Physiol Rev 90: 559–605, 2010;
doi:10.1152/physrev.00029.2009.

Molecular Background of Leak K^+ Currents: Two-Pore Domain Potassium Channels

PÉTER ENYEDI AND GÁBOR CZIRJÁK

Department of Physiology, Semmelweis University, Budapest, Hungary

I. Introduction 559
II. TWIK (Tandem of Pore Domains in a Weak Inward Rectifying K^+ Channel) 562
A. (Non-?)functional properties of the members of TWIK subfamily 562
B. Possible mechanisms restricting the functional expression of TWIK channels 562
C. TWIK channels at the gene, mRNA, and protein levels 563
III. TREK (TWIK-Related K^+ Channel) 564
A. Electrophysiological diversity in the TREK subfamily 564
B. Multiplex regulation of TREK/TRAAK channels 565
C. Physiological function and pathophysiology of TREK/TRAAK channels 571
IV. TASK (TWIK-Related Acid-Sensitive K^+ Channel) 579
A. Biophysical properties and the molecular mechanisms of acid sensitivity 579
B. Regulation by receptors, endocannabinoids, and interacting proteins 581
C. pH-dependent and other functions mediated by TASK channels 583
V. TALK (TWIK-Related Alkaline pH-Activated K^+ Channel) 590
A. Expression patterns, electrophysiology, and regulation by alkaline pH 590
B. Alkaline pH-related functions of TALK channels 592
VI. THIK (Tandem Pore Domain Halothane-Inhibited K^+ Channel) 593
VII. TRESK (TWIK-Related Spinal Cord K^+ Channel) 593
A. Unique single-channel behavior 593
B. Regulation by Ca^{2+} and protein interactions 594
C. Physiological significance of TRESK 595
VIII. Conclusions 596

Enyedi P, Czirják G. Molecular Background of Leak K^+ Currents: Two-Pore Domain Potassium Channels. *Physiol Rev* 90: 559–605, 2010; doi:10.1152/physrev.00029.2009.—Two-pore domain K^+ (K_{2P}) channels give rise to leak (also called background) K^+ currents. The well-known role of background K^+ currents is to stabilize the negative resting membrane potential and counterbalance depolarization. However, it has become apparent in the past decade (during the detailed examination of the cloned and corresponding native K_{2P} channel types) that this primary hyperpolarizing action is not performed passively. The K_{2P} channels are regulated by a wide variety of voltage-independent factors. Basic physicochemical parameters (e.g., pH, temperature, membrane stretch) and also several intracellular signaling pathways substantially and specifically modulate the different members of the six K_{2P} channel subfamilies (TWIK, TREK, TASK, TALK, THIK, and TRESK). The deep implication in diverse physiological processes, the circumscribed expression pattern of the different channels, and the interesting pharmacological profile brought the K_{2P} channel family into the spotlight. In this review, we focus on the physiological roles of K_{2P} channels in the most extensively investigated cell types, with special emphasis on the molecular mechanisms of channel regulation.

I. INTRODUCTION

The high resting potassium conductance of the plasma membrane was recognized in the era when the principal concepts of electrophysiology about ion channels and the generation of membrane potential were developed (135, 136). The high K^+ conductance could be most simply explained by the presence of (unregulated) potassium-selective pores in the plasma membrane and a background (leak) K^+ current conducted through these pores. On the basis of the constant field theory of Goldman, Hodgkin and Katz (114, 137), the current-voltage relationship of these hypothetical background K^+ channels could be predicted. However, the molecular entities responsible for the background K^+ currents have not been found for a half century. The first representative

(and several further) coding DNAs of all the other major (voltage-gated, inwardly rectifying, and calcium-dependent) K^+ channel families had already been cloned (8, 106, 179), when finally in 1996, the identification of TWIK (tandem of pore domains in a weak inward rectifying K^+ channel, now called TWIK-1) gave birth to the last, rapidly emerging family of mammalian background potassium channels (190). Actually, cloning and functional expression of the first K^+ channel with two pore domains per subunit was reported from *Saccharomyces cerevisiae*, and a new family of "potassium channels with two pore domains in tandem" was predicted in 1995 (159). However, this yeast channel, TOK1 (YORK) (159, 189), possessed eight putative transmembrane segments, and it was strongly outwardly rectifying. As TOK1 differs from the mammalian K_{2P} channels both structurally and functionally, we will not discuss it further in this review.

Between 1996 and 2003, the family of cloned mammalian background K^+ channels embraced 14 further members encoded by different genes (7, 11, 47, 84, 99, 112, 165, 170, 192, 194, 285, 286, 289, 294, 299). The members were divided into six subfamilies (TWIK, TREK, TASK, TALK, THIK, and TRESK) on the basis of sequence similarity and functional resemblance (Fig. 1). The categorization into subfamilies was reasonable despite the relatively low numbers of members, since the sequence variation between the different background K^+ channel subfamilies proved to be almost as high as that between the families of K^+ channels. Although the members of different subfamilies show relatively low sequence similarity (e.g., 28% identity between TWIK-1 and TREK-1 at the protein level; Ref. 99), all members of the background potassium channel family are characterized by the same general molecular architecture. The name of the family, "two-pore domain" potassium (K_{2P}) channels, was given on the basis of the distinguishing topology of the K^+ channel subunits. Each subunit contains two K^+ channel pore loop forming (P) domains, in contrast to the other K^+ channel families characterized by one P domain per one subunit stoichiometry. (Accordingly, K_{2P} subunits dimerize to constitute the functional K^+ selectivity filter containing four pore loop domains, a structure characteristic for all known K^+ channels). It is important to note that all mammalian K_{2P} channel subunits possess four transmembrane segments; the 4TM/2P structure defines the membership in the K_{2P} channel family (see Fig. 1). It is also worth mentioning that the K_{2P} channels are not restricted to mammals; their genes can also be found in lower organisms. ORK1 (later renamed by the authors to KCNKO), a *Drosophila melanogaster* background K^+ channel with 4TM/2P structure, was also reported in 1996 (116). An especially high number (>40 genes) of K_{2P} channels were found in *Caenorhabditis elegans* (76, 182). Although they had significantly different domain composition from most of the animal channels outside the 4TM/2P core, two-pore domain K^+ channels have also

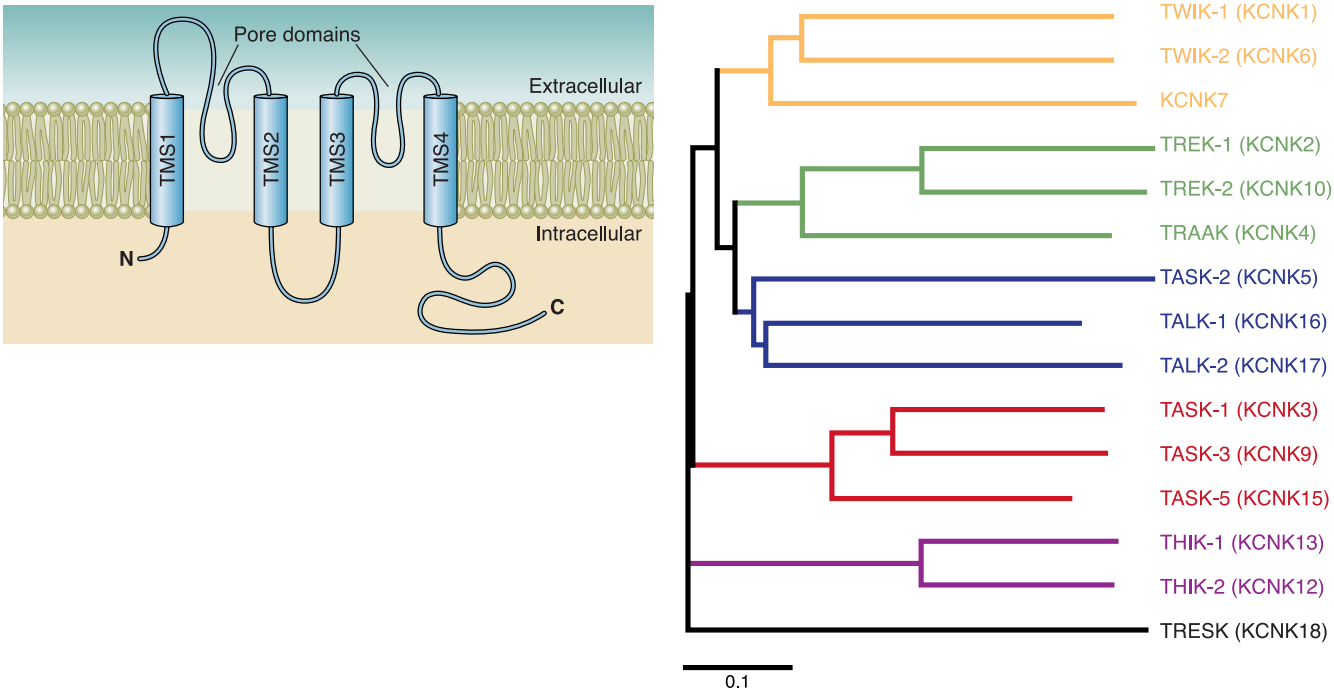

FIG. 1. Schematic transmembrane topology (*left*) and dendrogram of human two-pore domain potassium (K_{2P}) channels (*right*). Transmembrane segments are indicated by blue cylinders (TMS1-4). Note that the length of the COOH-terminal tail and the intracellular loop between TMS2 and -3 is highly variable in the different channels. The topology is not drawn to scale, and only one subunit of the functional dimer is depicted. On the dendrogram, both the conventional and systematic (HUGO) names are indicated. Note that KCNK8, KCNK11, and KCNK14 do not exist.

been cloned from different plants (62, 242), indicating that channels with the 4TM/2P architecture are widespread both in the animal and plant kingdoms.

In addition to the 4TM/2P topology, the electrophysiological features of K_{2P} channels are also similar. It is well-accepted in the literature that K_{2P} channels give rise to background K^+ currents. Therefore, it is practical to keep in mind what kind of properties an ideal background K^+ current should have if it followed the Goldman-Hodgkin-Katz (GHK) current equation. An ideal background K^+ current is not voltage dependent, meaning that the probability of opening (P_o) of the channels is the same at all membrane potential values. (P_o is also independent from the K^+ concentrations on the two sides of the plasma membrane.) Another important feature of the hypothetical background K^+ current is that the amplitude of the current instantaneously follows the changes of the membrane potential. [It is also said that the channel is "time independent" (190) or the channel does not have activation, deactivation, and inactivation kinetics (84).] In sharp contrast to the K_{2P} channels, the P_o of the voltage-gated channel types is regulated by the membrane potential. This is achieved via a relatively slow rearrangement of protein conformation. Therefore, the alteration of the voltage-gated K^+ current is delayed after the change of the membrane potential at the millisecond timescale (Fig. 2*A*). Since the membrane potential does not influence the P_o of the ideal background K^+ channel, and the driving force of K^+ is determined by the membrane potential at the submillisecond timescale, a rapid change of the membrane potential results in an "immediate" alteration of the background K^+ current; thus a voltage step in a voltage-clamp experiment induces a square wave-like K^+ current (Fig. 2*B*). Moreover, an ideal background channel is not rectifying; opposite driving forces (electrochemical gradients) of equal amplitudes induce opposite currents of equal amplitudes. This means that the apparent rectification in physiological solutions (mentioned as "open rectification" by some authors, Ref. 188) is caused exclusively by the unequal K^+ concentrations on the two sides of the plasma membrane (Fig. 3). (If $[K^+]$ was equal on both sides, then the current-voltage relationship would be a line passing through the origin.) If a K^+ current approximately meets the above criteria, then it can be considered as a background (leak) K^+ current. Although real K_{2P} channels do not perfectly fulfill these criteria (due to weak voltage dependence, interactions of multiple ions in the channel pore, rectification in symmetrical $[K^+]$, etc.), they provide the best approximation by far, compared with the other K^+ channel families. In the following sections we are going to highlight how the currents of the different K_{2P} channels deviate from the above principles, and also discuss the (possible or established) physiological roles of the given channel with special emphasis on the regulation of channel activity.

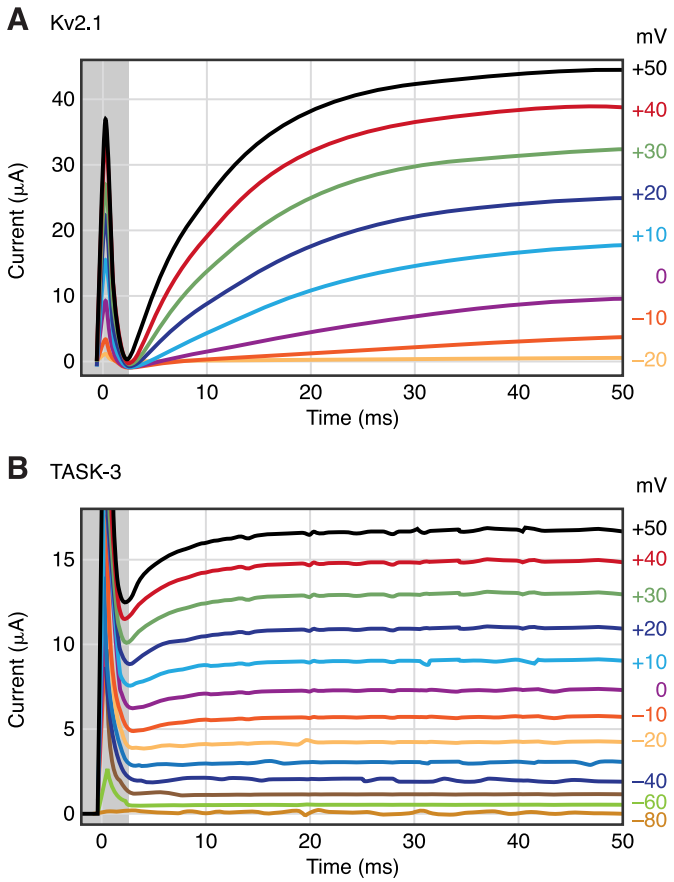

FIG. 2. Representative current traces of voltage-gated and background potassium channels. Kv2.1 voltage-gated (*A*) or TASK-3 background K^+ channels (*B*) were expressed in *Xenopus* oocytes. The currents were elicited by voltage steps from −80 to +50 mV in 10-mV increments in a solution containing 2 mM $[K^+]$. After the capacitative transient (indicated by the gray-shaded area), Kv2.1 is not yet active at 2.5 ms (*A*), whereas TASK-3 current is close to its maximum (*B*). TASK-3 recordings also contain a voltage-dependent component mainly reflecting the increased P_o of the channel at depolarized potentials (286). This whole oocyte recording is compatible with the instantaneous nature of the major fraction of TASK-3 current. (Kv2.1 was not activated by voltage steps from −80 to −30 mV.) The voltage labels of these curves on the *right* of *A* (and those of every second TASK-3 curves below −20 mV in *B*) were omitted. The holding potential was −80 mV for both cells.

In this review, where it is possible, we use the conventional names of K_{2P} channels (given by the researchers, generally beginning with the letter T), as these names can most often be found in the scientific literature. A systematic nomenclature was accepted by the Human Genome Organization (HUGO) for the K_{2P} channels genes (KCNK1-18) and another for the protein products (K_{2P}1-18) (115). (This latter nomenclature also takes the splice variants into account by extending the name with a dot and a further number, e.g., K_{2P}1.1.) In parentheses, we also give the systematic names of gene and protein product once for each channel.

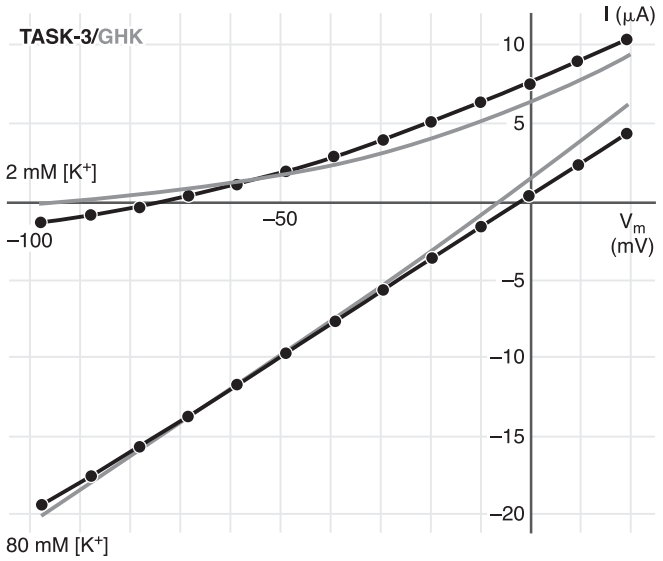

FIG. 3. Approximation of the current of TASK-3 with Goldman-Hodgkin-Katz (GHK) current equation. K^+ currents of a *Xenopus* oocyte expressing TASK-3 were evoked by depolarizing voltage steps from −100 to +20 mV in 2 or 80 mM extracellular [K^+]. The instantaneous components of TASK-3 current, measured at 2.4 ms after the initiation of the voltage steps, were plotted (circles connected with black lines). The data in 2 and 80 mM [K^+] were approximated by the GHK current equation (gray curves) in a single fitting process applying the least-squares method with the permeability constant and the intracellular [K^+] as variables. Note that the GHK curves only approximate the instantaneous component of the current, and the steady-state current (e.g., at 50 ms, see Fig. 2*B*, also including the voltage-dependent component of TASK-3 current) would be even less well fitted (not shown).

II. TWIK (TANDEM OF PORE DOMAINS IN A WEAK INWARD RECTIFYING K^+ CHANNEL)

A. (Non-?)functional Properties of the Members of TWIK Subfamily

Electrophysiological characterization and understanding of the functional significance of TWIK channels [TWIK-1 (KCNK1, K_{2P}1.1), TWIK-2 (KCNK6, K_{2P}6.1), and KCNK7 (K_{2P}7.1)] has been impeded by the low or absent functional expression in heterologous expression systems. TWIK-1 has been reported to give rise to a weakly inwardly rectifying K^+ current in *Xenopus laevis* oocytes in the first study of K_{2P} channels (190). In this original report, despite the high amount of injected cRNA, only small currents were induced (190), the amplitudes of which were close to those of endogenous currents of *Xenopus* oocytes (190). In subsequent independent experiments, TWIK-1 (also mentioned as HOHO1) could not be expressed in the same expression system (67, 117, 279, 283). This suggests that presently unidentified (perhaps oocyte preparation-specific) factors may have enabled the moderate functional expression in the first study. In symmetrical [K^+], TWIK-1 single-channel conductance was 34 pS (at −80 mV in symmetrical 140 mM [K^+]) in the first study (190); this value was also confirmed by others with a mutant form (K274E, see sect. II*B*) of human TWIK-1, producing higher current density than the wild-type channel (283). TWIK-1 was inhibited by intracellular acidification and activated by the application of phorbol 12-myristate 13-acetate (PMA, the pharmacological activator of protein kinase C), although the latter effect was suggested to be indirect (190, 191). These functional properties were also found to be characteristic for TWIK-2 current (47).

Expression of human TWIK-2 in *Xenopus* oocytes also resulted in small current amplitudes (<0.5–1 μA, in 115 mM [K^+] at −100 mV; Ref. 47), and as in the case of TWIK-1, others could not detect human or mouse TWIK-2 (also called TOSS) current in *Xenopus* oocytes (67, 279). Coexpression of TWIK-1 and TWIK-2 subunits also failed to induce K^+ current (279). Interestingly, rat TWIK-2 produced 15-fold higher currents than the human channel in COS-7 cells; thus rat TWIK-2 was more readily characterized (270). According to these (sometimes contradictory) reports, the expression of TWIK-2 may also be limited in the different expression systems (with the possible exception of rat TWIK-2).

TWIK-2 (like TWIK-1) induced a weakly inwardly rectifying current in symmetrical [K^+] (47, 270). The current deviated from that of an ideal background channel as the activity was influenced by the membrane potential. About 50% of TWIK-2 inactivated slowly ($\tau \sim 2$ s) at strong depolarization (steady-state half inactivation at +65 mV) (270), while the remaining fraction showed background K^+ current properties (270). The inactivation was also modified by the extracellular K^+ concentration. TWIK-2 inactivated at physiological [K^+] distribution, whereas no inactivation was observed in symmetrical high [K^+] (47, 270).

The third member of the TWIK subfamily, K_{2P}7 (KCNK7), could not be heterologously expressed in *Xenopus* oocytes or COS-7 cells (27, 294). (KNCK7 of different species was also called KCNK6 or KCNK8 in the first studies. Later KCNK6 was assigned to TWIK-2, and the KCNK8 name was omitted.) A structural trait of mouse KCNK7 is its COOH-terminal EF-hand (potential Ca^{2+} binding) domain (294), which is unique in the mammalian K_{2P} channels. Human KCNK7 has an unconventional sequence (GLE) in the second K^+ channel pore (P2) domain (294), whereas in other K^+ channels in homologous positions, the glycine residues are strictly conserved (GYG, GLG, or GFG) and considered as indispensable in forming the selectivity filter. This raises the question whether the human KCNK7 protein may function as a K^+ channel at all.

B. Possible Mechanisms Restricting the Functional Expression of TWIK Channels

Two different hypotheses were suggested to explain the low/absent functional expression of TWIK-1. Accord-

ing to the first one, TWIK-1 is mainly located in intracellular compartments, and its transfer to the plasma membrane is tightly regulated. Expressed TWIK-1 was present primarily in the pericentriolar recycling endosome in nonpolarized cell types (HeLa, CHO, and COS cells) and in the subapical recycling endosome in polarized (MDCK) cells (78). The native channel was also abundant in the subapical region of renal proximal tubule cells (78). An ARF6-dependent interaction was demonstrated between TWIK-1 and EFA6 (78). EFA6 is a GDP/GTP exchange factor for ARF6 small G protein, which is known to regulate membrane recycling, actin cytoskeleton organization, and vesicle trafficking (102). It has been hypothesized that sequestration of the channel in intracellular compartments may be the consequence of this ternary interaction, and the importance of TWIK-1 in the modulation of endocytosis and intracellular vesicle trafficking has also been suggested (78). Nevertheless, functional TWIK-1 expression in the plasma membrane has not been achieved by manipulation of the ARF6/EFA6 system (78).

According to the other hypothesis, TWIK-1 is inserted into the plasma membrane, but it is silenced by a special posttranslational modification: sumoylation (283). SUMO (small ubiquitin-related modifier) proteins are reversibly and covalently linked to the ϵ-amino group of a lysine residue located in consensus sumoylation sequences of target proteins (246). K274E mutation of the putative sumoylation site of TWIK-1 rendered the channel functional in *Xenopus* oocytes and in COS-7 cells (283). Sumoylation of wild-type TWIK-1 was biochemically verified; desumoylation of the channel with SENP1 enzyme resulted in an appropriate molecular weight shift of the protein. SENP1-treated wild-type and sumoylation-resistant K274E mutants were indistinguishable on Western blots. Coexpression of SENP1 increased TWIK-1 whole cell current in *Xenopus* oocytes, and application of the desumoylating enzyme to excised patches also increased the activity of the channel (283).

However, the theory of TWIK-1 sumoylation was soon challenged (96). It was shown that the current densities of wild-type and K274R-mutant TWIK-1 were identical, although this mutant could not be sumoylated. (In these experiments the HcRed-K_{2P}1 fusion construct was used, which resulted in measurable "wild-type" TWIK-1 current.) Therefore, it has been suggested that the higher current density of K274E mutant could be the consequence of a charge effect unrelated to sumoylation. Furthermore, the previous results on the wild-type channel regarding the molecular weight shift and functional consequences of desumoylation with SENP1 could not be reproduced (96). Because both sets of conflicting experiments (96, 283) seem to be convincing, further investigation is required to decide the principal question whether TWIK-1 is sumoylated or not.

Despite the small (47, 270) or absent (279) human TWIK-2 currents in *Xenopus* oocytes and the 15-fold difference between human and rat TWIK-2 currents in COS-7 cells (270), the mechanism restricting functional expression of TWIK-2 has not been examined so far. In contrast, the third member of the TWIK subfamily, KCNK7, clearly failed to induce K^+ current in heterologous systems, and therefore, the question was immediately raised whether the protein was unable to reach the plasma membrane or whether it was inactive on the cell surface. Immunofluorescence localization of KCNK7 in permeabilized COS-7 cells indicated that the channel protein was sequestered in the endoplasmic reticulum (294). This result suggests that KCNK7 may reside in the endoplasmic reticulum under physiological conditions or a presently unknown factor, absent from COS-7 cells, is required for its surface expression.

C. TWIK Channels at the Gene, mRNA, and Protein Levels

While the electrophysiology of TWIK channels remains enigmatic, an exciting direct interaction of KCNK1 gene has been recently revealed (20). A member of the p53 tumor suppressor family, TAp73, has been shown to transactivate the KCNK1 gene. TAp73 inhibits anchorage-independent growth of tumor cells, and it has been suggested that TWIK-1 might mediate its effect. In fact, silencing of TWIK-1 expression promoted growth of tumor cells similarly to the knockdown of TAp73. As TWIK-1 is downregulated in different tumors, including glioblastoma, melanoma, and advanced stages of ovarian cancer, it was plausible to assume that the channel modulated tumor aggressiveness and metastasis (20).

Expression of TWIK-1 has been detected in several tissues, including the kidney, brain, and lung (5, 190). In the kidney, TWIK-1 immunoreactivity has been found in different parts of the nephron; however, the expression pattern showed considerable differences in various species (59, 195, 233, 251, 261). Unexpectedly, the principal cells of cortical collecting duct of TWIK-$1^{-/-}$ knockout mice were hyperpolarized (233), and the increased urinary phosphate and free water clearance reflected reduced expression of the sodium-phosphate cotransporter in the proximal tubule and inappropriate internalization of aquaporin-2 in the collecting duct (251). Thus the absence of TWIK-1 at these locations appeared to interfere with proper targeting and/or regulation of other transporters. TWIK-1 was consistently expressed in the thick ascending limb of the loop of Henle in all examined species, raising the possibility that the function of TWIK-1 is related to the K^+ recycling in these cells, the mechanism of which is primarily attributed to the inwardly rectifying K^+ channel, ROMK (Kir1.1) (59).

TWIK-1 was also detected in the heart (86, 329), and its expression was altered in atrial fibrillation. However, these results are inconsistent as both increased (108) and reduced (86) TWIK-1 mRNA levels have been reported. Thus further work is required to elucidate whether TWIK-1 participates in the electrophysiological maladaptation characteristic of chronic atrial fibrillation (249, 335).

TWIK-1, like many other K_{2P} channel subunits, is expressed along the auditory and vestibular sensory system, including neurons and also nonsensory epithelia (53, 61, 138, 250). After bilateral cochlear ablation, TWIK-1 mRNA levels were reduced significantly (although not as dramatically as TASK-5 mRNA) in both the cochlear nucleus and colliculus inferior (61, 138), suggesting that TWIK-1 might also contribute to the deafness-associated sensitization of the neural auditory pathway.

TWIK-1 expression has been documented in several other tissues: in the brain (29, 175, 282), in airway epithelial cells (75, 143), and in the umbilical cord vein (266). Different theories were proposed for the physiological functions of TWIK channels at these locations. We will not discuss these theories further, as they remain clearly hypothetical until TWIK K^+ current is analyzed directly in the corresponding cell types.

In the absence of apparent functional expression, another successful line of investigation was the biochemical analysis of TWIK-1 protein (193). It was demonstrated that TWIK-1 subunits formed homodimers in vitro, which were dissociated by treatment with β-mercaptoethanol. A disulfide bridge, formed between the cysteines at residue 69 in the first extracellular loops (193), linked the two subunits. The experimental data suggested that TWIK-1 constitutes functional homodimers also in vivo, and both pore domains of TWIK-1 subunits contribute to the formation of K^+-selective channel pore (193). Although the same cysteine (and thus the disulfide bridge) is not conserved in all the other K_{2P} channels, a similar conclusion, regarding the dimeric structure, was derived in the case of the functional TASK-1 channel (213).

III. TREK (TWIK-RELATED K^+ CHANNEL)

A. Electrophysiological Diversity in the TREK Subfamily

The first member of the subfamily, TREK-1 (TWIK-related K^+ channel) (KCNK2, $K_{2P}2$), was discovered in 1996, as the second mammalian K_{2P} channel (99). Subsequent cloning of the closely related TRAAK (TWIK-related arachidonic acid activated K^+ channel, KCNK4, $K_{2P}4$) (100) and TREK-2 (KCNK10, $K_{2P}10$) (11, 194) completed this group. Functionally active alternative splice variants of both TREK-1 (340), TREK-2 (122), and TRAAK (263) also contribute to the diversity of the subfamily. [In addition, significant expression of a nonfunctional, truncated form (consisting of only 67 amino acids) of TRAAK (TRAAKt) has also been detected (100).] The structural difference of the functional splice variants is restricted to the extreme NH_2-terminal intracellular part. To our present knowledge, these minor variations influence neither the basic biophysical characteristics of the currents nor the regulatory processes of the channels (171, 269), although, intriguingly, the expression pattern of the splice variants shows significant tissue specificity (122, 340). It has been recently reported that the heterogeneity of both TREK-1 and TREK-2 is further increased by alternative translation initiation. In these alternatively translated forms of the channel, a longer segment of the intracellular NH_2 terminus is missing than in the splice variants. This structural alteration has significant consequences on the biophysical characteristics of the channels (see below).

TREK-1 has been originally characterized as an outwardly rectifying potassium channel (99). Two independent mechanisms underlie the deviation from the ideal leak conductance. In the absence of extracellular divalent cations, the single-channel current-voltage (*I-V*) relationship of TREK-1 in symmetrical K^+ solution is linear or slightly inwardly rectifying (194, 340). However, in the presence of physiological concentrations of extracellular Mg^{2+} or Ca^{2+}, the unitary conductance of TREK-1 is progressively reduced in the negative membrane potential range and has a tendency to saturate at very negative values (168, 269). This results in a marked outward rectification. The sensitivity to extracellular divalent cations (a mirror image of the mechanism, by which intracellular Mg^{2+} or spermine regulate the inwardly rectifying potassium channels) is unique for TREK-1 in the subfamily. The amplitude of TREK-2 and TRAAK single-channel currents is not influenced significantly by the presence of extracellular Mg^{2+} (11, 168, 194).

Voltage-dependent gating of TREK-1 is the other major factor responsible for outward rectification. TREK-1 single-channel activity has a characteristic, pronounced bursting behavior (99, 269). At highly positive membrane potentials, the P_o of TREK-1 can be as high as 0.6 (also depending on the mechanical activation). In turn, at negative membrane potentials, the P_o of the channel is greatly reduced (218), and the bursting activity completely disappears (269). Early reports described TREK-1 as an almost instantly activating channel (99). Closer analysis revealed that the instantaneous current change during depolarization (reflecting the alteration of the electrochemical driving force) is in fact accompanied by a fast (τ = 4–6 ms), time-dependent component, representing the voltage-dependent activation of TREK-1 (28). TREK-1 does not inactivate, and the channel has a low deactivation time constant (τ = 5–7 ms) (218). The rapid activation and deactivation kinetics may hide the voltage dependence of

TREK-1, when the voltage clamp is not efficient enough during whole cell measurements, and may manifest as an apparent rectification of the K^+ current.

Progressive deletion of the intracellular tail of TREK-1 gradually diminished the transient component of the current (evoked by depolarizing voltage steps), thus simultaneously reducing the apparent rectification of the channel (218). Studying hybrid constructs of TREK-1 and a less voltage-dependent K_{2P} channel, TASK-1, it was demonstrated that the COOH-terminal tail of TREK-1 was not only necessary for the voltage dependence, but its transposition to the core of TASK-1 conferred voltage sensitivity to the chimera (218). However, it should also be noted that the same domain, required for the effect of the membrane potential, is also prominent in a wide variety of other regulatory mechanisms. It is a salient feature of TREK-1 regulation that the highly divergent regulatory factors affect either directly or indirectly the proximal intracellular tail region, and many of these were also shown to modulate the voltage dependence (28, 218).

In symmetrical high (~140 mM) K^+ solution, the single-channel conductance of TREK-1 is 95–130 pS at positive membrane potentials (140, 173, 269, 340). At negative potentials, in the absence of inhibitory extracellular (EC) Mg^{2+}, the slope conductance is somewhat higher (28). In addition to this high conductance mode, another lower conductance level of TREK-1 was characterized more recently. Heterologous expression of either the longer or the shorter splice variants produced two populations of channels with the high and low single-channel conductance values (~100 and 40 pS, respectively), and the activity of the channels in both conductance modes was changed similarly by the different regulatory factors of TREK-1. Transition between the two conductance values was observed very rarely. Accordingly, it has been proposed that the different conductance levels might arise because of the interaction of the channel with unknown accessory intracellular proteins (340).

TREK-1 gene has a weak natural Kozak sequence, which may be skipped, and translation can initiate from another, internal start codon (AUG site 57 amino acids downstream of the expected NH_2 terminus). A truncated form of the TREK protein was detected in heterologous expression systems as well as in native tissues. The deletion construct (Δ1–56) was shown to have ~30% larger unitary current but lower P_o than the M57I mutant, in which the mutation prevents translation to the shorter deleted form. This mechanism clearly explains the previously observed heterogeneity of the unitary current of TREK-1 expressed from the same mRNA species. A quite unexpected property of the truncated channel was also observed, which may have striking consequences; the ion selectivity of the truncated channel was impaired. Although the missing part of the NH_2 terminus is located far from the selectivity filter, it has been found that TREK-1(Δ1–56) is also permeable to Na^+. Thus, considering the physiological ion concentrations, the high relative expression of the Δ1–56 channel form may induce depolarization toward the firing threshold (316).

Alternative translation initiation is not restricted to TREK-1. Three different TREK-2 channels are produced from the same mRNA as a result of skipping the first or the first two initiation site(s). It has long been known that expressed TREK-2 channels have low (~50 pS) and high (~220 pS) conductance levels and that these levels do not represent different subconductance states, as they are never converted from one to the other. The long TREK-2 variant turned out to be responsible for the lower, while the two shorter forms for the higher conductance channel. The previously reported channels of intermediate conductance may have reflected the heteromer assembly of the short and long variants. Unlike the shorter TREK-1 forms, all the TREK-2 variants preserve their selectivity for K^+. They were also identical in their response to different regulatory manipulations, which had previously been assigned to the proximal intracellular tail region (303).

TREK-2 shows high sequence similarity to TREK-1 in the proximal region of the intracellular COOH-terminal tail (in addition to the transmembrane segments). As expected on the basis of this resemblance, the membrane potential also affects the gating of TREK-2. The P_o of the channel at +40 mV was determined to be about twice (194) or four times (11) as high as at −40 mV. In contrast to TREK-1, however, depolarization decreases the unitary conductance of TREK-2 (11, 122, 168, 194). At the macroscopic (whole cell) current level, this inward rectification of the unitary current may balance the effect of the voltage dependence of the gating, resulting in an almost linear (11) or only slightly outwardly rectifying current (194) in symmetrical $[K^+]$ solutions.

TRAAK current is not influenced by EC Mg^{2+}, and its single-channel *I-V* relationship is only slightly inwardly rectifying in symmetrical high $[K^+]$ solutions (168). The slope conductance, in physiological $[K^+]$ solutions, is 45 pS measured in the positive membrane potential range (between 0 and +60 mV) (100). Although it has been reported that the single-channel activity (NP_o) of TRAAK in isolated membrane patches was increased three- to eightfold by depolarization (168, 217), at the whole cell level TRAAK behaves as a classical nonrectifying leak channel (100).

B. Multiplex Regulation of TREK/TRAAK Channels

The channels belonging to the TREK subfamily share complex regulatory properties. The first 30 amino acids of the cytoplasmic tail adjacent to the fourth transmembrane segment (TMS) turned out to be absolutely critical for

such diverse regulatory processes as the voltage dependence, mechano-, lipid-, and thermosensitivity as well as the modulation by G protein-coupled receptors. On the basis of the analogy with other potassium channels of known crystal structure (238), the second and fourth transmembrane segments of K_{2P} channels are envisioned to form the inner pore helices. Secondary structure predictions suggest that the fourth transmembrane α-helix extends intracellularly, and this rodlike extension apparently has a pivotal role in the regulation of channel activity. TREK-1 and TREK-2 are highly conserved in this region, explaining the very similar regulatory mechanisms of the two channels (see Fig. 4). Analysis of the response of TREK mutants to various stimuli pinpointed single amino acid residues in this α-helix, which are targeted during the different types of regulation. Aligning the sequences of the proximal COOH terminus in the three members of the family clearly shows that TRAAK differs from TREK-1 and TREK-2 at some critical positions. Accordingly, its regulation also deviates from that of the two TREK channels. (A homologous part plays an important role in the receptor-mediated regulation of TASK channels, suggesting that the intracellular helical structure following the fourth TMS is also a regulatory focal point in the other extensively examined K_{2P} channel subfamily.)

1. Mechanosensitivity

Under basal conditions, the activity of the TREK/TRAAK channels is rather low, while applying subatmospheric (negative) pressure to the patch pipette in cell-attached configuration reversibly activates TREK-1 (269), TREK-2 (194), and TRAAK (168, 217). Laminar shear stress stimulates TREK-1 (269), whereas the shrinkage of the cell induced by extracellular hyperosmolarity reduces the amplitude of TREK-1 and TRAAK currents. This indicates that the tension of the cell membrane efficiently regulates channel activity (222, 269). Mechanosensitivity does not depend on cellular integrity; rather, it is clearly membrane delimited. The response to negative pressure in the pipette is not only maintained after patch excision, but the physical disruption of cytoskeletal interactions by the isolation of the membrane patch even increases the basal activity and augments the susceptibility to mechan-

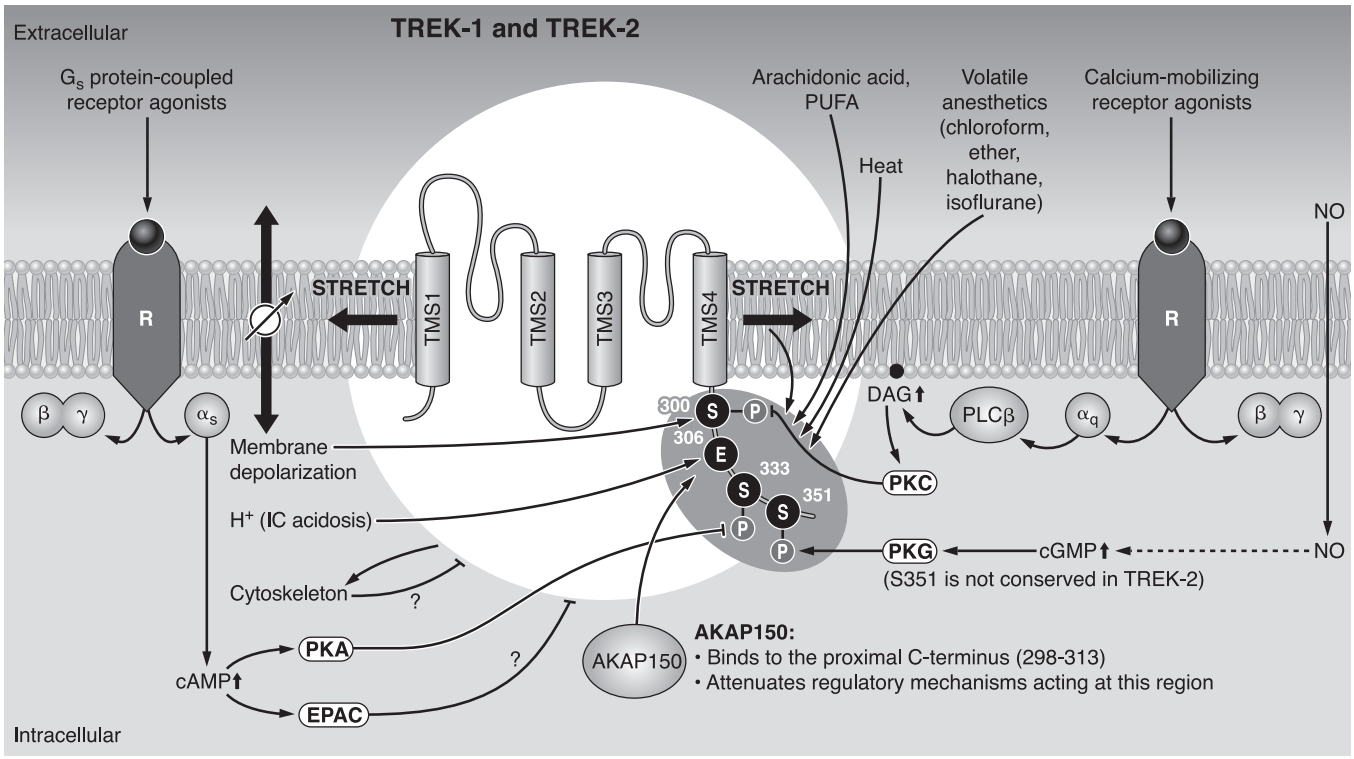

FIG. 4. Multiplex control of TREK-1 and TREK-2. The channels are activated by physicochemical changes, such as stretch or convex deformation of the plasma membrane, depolarization, heat, and intracellular acidosis. Polyunsaturated fatty acids (PUFA) including arachidonic acid (AA) and a wide variety of volatile anesthetics also open TREK channels. Activation of the G_s/cAMP/PKA and the G_q/PLC/DAG/PKC signaling pathways inhibit TREK channels by phosphorylating defined serine residues on the COOH-terminal tail. In some tissues, the effect of the elevated cAMP concentration is mediated by the small G protein EPAC. The interaction of the cytoskeleton with TREK channels has bidirectional consequences; the channels shape the cytoskeleton while being inhibited by it. Another established partner of TREK-1 is AKAP 150, which binds to the key regulatory domain of the channel and modifies its sensitivity towards various modulating factors. TREK-1 is activated via the NO/cGMP/PKG pathway, but the PKG phosphorylation consensus site is missing in TREK-2. (Arrows indicate stimulation; lines with ⊤ ending represent inhibition.)

ical stimuli (168, 186, 217). Pharmacological disintegration of the cytoskeletal network (pretreatment with colchicine or cytochalasin D) also activates these channels, suggesting that the cytoskeleton exerts a tonic inhibitory effect on them (168, 186). The action of the cytoskeleton might be transmitted by membrane shape or tension, which in turn directly regulates channel activity. Interestingly, the regulatory effect seems to be bidirectional; it has been reported that TREK channels influence the cytoskeletal organization (see more details in sect. III*C1*).

In general, the opening of all TREK/TRAAK channels is facilitated by convex membrane deformation. However, detailed characterization of their response to physical stress revealed delicate variations. TREK-1 (269) and TREK-2 (194) are activated by negative, and to a much smaller degree by positive, pressure applied to the extracellular side of the plasma membrane. On the other hand, TRAAK can be activated only by suction from the extracellular direction (positive pressure activates only from the intracellular side) (168, 217). Amphipathic molecules, which asymmetrically insert into the lipid bilayer, are known to modify the shape of the membrane characteristically. The anionic crenator trinitrophenol (TNP) causes convex curvature (like the negative pressure does) and activates TREK-1 (269) and TRAAK (217). The opposite (concave) change of shape created by the cationic cup former antipsychotic drug chlorpromazine inhibits TREK-1 but does not affect TRAAK (222).

Activation of the channel by the applied mechanical stimulus is graded and reversible. The negative pressure that activated half-maximally TREK-1 and TRAAK was −36 and −46 mmHg, respectively (221); however, these values significantly depended on the experimental system and on other regulating factors, such as the intracellular pH, membrane potential, and arachidonic acid (217).

Truncation of the COOH terminus results in the reduction of mechanosensitivity of TREK channels, if the region next to the fourth TMS is also truncated. A more distal deletion (after T322 in TREK-1), leaving the first 30 amino acids of the COOH-terminal tail intact, does not influence mechanosensitivity, whereas progressive truncation before this position gradually decreases mechano- (and other forms of) stimulation and also the amplitude of the basal current (269). The basal channel activity was rescued by fusing the COOH terminus of TASK-1 to the TREK-1 channel core (retaining only the first six amino acids of the COOH-terminal cytoplasmic part of TREK-1); however, this chimera remained insensitive to shearing forces (269). [The reverse chimera, in which the tail of TREK-1 was transferred to TASK-1, was also entirely insensitive to shear stress (269).] In contrast to the above results, a similar TREK-2/TASK-3C chimera (in which the two channel parts were joined exactly at the transmembrane/cytoplasmic border) was responsive to the negative pressure, applied directly to the membrane (168). The discrepancy between the two studies might have arisen because different members of the TREK and TASK subfamilies were used, or an alternative explanation may be that the −60 mmHg suction, applied directly to the membrane exerted a stronger mechanical stimulus than the shear stress (168). It is also possible that the important α-helix (the rodlike structure extending the fourth TMS in the cytoplasm) was better preserved in the TREK-2/TASK-3C chimera despite the shorter sequence retained from the mechanosensitive TREK channel. In addition to the above truncation and chimera experiments, the significance of the fourth TMS and its COOH-terminal cytoplasmic α-helical appendage in the determination of mechanosensitivity has been further supported by site-directed mutagenesis studies (140) (see further details in sect. III*B4*). These results together suggest that the transmembrane segments (primarily the fourth one) play a pivotal role in the mechanosensitivity, while an appropriate (but not necessarily TREK subfamily specific) COOH-terminal tail fragment is also necessary for proper regulation.

2. Arachidonic acid, phospho-, lysophospho-, and other lipids

Both TREK channels and TRAAK are activated by arachidonic acid (AA). In fact, the name TRAAK refers to this sensitivity. AA need not be metabolized to act, and other polyunsaturated fatty acids (PUFA), docosahexaenoic acid, linolenic acid, linoleic acid, etc., also directly stimulate TREK/TRAAK channels. On the contrary, saturated fatty acids are not effective (11, 73, 100, 194). In addition to the activation, PUFA sensitize the channels to mechanical stimulation; the channels open in response to less negative pressure. PUFA also interfere with the cAMP/protein kinase A (PKA)-induced inhibition of TREK-1 (269). Stimulation by PUFA does not rely on cellular integrity; it also develops in excised patches. PUFA are effective from either side of the membrane (100, 168); however, their effect is evoked more rapidly if they are administered to the intracellular compartment (11). The first 28–30 amino acids in the proximal COOH-terminal tail of TREK-1 (269) and TREK-2 (171) mediate the effect of PUFA; however, in the case of TRAAK, it has been suggested that this region is not absolutely critical and can be substituted by a homologous region of TASK-3 without losing the regulation (168).

Different lysophospholipids (independently of their charge) open TREK and TRAAK channels even more rapidly than AA (194, 222). In contrast to the fatty acids, however, the effect of lysophosphatidylcholine (LPC) needs cellular integrity. If LPC is applied to the intracellular side of excised membrane patches, then it becomes even inhibitory (222). Native TREK-1 in bovine adrenal fasciculata cells was activated by LPC and lysophosphati-

dylinositol (LPI) similarly to the heterologously expressed channel; however, the activation rapidly desensitized and subsequent stimuli were ineffective. These results suggest a more complex mode of action with the possible involvement of signaling, metabolism, or auxiliary channel subunit(s) (73). Unlike the lysophospholipids, lysophosphatidic acid (LPA) does not act from outside (neither on whole cells, nor on right-side-out vesicles) (50, 222). However, it activates TREK and TRAAK channels on inside-out vesicles, suggesting that LPA, formed intracellularly during the activation of phospholipase C (PLC) and phospholipase A_2 (PLA_2), may have a regulatory potential. LPA also shifts the mechanogating of the channels toward less negative pressure values and converts them to voltage-independent leak conductance (50).

Acidic inner leaflet membrane phospholipids, phosphatidylinositol-4,5-bisphosphate (PIP_2) and to a lesser degree phosphatidylserine (PS), also activate TREK-1 from the intracellular side (51, 212). It has been suggested that these phospholipids interact with positively charged amino acid residues in the proximal COOH-terminal domain (51). Quenching the charge of endogenous phospholipids by the polycationic agent polylysine significantly reduces the channel activity in excised patches. In response to the application of PIP_2 to the intracellular surface, the characteristics of TREK-1 current were also modified, e.g., the channel became less voltage dependent (51, 212). The PIP_2 level of the plasma membrane is reduced substantially by the activation of PLC, when the cells are stimulated via G_q protein-coupled receptors. Therefore, the PIP_2-mediated activation of K^+ current may also change dynamically, also depending on the strength of channel-PIP_2 interaction (212).

PA and its precursor, diacylglycerol (DAG), were shown to reduce the AA-activated TREK-1 and TREK-2 currents in patches excised from HEK293 cells expressing the channels heterologously (48). In a similar experiment (147), however, inhibition of TREK-2 by DAG was inconsistent; it was apparent only in ~25% of the examined patches. A potentially significant difference between the two experiments was that in the latter, the channels were not preactivated by AA (147). This suggests that the inhibition by PA and DAG may be either indirect even in the excised membrane patch, or (more likely) it depends on the simultaneous presence of other local regulating factors (e.g., on the lipid composition of the surrounding membrane).

3. Thermosensitivity

TREK-1 is activated gradually and reversibly, in response to elevation of the ambient temperature from 14 to 42°C (219). TREK-2 and TRAAK channels share this sensitivity in the same temperature range (146). The activity of TREK-1 increased most steeply between 22 and 42°C. In this range, the amplitude of TREK-1 (whole cell) current was enhanced about sevenfold (which is a much larger increase than the activation of most other K^+ channels under identical conditions, e.g., ~2-fold for TASK-1). Thermal activation was also apparent in cell-attached configuration in addition to whole cell measurements. However, interestingly, after patch excision, the thermosensitivity of TREK/TRAAK channels was completely lost (146, 219), under conditions when mechano-, AA, and pH regulation was maintained. Therefore, it has been hypothesized that thermosensitivity is not an inherent property of the channels and may depend on an auxiliary (sensor) protein (219). If this theory is correct, then the auxiliary protein must be widespread and present not only in specialized temperature sensor cells but also in a wide variety of other cell types (even in amphibian oocytes), since thermosensitivity was very similar in different expression systems (COS-7 cells, *Xenopus* oocytes) and in the cell types expressing the channels endogenously (146).

Single-channel conductance of TREK-2 is not influenced by temperature, and activation is exclusively due to the elevated P_o (146). Thus temperature affects the gating of these channels, similarly to the (above discussed) other regulatory factors. In the case of TREK-1, deletion of the COOH-terminal tail or its replacement with the COOH terminus of TASK-1 abolished the thermosensitivity of the construct (219). However, the similar chimera composed of the core of TREK-2 and the COOH terminus of TASK-3 remained thermosensitive, suggesting that, in this context, the TREK-specific COOH terminus was not absolutely critical (146). The apparent contradiction of the results obtained with the two different chimeras is quite similar to the discrepancy discussed more extensively in section III*B1* and suggests that mechano- and thermosensitivity may work through related mechanisms, which are structurally associated with the fourth TMS and the following COOH-terminal tail region.

4. Regulation by pH

A) TREK/TRAAK CHANNELS ARE EFFICIENTLY REGULATED BY PH FROM THE INTRACELLULAR SIDE. In contrast to the canonic acid- and alkaline-sensitive (TASK and TALK) K_{2P} channels, the activity of the members of TREK subfamily is modified predominantly by intracellular pH changes. Protons activate both TREK-1 and TREK-2 (171, 194, 221), and also sensitize these channel to mechanical stimuli. TRAAK is not influenced by the acidification, but it is stimulated by the alkalinization of the intracellular solution (from an initial value of pH 7.3) (168). The effect of pH on all TREK/TRAAK channels is direct and apparent not only in cell-attached and whole cell configurations but also in excised patches.

Truncation experiments indicated that the proton sensor function of TREK channels resides in a 30-amino acid stretch of their proximal COOH-terminal intracellular tail. Progressive truncation of this COOH-terminal region of TREK-1 (221) and TREK-2 (171) gradually decreased the proton sensitivity, and the effect of pH completely disappeared when the truncation approached E306 in TREK-1 or the homologous E333 in TREK-2. The chimera, assembled from the core of TREK-2 and the COOH terminus of TASK-3 (a K_{2P} channel which is not influenced by IC pH changes), was insensitive to acidification (171), indicating that the COOH terminus of TREK-2 was indispensable for this type of regulation. Glutamate-306 was identified as the cornerstone of the intracellular proton sensor in TREK-1 by alanine scanning mutagenesis. Its substitution with neutral or positively charged residues rendered the channel constitutively active, independent of the membrane stretch, and even restored the mechanosensitivity of a mutant, truncated more distantly at the COOH terminus. This latter result suggests that the mechanosensitivity is determined by the complicated interaction of the COOH terminus and the channel core, and the protonation of E306 has a pivotal role in the regulation of this interaction. At the same time, the robust activity of the E306A channel was resistant to cAMP-mediated inhibition (characteristic for wild-type TREK-1, see sect. III*B5*). This indicates that E306 intertwines the regulatory action of the intracellular pH not only with mechanosensitivity but also with the susceptibility to the stimulation of G_s protein-coupled receptors (140).

TRAAK also has a glutamate in the position homologous to E306 of TREK-1, but this channel is not influenced by intracellular (IC) acidification (below pH 7.2). Furthermore, the mutation of this glutamate to alanine does not affect channel activity (140). In addition, transposition of the COOH-terminal tail of TREK-1 confers acid sensitivity to TRAAK (221), indicating that the transmembrane segments and pore domains of TRAAK can be modulated (and the channel activated by IC protons), if an appropriate COOH-terminal proton sensor is installed artificially. Without this engineered proton sensor, wild-type TRAAK can be modulated by intracellular pH changes only in the alkaline range. Alkalinization activates the channel suggesting that the effect is mediated by deprotonation of a residue (or residues), which is protonated at neutral pH. Although the contributing amino acid(s) have not been unequivocally determined, it is clear that they are not located in the intracellular tail, as the whole cytoplasmic COOH terminus of TRAAK could be replaced by that of TASK-3 without losing alkaline activation. These results indicate that the elements involved in the pH regulation of TRAAK are entirely different from those of TREK-1 and TREK-2 channels (168).

B) EXTRACELLULAR PH MODERATELY INHIBITS HUMAN TREK-1. Although the investigation of the effects of intracellular pH changes on TREK/TRAAK channels has dominated the literature for almost a decade, the regulation by extracellular acidification has also been demonstrated and its mechanism recently analyzed in detail (60). Two histidine residues (H87 and H141) in the first EC turret loop (located before the P1 pore domain) of human TREK-1 provide significant pH sensitivity in the physiological pH range. (Human TREK-1 is inhibited by ~35% at pH 6.5, compared with the value measured at pH 7.5. The inhibition by acidification was characterized by a p*K* value of ~7.5 and a Hill coefficient of 0.51, suggesting that the H^+-binding sites interact with negative cooperativity.) However, the sensitivity of human TREK-1 to EC pH in the physiological range seems to be the exception rather than the rule in the subfamily. In murine TREK-1, a glutamine is located in the position corresponding to H87 of the human channel, and that explains the much lower acid sensitivity of the mouse ortholog. An analog of H87 is also absent in human TREK-2, in accordance with the low sensitivity of this channel to EC pH alterations.

Extracellular acidification reduces the P_o of human TREK-1, while it does not influence the single-channel conductance (60). It has been proposed that the protonated histidine(s) attracted glutamate-84, thereby displacing the residue from its normal pore structure-stabilizing location. The evoked collapse of the selectivity filter and reduction of the P_o resembled in many respects to the C-type inactivation of voltage-dependent K^+ channels: attenuation of the pH effect by high extracellular K^+ concentration, reduction of ion selectivity (K^+/Na^+) simultaneously with the proton induced destabilization of the channel pore, and sensitization of the channel to acidification by mutating the pore-proximal serine-164 to tyrosine. These characteristics suggested that the inhibitory effect of acidification is related to the conformational change of the external pore gate.

In conclusion, human TREK-1 should be considered as a channel regulated by pH from both sides of the plasma membrane; its activity is modified in the opposite direction depending on the intra- or extracellular dominance of acidification. These data also point to the importance of careful evaluation of the results, where the identification of a natural leak K^+ current as TASK or TALK relied predominantly on the sensitivity to pH.

5. G protein-coupled receptors and phosphorylation

The first publication about TREK-1 already described its G protein-mediated regulation (99). In *Xenopus* oocytes expressing TREK-1, intracellular microinjection of the nonhydrolyzable GTP analog GTPγS inhibited the background K^+ current. The inhibition was explained by the stimulation of PKA and protein kinase C (PKC), as

pharmacological activation of these kinases by forskolin plus 3-isobutyl-1-methylxanthine (IBMX) or PMA, respectively, also decreased the K^+ current. The effects of the maximal pharmacological activation of PKA and PKC were additive, suggesting that separate sites were phosphorylated (99).

The COOH-terminal region of TREK-1 possesses two putative PKA consensus sites (S333 and S351). Mutational analysis revealed that serine-333 is the primary target of PKA; the S333A mutant lost cAMP sensitivity (99, 219). In excised patch experiments, phosphorylation by PKA decreased the P_o of TREK-1 only at negative membrane potentials, and thus enhanced the degree of rectification. The S348D mutant (in the long variant of TREK-1, which corresponds to S333D mutation in the short ortholog), mimicking the phosphorylated state at the PKA consensus site, also showed reduced P_o at negative membrane potentials leading to the characteristic outward rectification (28). The opposite modification, treatment with alkaline phosphatase or mutation of the PKA target serine to alanine, converted TREK-1 (in the absence of Mg^{2+}) into a leak channel with high P_o. These results led to the conclusion that phosphorylation by PKA converted TREK-1 into a voltage-dependent channel (28). However, this explanation for the mechanism of cAMP inhibition has been challenged, as under whole cell conditions the current of the wild-type and the S333A mutant channel showed equal voltage dependence, i.e., the same proportion of their currents was activated instantly and time dependently (218).

Recent results suggested that cAMP may also influence TREK-1 by a PKA-independent mechanism. In bovine adrenal zona fasciculata cells, cAMP inhibited TREK-1 by activating the Epac2 pathway (208). As the distribution of Epac2 is not uniform, this inhibitory mechanism is restricted to a population of cells or tissues, which express this cAMP-regulated small G protein.

The first argument in favor of the PKC-mediated regulation of TREK-1 was the inhibition of the channel by PMA (99). Serine-300, located in a highly conserved region, at the border between the fourth TMS and the intracellular tail, turned out to be essential for this regulation. An interesting relationship between PKA- and PKC-induced phosphorylations was also revealed in elegant experiments using a series of mutant channels (247). The protein kinase target serines (S300 and S333) were replaced (either alone or in different combinations) by amino acids that mimic the phosphorylated or dephosphorylated state (aspartate or alanine, respectively). According to this study, PKA- and PKC-induced phosphorylations at S333 and S300, respectively, are intimately related. The basal current densities and the inhibition of these mutants by PKA and/or PKC suggested that the phosphorylation of TREK-1 by PKA at S333 predisposes the channel for subsequent phosphorylation by PKC at S300 (247).

In different native cells and expression systems, TREK-1 activity at negative membrane potentials is low and the channel shows marked outward rectification and voltage-dependent activation (28, 93, 99, 211, 247). Stimulation of the G_i-coupled mGluR2 (194), mGluR4 (43), or α_{2A}-adrenergic receptors (343) activated the expressed and native TREK currents, respectively. In accordance, application of protein kinase inhibitors activated wild-type TREK current while the current of the S333A/S300A mutant was unaltered, suggesting that a significant fraction of the wild-type channels was phosphorylated under basal conditions (43, 194). Moreover, the phosphorylation state may change during the course of patch-clamp experiments. A slow increase of the background K^+ current after establishing whole cell configuration was apparent in cells expressing native (93) or cloned TREK-1 (247). This gradual run-up of the current was attributed to dephosphorylation of the channel, since the phenomenon was absent in mutant channels, lacking the S300 or S333 phosphorylation sites (247).

TREK-2 possesses the conserved serines of regulatory importance (S326 and S359, corresponding to S300 and S333 of TREK-1). Accordingly, TREK-2 current was inhibited by a membrane-permeable cAMP analog (i.e., the channel was regulated by PKA identically to TREK-1) (194). Different (NH_2-terminal) splice variants of TREK-2 were also inhibited by PMA similarly to TREK-1, indicating that the PKC-mediated regulation of TREK-2 was also operational (122). TREK-2 was inhibited by the G_q protein-coupled M3 muscarinic receptor, and this effect was prevented by the PKC inhibitor bisindolylmaleimide (147). Alanine substitution of the regulatory serines resulted in high basal channel activity, whereas the replacement with negatively charged aspartate caused low basal channel activity. All of these TREK-2 mutants were also insensitive to acetylcholine acting on the coexpressed M3 receptor (147). Thus, to our present knowledge, inhibition of TREK-2 by PKA or PKC is indistinguishable from that of TREK-1. In addition to the kinases, regulated by G protein-coupled receptors, TREK channels turned out to be targets of the AMP-activated protein kinase (AMPK). The inhibitory effect of AMPK relies on phosphorylation of the same serine residues, which are the substrate sites of PKA and/or PKC. AMPK may influence the activity of TREK channels depending on the metabolic state of the cell (178).

Interestingly, serine-351 of TREK-1, originally predicted as a PKA phosphorylation site, was also found to contribute to regulation, although its mutation to alanine failed to interfere with the inhibition evoked by PKA. Closer analysis of the PKA-mediated regulation of TREK-1 revealed that robust activation of the kinase may result in a biphasic response. The initial inhibition was followed by

activation of the current after long-term (15 min) stimulation. The S351A mutant was not activated by PKA (173), indicating that slow phosphorylation of S351 was responsible for the second (activatory) phase of regulation. While S351 is a poor substrate for PKA, its phosphorylation is central in TREK-1 current activation by the nitric oxide/cGMP/protein kinase G pathway (173). As serine-351 is not conserved in TREK-2, this channel cannot be the target of nitrergic stimulation. From the regulatory point of view, this is an important difference between the two, otherwise nearly identical, TREK channels.

On the basis of the above studies, it is clear that the phosphorylation of TREK channels by PKA or PKC plays a pivotal role in the channel inhibition during G_s or G_q protein-coupled receptor stimulation, respectively. Indeed, phosphorylation by PKC proved to be indispensable for the inhibition of TREK-1 (or TREK-2) by the G_q-coupled thyrotropin releasing hormone (TRH)-, orexin-, and M3 muscarinic receptors (147, 247). However, during the G_q-coupled receptor activation, complex signal transduction pathways are activated, and several metabolites are formed with potential regulatory function. Considering the multiplex and hierarchical regulation of TREK channels, the direct effect of the generated DAG, phosphatidic acid (PA), or lysophospholipides and the breakdown of polyphosphoinositides must also be considered. While most (48, 147, 211), but not all (207), studies accept that PLC activation is necessary for TREK-1 inhibition, the relative importance of the complementary or alternative pathways activated simultaneously with PKC is less well defined and may be cell specific.

In contrast to the PKC dependence of TREK inhibition during the stimulation of TRH, orexin-B, or M3 receptors, the inhibition of TREK-1 and TREK-2 via mGluR1 glutamate receptor was not influenced by a PKC inhibitory peptide and staurosporine. In this case, the liberated DAG and PA were suggested to be the most important regulators, since a DAG lipase inhibitor slowed down the recovery of the current after glutamate application, and DAG and PA reduced the current of the channels preactivated by AA (48). Direct activation of TREK by phosphoinositides was clearly shown by different groups (52, 211, 212). Thus it has been hypothesized that the breakdown of PIP_2 in response to G_q activation contributed to the inhibition of TREK current. However, direct experimental demonstration of this mechanism has not been presented.

Neither PKA nor PKC influences TRAAK activity (100). The inefficiency of PKA can be predicted from the amino acid sequence, since TRAAK does not contain a serine in homologous position to S333 of TREK-1. In contrast, S261 of TRAAK corresponds to the PKC phosphorylation site (S300) of TREK-1, and the amino acids in its neighborhood are also highly conserved between the two channels. On the basis of the sequential phosphorylation theory of TREK channels (247), it may be speculated that S261 of TRAAK cannot be efficiently phosphorylated by PKC in the absence of the PKA phosphorylation site. In fact, TRAAK proved to be insensitive to the stimulation of M1 muscarinic receptor, under the same conditions when TASK and TREK channels were efficiently inhibited (212).

6. Interaction with partner proteins

The A-kinase anchoring protein AKAP150 is known as a scaffolding protein, which binds to several partners [including PKA, PDZ binding proteins (PSD95 and SAP97), and G protein-coupled receptors]. A proteomic approach revealed interaction between TREK-1 and AKAP150. The proximal tail of TREK-1 between V298 and R313, the region having the primary importance in the regulation of channel activity, was identified as the AKAP150-interacting domain (298). Coexpression of AKAP150 profoundly changed the functional properties of TREK-1 (and TREK-2 but not TRAAK). The channel was transformed into a voltage-independent leak conductance. The gained high basal activity could not be stimulated further by AA, stretch, or intracellular acidification. AKAP150 rendered TREK-1 resistant to PKC, which inhibited the channel by phosphorylating S300 within the AKAP-binding domain in the absence of the scaffolding protein. On the contrary, the inhibition by PKA, which phosphorylates distal to the AKAP-interacting site, was retained. The effect of β2-adrenergic receptor was even accelerated, probably reflecting that the channel and the receptor were assembled to a protein complex by AKAP150 (298).

Microtubule-associated protein, Mtap2, increases the surface expression of TREK-1 and TREK-2 without influencing their *I-V* relationship. The enhanced targeting depends on the simultaneous interaction of Mtap2 with the microtubular system. Mtap2 attaches to the amino acid stretch between E335 and Q360 on the COOH-terminal tail of TREK-1, which is clearly distinct from the AKAP150 binding site. This allows simultaneous binding of AKAP150 and Mtap2 to the channel with an additive intensifying effect on TREK current (297).

Interaction between TREK-1 and a cellular prion protein (PrP^C) was detected in a bacterial two-hybrid system. The interaction was verified in transfected eukaryotic cells by coimmunoprecipitation and by confocal microscopic visualization of the transfected proteins (9). Although the colocalization and binding of PrP^C to TREK-1 is interesting, demonstration of the functional consequences of the interaction would highly increase the significance of the finding.

C. Physiological Function and Pathophysiology of TREK/TRAAK Channels

Long before the discovery of K_{2P} channels, unusual outwardly rectifying and noninactivating potassium currents were described in different tissues, including neu-

rons (166), cardiomyocytes (163), smooth muscle (260), and adrenocortical cells (237). The currents were not inhibited by the traditional potassium channel blockers [TEA, 4-aminopyridine (4-AP), and quinidine], and some studies reported that they were activated by AA and phospholipids (163, 260), showed mechanosensitivity (161, 174), or were inhibited by PKA (91). Many of these properties correspond to the later discovered TREK or TRAAK channels and often allow retrospective identification of their native currents. After the cloning of the channels, their tissue distribution was explored at the mRNA and protein levels. Highest expression was found in different areas of the brain; therefore, the members of this subfamily were originally referred to as neuronal potassium channels. Later the presence of their mRNA and the channel proteins were found in several peripheral tissues, and their functional expression was also confirmed by electrophysiological studies. Further data have been accumulated about their importance in physiological regulatory processes, and their significance under pathological or disease condition was also demonstrated, showing promise that their pharmacological modulation could provide medical benefits.

1. *Cytoskeletal organization during neuronal morphogenesis*

During the development of the nervous system, the dynamic reorganization of the cytoskeleton with the accompanying shape changes and directional expansion of the neurons are especially important as they underlie the axonal growth, path finding, dendritic arborization, and final formation of the complex neural network. A background K^+ channel is concentrated in the developing neuronal growth cones of the model organism marine snail *Aplysia* (302). It has been suggested that this channel influences the local [Ca^{2+}] changes and plays an important role in neurite elongation. Several characteristics of this mollusk S-type K^+ current (e.g., its leak properties, inhibition by cAMP, and activation by stretch and AA) are shared by the mammalian TREK-1 channel (269). These similarities and the modification of TREK-1 activity by cytoskeletal elements inspired studies to elucidate whether TREK channels have a reciprocal effect and also influence the neural morphogenesis via the cytoskeleton. Overexpression of TREK-1 (or to a lesser extent TREK-2) altered the morphology of cultured neonatal hippocampal neurons; the surface area of the cells increased because of the formation of filopodia-like structures in their dendrites and axons. TREK-1 was preferentially targeted to these protrusions, where it was colocalized with actin and ezrin (a plasma membrane-actin cytoskeleton linker), suggesting that TREK-1 influenced the cytoskeletal organization and likely participated in the formation of the protrusions. Interestingly, the effect of TREK-1 on cytoskeletal remodeling did not depend on channel permeation, as it also developed in the presence of channel inhibitors or when EC [K^+] had been elevated. Instead, the phosphorylation of serine-333, the principal substrate of PKA in TREK-1, regulated the morphogenetic properties of the channel. The channel activity and the cytoskeletal interactions were modulated in the opposite direction by the phosporylation; overexpression of the electrophysiologically less active phosphomimetic S333D mutant of TREK-1 had more pronounced effect on cell morphology than the constitutively active S333A mutant (186).

Cultured striatal neurons of TREK-1 knockout mice developed significantly less growth cones and looked more condensed than those of the wild-type animals, suggesting that TREK-1 expressed at the physiological level is necessary for normal morphogenesis (186). Strong expression of TREK-1 mRNA in the human fetal brain (227) and the high and dynamically changing expression of TREK channels in mice during the prenatal and early postnatal period, mainly in the rapidly developing areas of the central nervous system, also supported the idea that these channels were important in brain morphogenesis (3). However, the gross brain morphology appeared to be normal in adult TREK-$1^{-/-}$ mice (131). Although it cannot be ruled out that the missing TREK-1 was substituted by other channel(s) (e.g., by TREK-2) during a critical period of development, such compensatory overexpression of other K_{2P} channels was not observed in the adult TREK-$1^{-/-}$ mice (131). It also remains to be established whether the functionally altered performance of the nervous system (without easily detectable morphological changes) in adult TREK-$1^{-/-}$ mice (e.g., resistance to depression, see below) is related to the absence of a temporary conditioning effect of TREK-1 during the important time frame of development (3). A reassuring answer to these questions awaits the availability of experimental models, in which the channel(s), possibly substituting TREK-1 function, are also absent. Alternatively, a conditional knockout might help to distinguish between the defects acquired during development in response to the continuous deficiency of the channel and the impairment caused by the elimination of TREK-1 function at a given time.

2. *Neuroprotection by PUFA*

PUFA, AA, docosahexaenoic acid, and linoleic acids have long been known to be beneficial in ischemia-induced neuronal degeneration (26). They also exerted an anticonvulsant effect in animal model experiments (26, 349) and reduced the epileptiform activity evoked in cell culture (327). PUFA were shown to inhibit voltage-dependent sodium and calcium currents and directly interfere with glutamatergic neurotransmission (104, 341). The consequent synaptic depression has been considered as a major factor in their neuroprotective effect. Members of

the TREK/TRAAK subfamily emerged as further potential candidates for neuroprotection, regarding their generally high level expression and characteristic activation by AA and other PUFA (100, 185, 194). Activation of these background potassium channels hyperpolarizes the neuronal plasma membrane and thus reduces excitability.

Linoleic acid dramatically improved the survival of hippocampal neurons after cerebral ischemia and reduced seizures and cytotoxicity induced by kainic acid (185). PUFA were also protective in granule cell culture in vitro, when glutamatergic synaptic activity was stimulated to a harmful level causing cell death. Linoleic acid, docosahexaenoic acid, and AA hyperpolarized these cells by increasing a potassium efflux insensitive to classical K^+ channel blockers, TEA and 4-AP. It is important from the potential therapeutic point of view that PUFA prevented the excessive electrical activity and reduced cell damage not only if added before the induction of electrical activity but also when administered after triggering the excitatory postsynaptic potential (EPSP) discharges (185). Saturated fatty acids, which do not modify TREK/TRAAK channel activity, failed to reduce neuronal death under identical conditions. The significance of TREK-1 in neuroprotection and its major contribution to the effect of PUFA were confirmed by analyzing the neuronal vulnerability in TREK-$1^{-/-}$ mice. The striatal neurons of these animals had no AA-sensitive potassium conductance, they showed much higher sensitivity to kainate than their wild-type littermates, and the epileptogenic effect of kainate was not influenced by PUFA. Experimental brain ischemia in the region supplied by the carotid artery and ischemia of the spinal cord caused several times higher death rate in TREK-$1^{-/-}$ than in wild-type mice. The surviving TREK-$1^{-/-}$ animals showed paralytic symptoms for several days, while the recovery period of the wild-type animals was shorter (131). Most of the above studies focused on the role of TREK-1 in mediating the beneficial effect of exogenous PUFA. However, during ischemic conditions, multiple factors tend to activate the channel: intracellular acidosis, cell swelling, and the liberated AA or lysophospholipides may all stimulate TREK currents leading to neuroprotection. Beyond the direct effect on neurons, these factors may also influence the local circulation through TREK channels expressed in the vasculature (see sect. III*C6*). Although the relevance of the above conclusions has been questioned by reports which suggested that TREK current is not stimulated under hypoxic conditions (235, 236), the effect of PUFA on TREK was repeatedly corroborated by other studies (35, 44).

Considering that the activation of TREK-1 is beneficial during excitotoxicity and under ischemic conditions, the effect of riluzol, a clinically used neuroprotective drug, was also related to the modulation of this K^+ channel (132, 224). However, riluzol biphasically affects TREK-1. The immediate activation of TREK-1 current is followed by inhibition within minutes. The immediate effect of riluzol was also demonstrated in excised patches, suggesting a direct interaction of the drug with the channel. The second inhibitory phase was indirect and related to the activation of the adenylate cyclase/cAMP/PKA messenger system (85). Therefore, regarding the short-lived initial activating phase, it is unlikely that riluzol causes neuroprotection via TREK-1. Other effects of riluzol on voltage-dependent sodium channels (129) and glutamatergic neurotransmission (107) may well explain the evoked neuroprotection during ischemia.

While the knockout studies underscored the contribution of TREK-1 to physiological and pharmacological neuroprotection, elimination of TRAAK neither increases the vulnerability of the nervous system nor affects the sensitivity of the animals to epileptogenic factors. The absence of protecting effect probably reflects the relatively moderate expression of TRAAK in the typically affected regions of the CNS (131).

3. Silencing of thermal and mechanical nociception

Pseudounipolar sensory neurons, residing in dorsal root ganglia (DRG) and trigeminal ganglia, innervate peripheral tissues with their long axons, and their nerve terminals detect mechanical forces, chemical stimuli, and the ambient temperature. An important function of this system is the detection of excessive, actually or potentially harmful, stimuli, called nociception. Neurons of small and medium-sized cell bodies are engaged in nociception. The immediate pain is mediated by the rapidly conducting peripheral Aδ fibers, whereas slowly conducting C fibers are engaged in the poorly localized slow pain (cf. Ref. 15). Activation of the nocipeptive neural mechanisms is essential (sometimes vital) to evoke the appropriate protective behavior. However, there are conditions when the system is persistently activated or becomes oversensitized. The nociceptive response to normally innocuous stimuli (allodynia) or exaggerated pain response (hyperalgesia) results only in pointless suffering. Therefore, it has been a long-standing desire to understand the regulatory mechanisms of nociception and to control them for alleviating pain.

Thermoreception primarily relies on nonspecific cation channels, which depolarize the cell upon activation leading to more frequent afferent discharge. These channels belong to the TRP family, which has both heat- (TRPV1-4) and cold-activated (TRPM8 and TRPA1) members (cf. Ref. 80). TRPV1, TRPV2, and TRPV4 also function as polymodal sensors; their activity is also influenced by mechanical and osmotic stimuli (cf. Ref. 199). In addition to TRP channels, epithelial sodium channels (ENaC) (318), acid-sensing ion channels (ASIC) and undefined nonspecific mechanosensitive cation channels may contribute to the depolarizing shift of the membrane potential

during nociception. The contribution of these channels to thermal reception and nociception has been supported by the availability of specific agonists, like capsaicin for TRPV1, menthol for TRPM8, and allylisothyocyanate for TRPA1.

The extreme temperature sensitivity of TREK and TRAAK channels has led to the assumption that they are also involved in the thermoreception at peripheral nerve terminals (219). Indeed, abundant expression of TREK-1 (219) and TRAAK (227) was detected in DRG . A detailed analysis revealed that TREK-1 mRNA was expressed in a large percentage of both the capsaicin-sensitive (TRPV1+) and -insensitive (TRPV1−) small-diameter neurons, peptidergic and nonpeptidergic cells. Especially high percentage of the probably C-type, nonpeptidergic isolectin IB4+ neurons showed TREK-1 positivity (4). The results clearly showed that TREK-1 expression is rather broad, and the channel is present in neurons with either C or Aδ fibers. Although such a detailed analysis of the localization of TRAAK (or TREK-2) channels has not been performed, functional studies on wild-type, TREK-1$^{-/-}$, TRAAK$^{-/-}$, and double-knockout animals strongly suggested significant coexpression of TREK-1 and TRAAK in DRG neurons (254).

The ion channels, responsible for the sensitivity of the peripheral receptors to different stimuli, are produced in the cell body, and they reach their final location in the nerve terminal by vesicular transport along the axon (19). These channels may also be present in the plasma membrane of the cell bodies, where they are experimentally more accessible than in the much smaller terminals embedded in the peripheral tissues. Electrophysiological experiments on DRG or trigeminal neuron preparations using pharmacological agents of limited selectivity provided data in favor of (287), but also against (318, 346), the contribution of TREK and TRAAK channels to the temperature-dependent K^+ conductance changes. Recently, however, this apparent controversy was resolved by the application of gene knockout animals. These results suggest an even broader function for these K2P channels in the nociceptive signal processing than originally expected. TREK and TRAAK reduce the efficiency of different activating thermo- (both cold and hot) and mechanosensitive receptive mechanisms.

AA-activated background K^+ currents were found in about half of the DRG neurons (and in almost all of the TRPV1+ ones). These currents were abolished in cells obtained from TREK-1$^{-/-}$ mice (4). The proportion of capsaicin-insensitive DRG neurons that gave a calcium signal to temperature change from 32 to 48°C in culture increased significantly both in TREK-1$^{-/-}$ and in TRAAK$^{-/-}$ animals (254). However, this population was not further increased, when the two channels were deleted simultaneously, suggesting the coexpression of TREK-1 and TRAAK in the same neurons. Interestingly, the TRPV1+ cells became more responsive to the same temperature elevation only when both channels were simultaneously eliminated, also suggesting the combined action of TREK-1 and TRAAK. Similarly, the sensitivity of DRG neurons to cooling from 30 to 10°C was increased only in TREK-1$^{-/-}$/TRAAK$^{-/-}$ double knockouts (mainly in the lower threshold, menthol and allyl-isothiocyanate-insensitive TRPM8−, TRPA1− cell population).

While DRG cell bodies in culture are often regarded as the model of the whole sensory neuron, the mechanisms, determining the sensory transduction in the nerve terminals in vivo may be different. In addition, local nonneuronal elements (e.g., odontoblasts) expressing TREK-1 (216)) may influence the afferent signal generation. Thus comparison of the wild-type, TREK- and/or TRAAK-deficient animals in behavioral studies and the response of their ex vivo skin-nerve preparations provided valuable additional information.

Both TREK-1$^{-/-}$ and TRAAK$^{-/-}$ mice became hypersensitive to moderate thermal pain in the range of 46–50°C (with tail immersion or hot plate test). The higher peripheral sensitivity was also confirmed by direct measurement of C fiber activity of a nerve-skin preparation. The afferent discharge rate of C-fibers in the knockout animals highly exceeded that of the wild type at moderately noxious temperatures below 45°C, and the threshold of heat-induced firing in the knockout was significantly reduced (4, 254). Only the thermal sensitivity to moderate heat was increased; at higher temperatures, the C fiber activation of TREK-1$^{-/-}$ and wild-type animals was not significantly different. Similarly to the thermal pain, the sensitivity of both TREK-1$^{-/-}$ and TRAAK$^{-/-}$ animals to moderate nociceptive mechanical stimuli increased, but there was no difference between the response of the knockout and wild-type animals during stronger noxious mechanical stimulation (4, 254). In contrast, the cold-sensitive afferent C fiber activity was shifted to higher temperatures only in the double-knockout animals, similarly to the threshold of the evoked cold-sensitive behavior (254). Thus the concerted hyperpolarizing effect of TREK-1 and TRAAK is necessary to reduce the efficiency of the cold-sensitive TRP (TRPM8, TRPA1) and other activating mechanisms in the peripheral cold receptors.

On the basis of these results, a general contribution of TREK-1 and TRAAK channels to nociception can be proposed: they may function as silencers or brakes of various activating sensory mechanisms, particularly in the moderate range of the stimulus. Thereby their presence allows more graded response in a wider range and helps distinction of innocuous and noxious conditions (4, 254). From the pathophysiological and therapeutical point of view, it is important that TREK-1 and TRAAK also function in inflammatory and chronic pain conditions, suggesting that they may be considered as potential therapeutic targets (254).

Osmotic nociceptive stimuli also increase C fiber discharge and cause pain, predominantly via TRPV4 activation. The effect is robustly potentiated by the inflammatory mediator prostaglandin E_2 (PGE_2). The response to osmotic stimuli was significantly blunted in TREK-$1^{-/-}$ mice, suggesting that the K2P potassium channel acts synergistically with the TRPV4-mediated mechanism in this type of pain sensation. This result is surprising and is in sharp contrast to the above discussed role of TREK-1 in noxious thermo- and mechanoreception. TREK-1 K^+ current would also be expected to alleviate the depolarization induced by TRPV4; however, it seems that TREK-1 somehow enhances the effect of the nonspecific cation channel. Further studies are needed to establish the mechanism of interaction between the two channels in noxious osmoreception (4).

Cold-sensitive neurons are also present in the central thermoregulatory area in the anterior and preoptic hypothalamus. They command heat balance and respond to cooling by enhanced action potential firing. The presence of TREK-1 in this region led to the assumption that this background K^+ channel might be a central temperature sensor. Although the thermoregulation in the TREK-$1^{-/-}$ knockout mice was unaltered (131), it will be interesting to see whether the central cold receptors are similarly affected by the simultaneous deletion of TREK and TRAAK as the peripheral ones.

4. Mechanoelectrical feedback in the heart

The resting membrane potential of atrial and ventricular cardiomyocytes is maintained between −70 and −90 mV, primarily by the high K^+ conductance of the sarcolemma. Inward rectifiers Kir2.1, Kir3.1, Kir3.4, and under ischemic conditions Kir6.2-SUR2A provide the high resting conductance. Different K_{2P} channels are also expressed in cardiomyocytes and may function not only under resting conditions but also during the action potential. Expression of several members of the K_{2P} channel family (TWIK-1, TWIK-2, TASK-1, TASK-2, TASK-3, TREK-1, TREK-2, TRAAK, and KCNK6) has been demonstrated at the mRNA level in rat heart (209), and the functional significance of TREK-1 and TASK-1 has also been proposed.

In the adult rat, strong expression of TREK-1 has been found both in atrial (313) and ventricular (1, 209, 313, 340) cardiomyocytes. Whereas the functional expression of TREK-1 in the ventricular myocardium of adult rat is unequivocal, it must also be mentioned that the level of TREK-1 expression depends on species, age, and location of the examined myocardial tissue. For example, in the human organ (313), the quantity of TREK-1 mRNA was found to be relatively low. In contrast, in 11-day-old chicken embryos, the resting membrane potential of atrial cells was determined primarily by TREK currents, but inwardly rectifying K^+ channels dominated in the ventricular cardiomyocytes, and this difference correlated well with the expression levels of TREK-1 and TREK-2 mRNAs (356).

In the rat, age-related differences were also observed; the expression was sparse in the embryonic heart, compared with the adult tissue (209). In addition, the channel was unevenly distributed across the wall of left ventricle. Stronger TREK-1 mRNA expression was found in the subendocardial than in the subepicardial region, in good correlation with the larger subendocardial chloroform-activated K^+ current (311). Subcellular immunolocalization of TREK-1 revealed that the protein was arranged in longitudinal stripes along the cell surface of cardiomyocytes (340). The mechanosensitive regulation of TREK-1 in the beating heart, by the rhythmically changing level of actual stretch at different locations, attracted particular attention, especially in the light of the known effect of mechanical forces on the electrical activity, known as mechanoelectrical feedback. Longitudinal stretch tends to depolarize cardiomyocytes via stress-activated nonspecific cation channels of the TRP family (351), while activation of the volume-sensitive Cl^- current (134) and the mechanosensitive K^+ current is expected to buffer the depolarizing effect. The degree of cardiomyocyte stretch varies significantly, depending on the location and the orientation of the muscle fiber. The pressure fluctuations are less pronounced in the subepicardial region, and it has been proposed that the transmural gene expression pattern of TREK-1 might be influenced by mechanical factors in the ventricular wall (311). This may provide heterogeneous sensitivity to the varying strain and contribute to the different responses to pressure/volume changes of the subepicardial and subendocardial fibers, also reflected in the differential mechanical modulation of diastolic depolarization, action potential duration, and refractory periods (154).

Background K^+ currents of cardiomyocytes share several characteristics of TREK channels. AA (163, 313), intracellular acidosis (1), mechanical stretch/negative pressure (340), and volatile anesthetics (313) activate these myocyte K^+ currents, whereas EC acidosis moderately inhibits them (1). The AA-sensitive, stretch-activated K^+ current of rat atrial cells was diminished by membrane-permeant cAMP analogs and also by the β-adrenergic agonist isoproterenol, suggesting that TREK channels are phosphorylated by PKA in response to β-adrenergic stimulation and are presumably involved in the generation of positive inotropic effect (313).

It has been suggested that TREK-1 activation has functional significance during myocardial ischemia (1) (similarly to the well-known protective role of the activation of K_{ATP} channels). Under ischemic conditions, purinergic agonists are liberated, and extracellular ATP was shown to indirectly stimulate TREK-1 via AA released by

PLA_2 in response to the activation of p38 and p42/44 MAPK pathways (1). Intracellular acidosis is another factor that may activate TREK-1 during ischemia. Since a growing body of evidence indicates that PUFA are not only neuroprotective but also reduce myocardial infarct size and arrhythmias (342), the role of TREK channels may also be considered to mediate the cardioprotective effect of PUFA.

5. *Adaptive relaxation of visceral hollow organs*

The volume and diameter in the gastrointestinal system can change dramatically. Stretch of the smooth muscle cells in the stomach and intestine directly stimulates mechanosensitive ion channels. The activation of nonselective cation channels as well as Ca^{2+}- and swelling-dependent chloride channels leads to depolarization and contraction. However, there are well-defined, functionally distinct areas of the gastrointestinal tract, where the response to distension is reversed. A significant amount of chyme can be stored temporarily before forwarding at these sites. At these locations, the activation of mechanosensitive K^+ channels of the smooth muscle cells may provide a hyperpolarizing outward current and allow adaptation to the increased luminar content by relaxation and increased compliance. Stretch-activated background K^+ channels in murine colonic myocytes were activated by nitric oxide donors (174, 265). Subsequently, the channels responsible for the hyperpolarizing current were identified: TREK-1 in gastrointestinal, bladder, and uterine smooth muscles and TREK-2 in the gastric antrum. TRAAK was not present in these locations (173). The mechanosensitive K^+ channels were activated by negative pressure, applied to the cell-attached patch pipette, and also by the elongation of the smooth muscle cell with two attached microelectrodes (mimicking the extension of colon; see Fig. 5) (296).

The urinary bladder also accommodates a relatively large volume without significantly increasing the luminar pressure. When human or rat bladder myocytes were treated with the bladder relaxant BL-1249, the compound activated a leak K^+ current with pharmacological properties of the TREK channels (314). Relatively high expression of TREK-1 was also demonstrated in human bladder cells versus aortic myocytes, in which BL-1249 failed to cause relaxation (314). The functional significance of TREK-1 in urinary bladder myocytes was further supported by pharmacological profiling of the background K^+ current (10).

Nitric oxide (NO), liberated either from endothelial cells or from nerve terminals of the visceral organs, diffuses to the nearby smooth muscle cells and activates guanylate cyclase. Carbon monoxide, also activating soluble guanylate cyclase, is also considered as a transmitter in the enteric nervous system. Thus cGMP-mediated activation of TREK-1 and the concomitant hyperpolarization contribute to the relaxation of visceral smooth muscle cells (72, 173, 174).

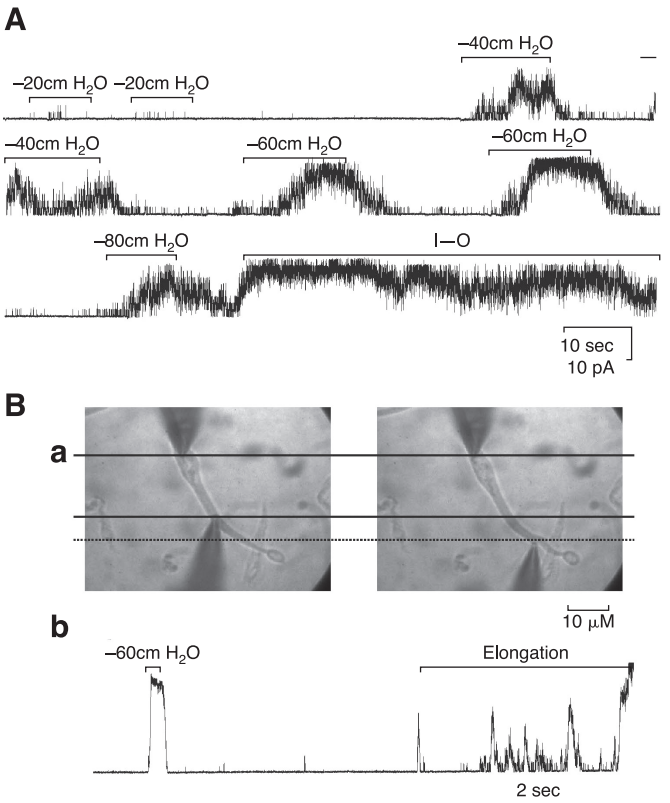

FIG. 5. TREK-1 contributes to adaptive relaxation of hollow organs. *A*: effect of negative pressure (from −20 to −80 mmHg) and patch excision [formation of inside-out vesicle (I-O)] on the activity of TREK-like K^+ channel in murine colonic myocytes. *B*: elongation of a colonic myocyte with two patch pipettes sealed to the same cell (*a*); stretch-dependent current is activated by negative pressure applied to the patch pipette and also by elongation of the cell (*b*). [From Sanders and Koh (296), with permission from Wiley-Blackwell.]

6. *Cerebrovascular and mesenteric vasodilation by PUFA and acetylcholine*

AA regulates the vascular tone in different regions of the systemic circulation. In some vessels the effect mainly depends on the conversion of AA to cyclooxygenase or lipoxygenase products. At selected locations, including cerebral circulation, AA directly induces vasodilation by activating potassium channels in vascular smooth muscle cells (VSMC). At these sites, other polyunsaturated (but not the saturated) fatty acids often act similarly to AA. It has been known for a long while that PUFA increase the blood supply to the brain (in addition to their direct neuroprotective effect). Thus PUFA have been used therapeutically during or even after the occlusion of cerebrovascular blood flow.

AA and other PUFA dilated middle cerebral artery of the rat by an endothelium-independent mechanism. PUFA

activated a leak K^+ current and robustly hyperpolarized VSMCs. The mRNA of several AA-activated K_{2P} channels has been found in the whole vessel, while in isolated cerebral artery VSMCs, only TWIK-2 mRNA and immunoreactivity were detected. Therefore, the vasodilator effect of AA was originally attributed to TWIK-2 (34), although this channel is only moderately influenced by AA, compared with the members of TREK subfamily (270).

Further studies revealed significant expression of TREK-1 both in the smooth muscle and endothelial layer of the basilar artery and highlighted its importance in the adjustment of the vessel tone (Fig. 6). Linoleic acid induced robust vasodilation in basilar artery preparations, but the response was absent when the vessels were isolated from TREK-$1^{-/-}$ animals (25). Accordingly, in the knockout mice, linoleic acid failed to increase cerebral blood flow in the basilar artery region (25). These results implicate that during an ischemic attack TREK channels mediate the beneficial effect of PUFA, not only by hyperpolarizing and thus reducing the vulnerability of neurons, but also by promoting the circulation in or nearby the affected region (25). The vascular reaction to acetylcholine was also impaired in TREK-$1^{-/-}$ mice, indicating the importance of TREK-1 in the process of endothelium-dependent vasodilatation (25). However, these mechanisms are not general in all regions of the cerebral circulation. TREK-1 expression in the carotid artery was negligible, and accordingly, the tone of this vessel was only marginally affected by PUFA (25).

At the same time, TREK-1 expression is not restricted to the vasculature of the brain. The channel was also detected in mesenteric arteries (110, 111). In these vessels of TREK-$1^{-/-}$ mice, the myogenic vasoconstriction (in response to elevated intravascular pressure) and the effect of adrenergic stimulation, which directly activates VSMCs, were maintained. Furthermore, the endothelium-related flow-dependent vasodilation was also preserved. However, vascular responses to acetylcholine and bradykinin, which are mediated by endothelial receptors, were diminished (Fig. 6.) (111).

Cutaneous microvessels dilate in response to local pressure, thereby defending the skin from ischemia. The vascular reaction depends on endothelial function and relies on the formation of NO. TREK-1 is also expressed in these vessels, predominantly in the endothelial layer. Its functional significance is underlined by the observation that the vasodilation, induced by local pressure, was substantially decreased in TREK-$1^{-/-}$ animals (Fig. 6.) (111).

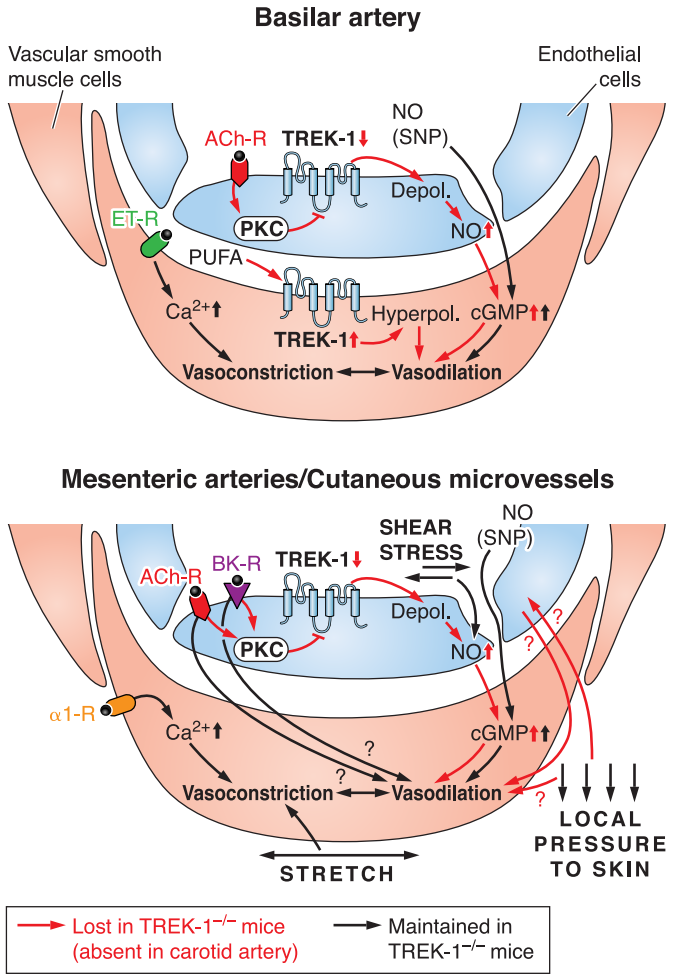

FIG. 6. Mechanistic model of TREK-1 regulation in the systemic circulation. *A*: TREK-1 is expressed in both the endothelial and the smooth muscle (VSMC) layer of the basilar artery. PUFA hyperpolarize and promote vascular relaxation by activating TREK-1 in the VSMC. In endothelial cells, acetylcholine binds to and activates muscarinic receptors, and TREK-1 is inhibited by PKC phosphorylation. In response to the following depolarization, NO is generated, and it diffuses to the neighboring VSMCs and relaxes them. These effects are lost in basilar arteries of TREK-$1^{-/-}$ animals and are also absent in the carotid artery, in which no TREK expression was detected. Vasoconstriction evoked by endothelin and the vasodilatory effect of the nitric oxide donor sodium nitroprusside (SNP) are independent from TREK-1. *B*: in the case of mesenteric arteries, the relaxing effect of endothelial G_q-coupled (muscarinic and bradykinin) receptors was significantly reduced (but was not abolished completely) in TREK-$1^{-/-}$ animals. On the other hand, vasodilation in response to endothelial shear stress and vasoconstriction evoked by distension of the vessel wall were preserved similarly to the response to SNP and α_1-adrenergic receptor stimulation. The vasodilatory response of skin microvessels, induced by local pressure applied to the skin, was also TREK-1 dependent (see more details in Refs. 25 and 111).

7. *Regulation of aldosterone and cortisol secretion in the adrenal gland*

Zona glomerulosa, fasciculata, and reticularis of the adrenal cortex produce mineralocorticoids, glucocorticods, and androgen hormones, respectively. Inhibition of K^+ channels and the subsequent activation of voltage-gated Ca^{2+} channels by depolarization is one of the important mechanisms by which hormone production is regulated in these cell types (305). A noninactivating, ACTH- and angiotensin II-sensitive potassium current of bovine fasciculata cells (IAC) was already described in

1993 (237), and considered to be the major determinant of the resting membrane potential. Subsequent characterization of the channel showed several features of TREK-1 (89, 92). IAC was also inhibited by ACTH (and by a cell-permeable cAMP analog) in fasciculata (91) and by angiotensin II in glomerulosa cells (88). [Interestingly, as a long-term effect, cAMP also increased the expression of IAC (87).] On the basis of the above data, IAC was convincingly assigned to TREK-1, even though the native current also showed some important differences compared with heterologously expressed TREK-1. IAC was activated by intracellular ATP and also by its nonhydrolyzable analog 5′-adenylylimidodiphosphate (AMP-PNP) in the millimolar range (90, 92). Considering the similarities between IAC and TREK-1, it has been suggested that the regulation by ATP is the consequence of an ATP-binding auxiliary protein, which is not present in the heterologous systems and is influenced by the metabolic state of adrenocortical cells (92). Another unusual observation was the mechanism of inhibition of the native TREK-1-like channel by the G_q-coupled angiotensin receptor, which was mediated by signaling pathway(s) bypassing PLC (207).

While TREK-1 is responsible for the majority of the background potassium current in bovine fasciculata and glomerulosa cells (88), it is important to emphasize the existing species differences. TASK-3 channels dominate the potassium conductance in the rat adrenal glomerulosa (64), whereas both TASK-3 and TREK-1 expression were reported in a human glomerulosa-like adrenocortical cell line, H295R (31).

8. General anesthesia

Ligand-gated ion channels, primarily $GABA_A$ receptors, have been regarded as the major targets of general anesthetics (103). The discovery that volatile anesthetics activate different K_{2P} channels, leading to hyperpolarization and decreased excitability, shed light to another mode of action of these compounds. TREK-1 and TREK-2 are robustly activated by a high variety of anesthetics including chloroform, diethyl ether, halothane, and isoflurane (268). The efficiency of the anesthetics shows only minor variation between the two closely related channels (194). TASK-1 is activated only by halothane and isoflurane, while TRAAK is entirely resistant to these anesthetics (268). Because of the localization of TREK-1 in the CNS, and its high sensitivity to clinically relevant concentrations of the volatile anesthetics, it has been proposed that TREK-1 is the best candidate to have an important role in anesthesia (268). In support of this assumption, further anesthetics, which do not influence $GABA_A$ receptors, chloral hydrate (127), N_2O, xenon, and cyclopropane (121) were also found to activate TREK-1, but not TASK-1. Even more convincing evidence for the involvement of TREK-1 in the anesthetic action was provided by experiments on a knockout model. In TREK-1-deficient animals, the anesthetic efficiency of chloroform, halothane, sevoflurane, and desoflurane was significantly reduced; their anesthetic action developed with delay, and the minimum alveolar concentration (MAC), which is required to suppress motor reactions to painful stimuli, was increased (131). The reduced anesthetic sensitivity was not the simple consequence of general hyperexcitability, since the efficiency of pentobarbital, a drug which acts via $GABA_A$ receptors but does not influence K_{2P} channels, was identical in the wild-type and TREK-$1^{-/-}$ mice (131).

Volatile anesthetics modulate synaptic transmission both on the pre- and postsynaptic side. Immunohistochemical studies detected TREK-1 presynaptically, colocalized with synapsin. Therefore, the role of this channel in the presynaptic effects of anesthetics has been anticipated (185). Clinically relevant concentrations of isoflurane, enflurane, and halothane inhibited the release of glutamate from excitatory nerve terminals (and also from cerebrocortical synaptosomes), while the release of the inhibitory neurotransmitter GABA was not influenced or even increased (333). In the synaptosomes prepared from TREK-$1^{-/-}$ mice, the sensitivity of transmitter release to halothane was reduced in accordance with the increased MAC of the anesthetic (334), indicating the functional significance of TREK-1 in the presynaptic modulation.

9. Depression and selective serotonin reuptake inhibitors

Impaired function of the serotonergic system plays a major role in the development of affective disorders. The most widely used and popular medical treatment of depression is based on drugs (selective serotonin reuptake inhibitors, SSRI), which selectively inhibit serotonin reuptake and thus augment serotonergic transmission in the brain. Selectivity of these drugs on the serotonin transport is relative; many of them have additional pharmacological targets contributing to the therapeutic efficiency. Several clinically used SSRI, fluoxetine, norfluoxetine, paroxetine (133, 157, 317) and sipatrigin (321), were found to inhibit TREK-1 and TREK-2 (but not TRAAK) current. TREK-1 is abundantly expressed in the cortical and subcortical brain regions (e.g., in the prefrontal cortex, hippocampus, striatum, and amygdala), which have been related to the cognitive and emotional dysfunctions in depression. Therefore, the role of this K_{2P} channel in the susceptibility to the behavioral disturbance has been addressed using TREK-$1^{-/-}$ mice. In five different experimental models testing depression-like behavior, TREK-1 knockout mice proved to be resistant to depression (133). For example, the period of transient immobility after placing the animal into a tank of water, representing a "behavioral despair," was substantially shortened by the

genetic elimination of TREK-1. TRAAK$^{-/-}$ mice performed identically to the wild type in these tests.

Interestingly, TREK-1$^{-/-}$ mice behaved similarly to the wild-type animals pretreated with SSRI drugs, and the acute or chronic administration of SSRI compounds to TREK-1$^{-/-}$ mice did not improve their test results further. This suggested a higher serotonergic tone in the knockout animals. Indeed, the serotonergic neurotransmission of the structures associated with affective and memory disturbances in depression (dorsal raphe nuclei and CA3 pyramidal neurons of the dorsal hippocampus) was found to be enhanced in TREK-1$^{-/-}$ mice (133). Accordingly, it has been proposed that the clinical usefulness of SSRI antidepressants is complemented by the inhibition of TREK-1 channels (133, 317). This suggests that the blockers of this background K^+ channel are of considerable therapeutic interest for the future management of psychiatric diseases (223, 224, 317). TREK-1 and TREK-2 (but not TRAAK) channels are also inhibited by several neuroleptic drugs, such as chlorpromazine (269), fluphenazine, haloperidol, and penfluridol (317). Further studies are needed to evaluate the significance of this effect in the therapeutic potential of neuroleptics.

10. Proliferation of prostate cancer

While epithelial or stromal cells of normal prostate tissue or benign adenomas do not express detectable TREK-1 immunoreactivity, a high level of expression was detected in prostate cancer samples and malignant cell lines (326). The subcellular distribution of TREK-1 was surprising; the nuclear region of the cells showed the highest labeling with the antibody. The overexpression positively correlated with the stage of the disease; invasive prostatic carcinomas expressed the channel in high proportion of the cancer cells. TREK-1 expression was also verified functionally. In the prostate carcinoma PC3 and LNCaP cell lines, an outwardly rectifying K^+ current was detected, which was absent in normal prostatic epithelial cells. This current was sensitive to the TREK-1 inhibitor sipatrigin and could also be neutralized by the overexpression of a dominant negative mutant of TREK-1 in these cells. The causal link between channel expression and abnormal cell proliferation was indicated by the experiments, in which the proliferation of isolated cancer cells was inhibited by sipatrigin treatment or the transfection of the dominant negative TREK-1 construct. In addition, overexpression of TREK-1 in normal prostate epithelial cells or in CHO cells increased the proliferation rate (326). Based on these observations, functionally active TREK-1 was suggested to be a significant factor and a potential therapeutic target in prostate cancer. According to an interesting recent observation, curcumin, an agent inducing apoptosis of prostate cancer cells (82), efficiently inhibits TREK-1 (89), possibly contributing to its antitumor action.

IV. TASK (TWIK-RELATED ACID-SENSITIVE K^+ CHANNEL)

The third mammalian K_{2P} channel, cloned from human kidney, showed extreme sensitivity to variations of extracellular pH in the physiological range (84). Therefore, the name TASK (TWIK-related acid-sensitive K^+ channel) was given to the channel, and later extended to TASK-1 (KCNK3 or $K_{2P}3$ in the HUGO nomenclature), when further members of the subfamily were discovered. Two other channels, TASK-3 (KCNK9, $K_{2P}9$) and TASK-5 (KCNK15, $K_{2P}15$), belong to this subfamily. TASK-3 is the closest structural relative of TASK-1; it is also inhibited by EC acidification and several regulatory factors influence the activity of the two channels in the same direction (Fig. 7). TASK-1 and TASK-3 are also closely related at the molecular level. These are the only subunits that have been reported to form functional heterodimers in the K_{2P} channel family. A unique feature of TASK-3 among the K_{2P} channels is that its gene, located on chromosome 8, is genetically imprinted; it is exclusively expressed from the maternal allele (215). A dominant negative mutation of TASK-3 (KCNK9) gene was implicated in the maternally inherited disease with mental retardation and characteristic dysmorphism (13). In contrast to TASK-1 and TASK-3 channels, TASK-5 cannot be functionally expressed, although its mRNA is abundantly expressed in several tissues. In the absence of functional data, the categorization of TASK-5 into the TASK subfamily was based primarily on structural similarity. Two other channels, TASK-2 and TASK-4, do not belong to the TASK subfamily. They show low amino acid sequence similarity to TASK-1 and are sensitive to pH in the alkaline range. Therefore, TASK-2 and TASK-4 (also called TALK-2) are classified in the TALK subfamily of alkaline pH-sensitive K_{2P} channels.

A. Biophysical Properties and the Molecular Mechanisms of Acid Sensitivity

Heterologous expression of TASK-1 in *Xenopus* oocytes or mammalian cell lines resulted in an instantaneously activating and noninactivating K^+ current (84). The current-voltage relationship of the macroscopic current was described well by the GHK equation. Rectification mainly reflected the different driving forces in asymmetric K^+ concentrations; thus the channel approximated the criteria for a voltage- and time-independent leak conductance. However, at low external [K^+], a significant deviation from this ideal relationship has already been described in the first study. Elevation of EC [K^+] increased not only the amplitude of the macroscopic inward

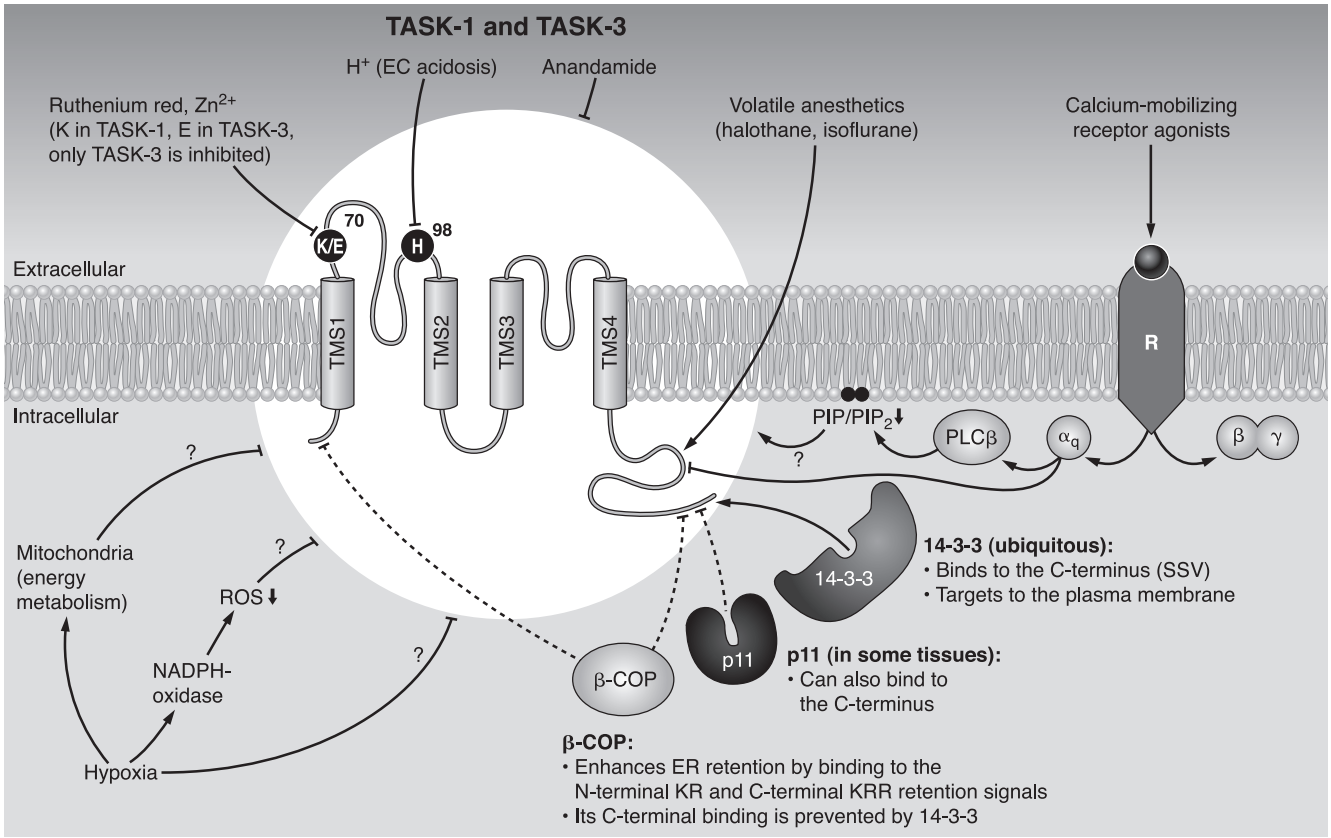

FIG. 7. Regulation of TASK-1 and TASK-3. The channels are inhibited by EC acidification as a result of protonation of H-98 in the first extracellular loop. Anandamide inhibits both TASK-1 and TASK-3 (with moderate species differences). G_q-coupled receptor activation reduces TASK currents; the effect is mediated by liberation of $G_q\alpha$, which binds directly to and inhibits the channels. Depletion of the plasma membrane polyphosphoinositide pools may complement the inhibitory effect. Hypoxia inhibits TASK current indirectly, and only in selected cell types; the effect is mediated by multiple signal transduction pathways, which may be different and characteristic for the particular tissue. TASK channels are activated by halothane and isoflurane, but (unlike TREK channels) they are not influenced by chloroform or ether. The polycation ruthenium red and Zn^{2+} allow pharmacological distinction between the two closely related channel subunits. The structural background of the differential sensitivity to inhibitory cations is a single glutamate residue in the first extracellular loop. Interaction of TASK channels with partner proteins, 14-3-3, β-COP, and p11, influence channel targeting to the plasma membrane. Dashed lines represent effects on targeting.

current but also the outward current (with $[K^+]_{0.5}$ ~2 mM) (84), indicating that in addition to being a charge carrier, K^+ activated TASK-1. The P_o of TASK channels is typically low ($P_o < 0.1$), and it is highly sensitive to low EC $[K^+]$. Thus it has been speculated that the anomalous K^+ dependence may be caused by the stabilizing effect of K^+ on the open pore structure (252). At the single-channel level, TASK-1 current shows brief openings (~1 ms) and 14–16 pS unitary conductance in symmetrical 150 mM $[K^+]$ (148, 164, 188). Single-channel current could be measured in cell-attached configuration (164) as well as in inside-out patches, although rapid rundown of the current was usually observed after patch excision (169, 172, 212).

Extracellular acidification inhibits TASK-1 with a p*K* value of 7.3 and a Hill coefficient of 1.6, whereas intracellular pH changes do not affect channel activity (84). The inhibition is voltage independent, suggesting that the proton sensor is located outside the transmembrane electric field (84). Elevation of EC $[K^+]$ reduces pH sensitivity, and this may also contribute to the apparent activating effect of potassium (210, 241). Mutational analysis of TASK-1 revealed that pH sensitivity was conferred primarily by the protonation of H98, but the smaller contribution of two other amino acid residues, H72 and K210 (all located on the extracellular loops), was also demonstrated (241).

TASK-3 was first cloned from rat cerebellum and was found to share 55–60% sequence identity with TASK-1 in different species (170, 286). The transmembrane segments, the pore regions, and the extracellular loops are highly conserved between the two channels, while the COOH termini show less similarity. Heterologous expression of TASK-3 resulted in a K^+ current, initially characterized as time independent and noninactivating (170). However, more detailed analysis indicated that a fraction of guinea pig TASK-3 current was not instantaneous (286), and depolarization from −80 to at least −20 mV also induced a small time-dependent current component of

human TASK-3 with a time constant of 10 ms (226). The deactivation of the current was even faster and hard to resolve (226). In accordance with this voltage-dependent component of the macroscopic current, the P_o of TASK-3 was also found to be higher at more positive potentials (286). In inside-out patches, the unitary *I-V* relationship of TASK-3 showed weak inward rectification in symmetrical 140 mM [K^+] and 2 mM EC [Mg^{2+}]; the single-channel conductance was 27 pS at −60 mV and 17 pS at +60 mV (170). When divalent cations were omitted from the EC side, the inward rectification (and the unitary conductance at negative potentials) became even more pronounced (286). The inward rectification of unitary current and the voltage dependence influence the curvature of macroscopic *I-V* relationship in opposite directions, with a net result of slight outward rectification in symmetrical [K^+] at the whole cell level (286).

TASK-3 is less sensitive to acidification than TASK-1. The channel is maximally active at pH 7.4 and is inhibited with a p*K* value of 6.7 and a Hill coefficient of 1.8–2 (170). Similarly to TASK-1, a single amino acid residue, histidine 98, primarily determines the pH sensitivity of TASK-3 (170, 286).

Heteromeric subunit assembly greatly increases the diversity of voltage-dependent and inwardly rectifying potassium channels; however, only TASK-1 and TASK-3 have been shown to form functional heterodimers in the K_{2P} channel family (63). Homodimeric TASK-1 and TASK-3 channels have distinct biophysical, regulatory, and pharmacological characteristics, and the heterodimer disproportionally inherits the properties of the parent subunits (63). In some respects, the TASK-1/TASK-3 heteromer is similar to TASK-1 homodimer. The polycationic dye ruthenium red and Zn^{2+} exclusively inhibit TASK-3 homodimer, whereas the heterodimer and the TASK-1 homodimer are not affected by them (57, 58, 65, 248). In other respects, the heterodimer is indistinguishable from the TASK-3 homodimer. The single-channel conductance of the heterodimer equals that of the TASK-3 homodimer in the presence of EC Mg^{2+} (i.e., about twice as high as the conductance of homodimeric TASK-1) (148, 162). Some properties of the heterodimer can be intermediate between the homodimers of the parent subunits, e.g., this is the case with the pH sensitivity (63) and the single-channel conductance in the absence of EC Mg^{2+} (162).

In native tissues, TASK-1/TASK-3 heterodimer is assembled as efficiently as the homodimeric channels, if the ratio of expression of the two subunits is appropriate. TASK-1/TASK-3 heterodimers were reported to be responsible for 44% of the "standing outward" current in cerebellar granule neurons (148), 52% of the background K^+ current in motoneurons (21, 184), and 75% of the pH-sensitive background K^+ current in rat carotid body glomus cells (162). Heteromers were also detected in dorsal lateral geniculate thalamocortical relay neurons (228) and in hippocampal CA1 pyramidal neurons (319). Heteromerization of the two TASK subunits provides high differential pH sensitivity around an intermediate p*K* value (between the p*K* values of the homodimers).

TASK-5 cDNA has been cloned on the basis of its sequence homology to TASK-3 (165, 325). In addition to the overall sequence identity (51%), TASK-5 also has a histidine located immediately downstream of the GYG signature sequence of the first pore domain. The position of this residue corresponds to histidine 98, ensuring pH sensitivity of TASK-1 and TASK-3 channels. However, the sensitivity of TASK-5 to acidification could never be examined, as the channel did not induce current either in oocytes or in mammalian expression systems. Replacement of the COOH terminus of TASK-5 with that of TASK-3 also failed to result in functional expression (165), although the channel was shown to reach the plasma membrane (7). In another study, impaired targeting of the channel was reported (153); however, deletion of a putative NH_2-terminal ER retention signal did not help the expression of TASK-5 current (7). TASK-5 is expressed abundantly in adrenocortical cells (165) and in the central auditory system (153), where TASK-1 and/or TASK-3 are also present. However, the idea that TASK-5 would influence the activity of its close structural relatives could not be verified (7, 153). Furthermore, a polymorphism of the human TASK-5 gene, which was expected to disrupt the K^+ channel function (153, 165), had no phenotypic consequence even in homozygous form (153). Accordingly, the function of this silent K_{2P} channel remains to be established.

B. Regulation by Receptors, Endocannabinoids, and Interacting Proteins

1. *Inhibition by G_q protein-coupled receptors*

Native TASK-like currents were unequivocally inhibited by the stimulation of G_q-coupled receptors in different tissues: in adrenortical glomerulosa cells by angiotensin (68) and in hypoglossal motoneurons by TRH, serotonin, and metabotropic glutamate receptors (309). These observations were also extended to cerebellar granule (30, 48), brain stem respiratory (18), and thalamocortical neurons (230). The inhibition by angiotensin II (68), acetylcholine (234), as well as TRH and serotonin (309) was reproduced by coexpressing TASK-1 with the respective receptor in different heterologous systems, indicating that G_q inhibits TASK-1 in general. TASK-3 homodimers were less inhibited by the stimulation of AT_1 angiotensin receptor in *Xenopus* oocytes than TASK-1 homodimers, and the TASK-1/TASK-3 heterodimeric channel showed intermediate inhibition, closer to TASK-1 than to TASK-3 (63). After the discovery of TASK-3, the source of the pH-sensitive background K^+ current in different native tis-

sues has been reevaluated, but the regulation by G_q protein was confirmed irrespectively of the found subunit composition of TASK channels (21, 64, 141, 148).

Different hypotheses were proposed on the mechanism of TASK inhibition; however, it was generally accepted that dissociation of $G_q\alpha$ from $\beta\gamma$-subunit was required for the receptor-mediated regulation (48, 69). Major effectors of $G_q\alpha$, inositol 1,4,5-trisphosphate (IP_3), and the elevated cytoplasmic [Ca^{2+}], were not responsible for the regulation (48, 69). Robust pharmacological activation of PKC by the phorbol ester PMA inhibited human (324, 325) and rat (324) TASK-3. However, the receptor-mediated inhibition was not influenced by pharmacological inhibition of PKC (48). Furthermore, a TASK-3 mutant, lacking all the PKC phosphorylation consensus sites, was inhibited as efficiently as the wild-type channel by muscarinic (M3) receptor agonists (324). PMA did not affect TASK-1 activity, and PKC inhibitors also failed to influence the receptor-mediated inhibition (48, 69, 84, 188). A pH-sensitive TASK-like potassium current in rat ventricular cardiomyocytes was reduced by platelet activating factor; the effect was attributed to PKC-ε (12, 22); however, this inhibition was marginal, compared with the robust regulation by most G_q-coupled receptors. Thus PKC cannot be the major mediator of TASK inhibition.

$G_q\alpha$ activates PLC-β, which breaks down PIP_2 in the plasma membrane. As polyphosphoinositides are known to modify the function of several membrane proteins, including potassium channels (292, 355), their depletion was suspected to result also in TASK inhibition (69). In excised patches, the rundown of TASK-1 and TASK-3 currents was attributed to the breakdown of PIP_2 by membrane-associated phosphatases, since the addition of PIP_2 to the intracellular surface of the plasma membrane restored channel activity. This effect was neutralized, with a specific PIP_2 antibody (48, 212), confirming that TASK channels were activated by this polyphosphoinositide in excised patches.

However, the significance of PIP_2 during receptor-mediated inhibition is controversial. The inhibition of TASK-1 and TASK-3 was (48, 69), or was not (30, 308), attenuated in the presence of the PLC inhibitor U-73122. High concentrations of wortmannin, a nonspecific inhibitor of phosphatidylinositol 4-kinase, which prevents the replenishment of the plasma membrane PIP and PIP_2 pools, decelerated the recovery of TASK-1 and TASK-3 currents after the stimulation of angiotensin or glutamate receptor (48, 69, 147). On the basis of these relatively nonspecific pharmacological approaches, it could not be unequivocally decided whether PIP_2 contributed to the receptor-mediated regulation or not.

In a comprehensive study, TASK-1 and TASK-3 channels were identified as direct targets of $G_q\alpha$ (54). A constitutively active form of $G_q\alpha$ associated with TASK-1 or TASK-3 and inhibited the channels, even if a mutated version of the G protein, unable to activate PLC, was used. Overexpression of the phosphoinositide-specific 5-phosphatase IV, which converts PIP_2 to PIP, did not affect TASK current under conditions when other PIP_2-sensitive channels were inhibited. Moreover, the recovery of TASK current after TRH-induced inhibition did not change significantly in the PIP_2-depleted cells (54). These results, which were confirmed independently (324), clearly demonstrated the direct effect of $G_q\alpha$ on TASK channels. They also argued against the significance of the breakdown of PIP_2 in the receptor-mediated regulation. However, it should be recalled that 5-phosphatase (unlike PLC) does not deplete PIP in the plasma membrane (in fact, PIP is formed by the dephosphorylation of PIP_2). If both PIP and PIP_2 modulate TASK channels (similarly to K_{ATP} channels, Ref. 301), then overexpression of 5-phosphatase does not have an equivalent effect to PLC activation. In this case, the inhibition of TASK channels by polyphosphoinositide breakdown during G_q protein-coupled receptor stimulation cannot be excluded.

The receptor-mediated regulation of TASK-1 and TASK-3 depends on the first six amino acids of the COOH-terminal tail (VLRFMT and VLRFLT, respectively). When these amino acids of TASK-1 were replaced with the corresponding residues of TREK-1 (308), the receptor-mediated inhibition was completely lost. Deletion of the VLRFLT motif in TASK-3 had a similar effect. Thus the proximal COOH-terminal tail of TASK channels appears to be as important in the receptor-mediated regulation as the corresponding region of TREK channels in their sensitivity to arachidonic acid and volatile anesthetics.

2. Anandamide and methanandamide: nonspecific TASK inhibitors

Anandamide and some synthetic cannabinoid receptor agonists (WIN552122 and CP55940) were found to be potent inhibitors of human TASK-1. The effect was not mediated by cannabinoid receptors; the receptor antagonist SR141716A did not interfere with the inhibition, and other receptor ligands, the endogenous 2-arachidonoylglycerol and the synthetic receptor agonist (HU210), were ineffective. Thus TASK-1 was suggested to be a direct and possibly physiological target mediating receptor-independent endocannabinoid effects (220). Originally, anandamide was reported to be highly specific for TASK-1 within the K_{2P} family (220). Based on this original report, anandamide and methanandamide were routinely used for the identification of TASK-1 in native tissues, glomus cells (95), smooth muscle cells of the pulmonary artery (123), cardiomyocytes (280), and cerebellar granule neurons (220). However, reexamination disproved the specificity; anandamide and methanandamide were found to inhibit TASK-1 and TASK-3 with comparable potency in different species (2, 21, 323). Thus, in the TASK subfamily, (meth)

anandamide cannot be regarded as a distinctive pharmacological tool (unlike ruthenium red, which inhibited only TASK-3 in all examined species; Refs. 21, 63, 65, 148, 162, 184, 187). The inhibition of both TASK-1 and TASK-3 may contribute to the receptor-independent effects of anandamide. However, it is worth mentioning that similar concentrations of endocannabinoids, which inhibit TASK-1 and TASK-3, modulate several other ion channels, including tetrodotoxin (TTX)-sensitive Na^+ channels (167), the vanilloid receptor (TRPV1; Ref. 357), the T-type Ca^{2+} channel (49), and also Shaker-type voltage-gated K^+ channels (277).

3. Targeting of TASK channels to the plasma membrane

Interaction with auxiliary proteins modifies the targeting of TASK-1 to different locations within the cell. Deletion of the last three amino acids (SSV) of the COOH-terminal tail interfered with forward traffic of the channel to the plasma membrane. It was demonstrated that the SSV motif binds 14-3-3 adaptor proteins, and their phosphorylation-dependent interaction is required to prevent trapping of the channel in the endoplasmic reticulum (ER) (255, 284). Retention of the ΔSSV channel in the ER is also facilitated by partner protein(s). Two endoplasmic retention signals were recognized in TASK-1: one at the NH_2 terminus and the other on the COOH-terminal tail. It was also demonstrated that the channel binds to β-COP (a subunit of coatomer protein complex I, COPI) via the NH_2- and the COOH-terminal basic residues. When either the NH_2- or the COOH-terminal basic motif was mutated, the high-affinity β-COP binding was lost, and the mutant channels reached the surface (256). These mutants produced K^+ current even if their SSV motif was also deleted [i.e., they no longer needed the interaction with 14-3-3 for proper targeting (113, 255, 256, 284, 323)]. In binding experiments, association of the channel with 14-3-3 and β-COP was mutually exclusive, suggesting that 14-3-3 enhanced surface expression of TASK channels by preventing β-COP-mediated ER retention.

Interaction of the annexin II subunit P11 with TASK-1 was first detected in yeast two-hybrid experiments, and the protein was also coimmunoprecipitated with TASK-1 but not with the ΔSSV truncated channel (113). Covalent attachment of P11 to the ΔSSV mutant rescued targeting to the plasma membrane, suggesting that P11 promoted forward traffic (113). Later, P11 was found to associate with TASK-1 only in the presence of 14-3-3 (256), and according to other data, it did not interact with the SSV motif but with a more extended helical structure at the proximal COOH-terminal tail of the channel (288). Since the knockdown of P11 with siRNA promoted trafficking of TASK-1 to the surface, it has been concluded (in contrast to the original P11 study) that the interaction with P11 inhibited plasma membrane targeting (288). Regarding the contradictory results and the apparent complexity of the system, the physiological role of P11 in TASK trafficking is difficult to evaluate at present, although it is generally accepted that P11 is an important interacting partner of the channel.

C. pH-Dependent and Other Functions Mediated by TASK Channels

1. Chemoreception in the carotid body

Carotid and aortic bodies are the primary sensors of hypoxia, metabolic acidosis, and elevation of EC $[K^+]$, all of which stimulate respiration. In type I (glomus) cells of carotid bodies, several ion channels are influenced by both acidosis and hypoxia, leading to depolarization, voltage-dependent calcium influx, and release of transmitters, which increase the discharge of afferent neurons. With respect to K^+ conductance, different calcium-activated K^+ channels were first suggested to be inhibited by the reduction of EC pH (271) and hypoxia (272) and contribute to depolarization and the subsequent Ca^{2+} signal (36, 37). Reduced depolarizing effect of hypoxia was also reported after blocking voltage-gated K^+ channels of the Kv2, Kv3 (274), and Kv4 (275) families. However, the above channels are activated only in stimulated cells (in response to depolarization or elevated $[Ca^{2+}]$). Accordingly, their inhibition may delay repolarization and prolong the hypoxic response, but cannot be responsible for the initial depolarization.

The initial chemosensitive response depends on the alteration of the resting membrane potential, principally determined by an acid-sensitive background K^+ conductance. Expression of several K_{2P} channels has been detected in type I cells, including TASK-1, TASK-2, TASK-3, TREK-1, and TRAAK (38, 347, 348). The pharmacological profile of oxygen-sensitive background K^+ current, together with the strong mRNA expression, suggested that TASK channels played the primary role in sensing acidosis and hypoxia in glomus cells (38). Recently, using pharmacological approach, as well as single-channel current analysis, TASK-1/TASK-3 heterodimers were found to be responsible for the major part of the oxygen-sensitive TASK-like background K^+ conductance (162). The importance of TASK-1 was also supported by the blunted (although not abolished) ventilatory response to hypoxia in TASK-$1^{-/-}$ mice, while the deletion of TASK-3 had no significant effect (320). The hypoxic response of TASK-$1^{-/-}$/TASK-$3^{-/-}$ knockout animals was partially preserved, similarly to that of the TASK-$1^{-/-}$ mice (320), or was not significantly changed compared with wild type in another study (245). This suggests that oxygen-sensitive mechanisms other than TASK also operate in glomus cells

or at least the knocked out channels are substituted for by compensatory changes.

In contrast to acidosis, hypoxia-induced inhibition of TASK channels depends on cellular integrity (38) and the cell type in which the channel is expressed [e.g., it is absent in *Xenopus* oocytes (267), but operates in HEK cells (156, 196)]. Several indirect mechanisms have been proposed by which hypoxia influences the activity of oxygen-sensitive potassium channels. These include altered mitochondrial function and energy metabolism as well as generation of reactive oxygen species by NADPH oxidases and heme proteins (cf. Ref. 181). In glomus cells, mitochondrial regulation seemed to dominate, since different inhibitors of oxidative phosphorylation inhibited the background K^+ current. Furthermore, in the presence of these inhibitors, hypoxia did not have any additional effect (338). One mechanism, by which the impaired energy metabolism of the cell may regulate the background (and also the calcium-activated) K^+ conductance is phosphorylation by the AMPK (94). Inhibition of AMPK prevented the effect of hypoxia, whereas its pharmacological activation induced depolarization and voltage-dependent Ca^{2+} influx (180, 339). However, the AMPK-mediated activation of glomus cells appeared to be independent of TASK channels, as neither TASK-1 nor TASK-3 currents were affected by AMPK in a heterologous expression system. In contrast, TREK-1 is efficiently inhibited by AMPK via the phosphorylation sites also targeted by PKA and/or PKC in the channel (178). These results, also taking into account the knockout data, highlight the complexity of oxygen sensing in the glomus cells.

Local paracrine and efferent mechanisms also modify the activity of chemosensitive cells. Type I chemoreceptors have an autoregulatory negative-feedback circuit; they secrete GABA and express $GABA_B$ receptors. The $GABA_B$ agonist baclofen activated a TASK-1-like K^+ conductance, while GABA antagonists potentiated the hypoxia-induced depolarization in cultured cell clusters, suggesting that this paracrine mechanism had physiological relevance. Reduction of the cAMP level was proposed to mediate the effect GABA via G_i-coupled receptors (95). In accordance with the theory of cAMP-dependent regulation, PACAP, a peptide signaling via G_s protein, inhibited a TASK-like K^+ current in type I cells and induced depolarization and calcium signal. The blunted ventilatory response of $PACAP^{-/-}$ mice to hypercapnia and hypoxia fits well with the contribution of PACAP to the regulation of glomus cells (344). Adenosine, acting via A_{2A} receptors coupled to adenylate cyclase, also inhibited the background K^+ conductance of type I cells. Inhibition of the TASK-like current by adenosine was suggested to induce depolarization and calcium signal and augment the response to hypoxia (345).

2. Detection of hypoxia by neuroepithelial bodies

Neuroepithelial bodies reside in the bronchiolar bifurcation and sense P_{O_2} changes in small airways (155). Hypoxia reduces the K^+ conductance of neuroepithelial cells and releases vasoactive amines (e.g., serotonin), which contribute to the local vasomotor tone in the lung (and the optimization of ventilation-perfusion ratio), and also function as neurotransmitters for the afferent pathways to respiratory centers. In contrast to glomus cells, the primary target of hypoxia (with respect to the regulation of K^+ conductance) is NADPH oxidase in this tissue, while the mitochondrial involvement is negligible (300). It has been suggested that NADPH oxidase maintains oxidizing environment required for tonic K^+ channel activity, and this is abolished during hypoxia (257). In a well-established model of neuroepithelial cells, in the human H146 carcinoma cell line, RT-PCR revealed the expression of TASK-1 (258) and TASK-3 (128). Hypoxia also reduced a TASK-like K^+ conductance, which first appeared to be resistant to acidification (compared with the extreme sensitivity of TASK-1; Ref. 258). However, its pH dependence was later found to correspond well to the less acid-sensitive TASK-3 subunit. TASK-1 and TASK-3 siRNA pretreatment eliminated the hypoxia-sensitive potassium conductance, confirming that TASK channels are responsible for this current in H146 cells (128).

3. Central chemoreceptors: dispensable TASK channels?

Different brain stem areas, dynamically monitoring P_{CO_2} changes as local pH alterations, are integrated with multiple respiratory nuclei in a complicated neural circuitry. During hypercapnia, the increased tonic drive of chemosensitive neurons activates respiration and also influences arousal from sleep (312, 328). Since the precise detection of local pH is central to the mechanism, the possible contribution of TASK channels was anticipated shortly after their discovery. Of the brain stem chemoreceptive areas, the noradrenergic locus coeruleus, the serotonergic raphe nuclei, and more recently the glutamatergic retrotrapezoid nucleus received the greatest attention in this regard.

TASK-1 and TASK-3 mRNAs were detected in neurons of locus coeruleus (18, 304) and raphe nuclei (310). Acidosis increased the action potential firing of locus coeruleus cells via multiple ion channel targets. One of these was a TASK-like conductance, which was inhibited by EC protons (98). Halothane activated the acid-sensitive TASK-like channel, hyperpolarized these neurons, and abolished their spontaneous activity (304). Serotonergic cells of the dorsal raphe nucleus expressed similar acid-sensitive and halothane-activated background K^+ current, attributed to TASK-1, TASK-3, and their heterodimers (331). Accordingly, TASK channels have been proposed

as the main (but not exclusive) targets of hypercapnia in the above brain stem regions.

Despite the undoubtedly strong functional expression of TASK channels in these areas, recent investigations challenged the conclusion that TASK channels contribute to the central respiratory chemosensitivity. In vivo, individually identified serotonergic lower brain stem neurons failed to respond to moderate hypercapnic acidosis, suggesting that these neurons were not real P_{CO_2} sensors (244). Another argument against the role of TASK channels in the central ventilatory chemoreception was raised in knockout experiments. While simultaneous deletion of TASK-1 and TASK-3 completely abolished the acid-sensitive background K^+ current of raphe neurons in brain slices, the ventilatory response of double knockout mice to hypercapnic acidosis was unaffected (245). In contrast to serotonergic raphe neurons, cells of the glutamatergic retrotrapezoid nucleus (RTN) responded even to moderate hypercapnic acidosis with robustly increased spiking activity (244). The ionic basis of the acid-sensitive response was the inhibition of a background K^+ current, which was not activated by halothane. Moreover, halothane inhibited an acid-insensitive K^+ conductance in these cells. Lack of activation by halothane strongly argued against TASK channels in the RTN. Indeed, the sensitivity of RTN neurons to hypercapnic acidosis was preserved in TASK double-knockout mice (245, 320). Accordingly, RTN neurons, with their unidentified non-TASK pH-sensitive background K^+ conductance, were suggested to be the primary central respiratory chemoreceptors (245).

Hypothalamic orexin neurons function as important orchestrators of adaptive responses, including the modulation of ventilation. Their firing activity is also profoundly influenced by alterations of EC pH and P_{CO_2}. Acidification activates these cells, and the effect is related to the reduction of their leak K^+ conductance (336). However, as it turned out in the case of RTN neurons, the pH response of orexin cells was preserved in TASK-$1^{-/-}$/TASK-$3^{-/-}$ double-knockout animals (119, 124).

4. *Pulmonary vasoconstriction in hypoventilated areas*

In sharp contrast to the systemic circulation, the smooth muscle cells of pulmonary arteries depolarize in response to reduced P_{O_2} and elevated P_{CO_2} in the neighborhood of hypoventilated alveoli. The resulting voltage-dependent calcium influx induces vasoconstriction. Under physiological conditions, this mechanism directs the blood to better ventilated areas of the lung. However, in chronic generalized lung disease, this mechanism is responsible for the development of the pulmonary hypertension. Depolarization of the smooth muscle cells mainly relies on the inhibition of their resting potassium conductance by hypoxia and hypercapnic acidosis. Several oxygen-sensitive, voltage-dependent (Kv1.2, Kv1.5, Kv2.1, and Kv3.1), and inwardly rectifying potassium channels have been detected in pulmonary arterial smooth muscle cells. TASK-1 came into focus more recently, as it also functions at resting conditions and has high mRNA and protein expression in pulmonary smooth muscle cells of different species (110, 123, 259). The pharmacological characteristics of the background K^+ current in the rabbit were similar but not identical to those of TASK-1, suggesting that other K^+ channels also contributed to the conductance (123). As the native conductance was only moderately facilitated by halothane (much less than TASK-1 by itself), the additional presence of a halothane-inhibited K_{2P} channel, THIK-1, has also been hypothesized (123). Indeed, in a later study, together with TASK-1, significant THIK-1 and TWIK-2 mRNA and protein expression were demonstrated (110). Nevertheless, the major role of TASK-1 in human pulmonary vascular smooth muscle was indicated by the efficient knock-down of the acid- and hypoxia-sensitive K^+ conductance by TASK-1 siRNA, and the concomitant depolarization of the cells (259).

5. *Tasting sour*

Several acid-sensing ion channels have been proposed to mediate sour taste perception, including ASIC-2, ENaC, HCN1, and chloride and potassium channels (201). In addition, TASK-1 and TWIK-1 mRNA expression were detected in the mouse (290), while TASK-1, TASK-2, TASK-3, and TALK-1 were detected in rat taste receptor cells (200). An acid-sensitive leak potassium conductance contributed to the negative resting membrane potential, but a particular channel could not be unequivocally identified. Further studies are required to establish the significance of K_{2P} channels in sour-tasting (290).

6. *Excitation of motoneurons by TASK inhibition*

In the brain stem, high levels of TASK-1 mRNA expression were found in motoneurons of the ambigual, motor trigeminal, facial, vagal, and hypoglossal nuclei (309). Significant expression was also detected in the ventral horn of the spinal cord (18). In hypoglossal motoneurons, extracellular acidification to pH 6.5 caused depolarization and increased input resistance, suggesting that the inhibition of a pH-sensitive K^+ current was responsible, at least in part, for the change of the membrane potential (18). In some cells, the acidification-induced depolarization reached the threshold of action potential generation (309). The properties of the pH-sensitive K^+ current were similar to expressed TASK-1 (18, 309). Later strong TASK-3 coexpression with TASK-1 was also demonstrated by in situ hybridization in motor nuclei of cranial nerves (153) and also in somatic motoneurons of the

spinal cord (310). When the pharmacological characteristics of the background K^+ conductance of medullary motoneurons were analyzed in more detail, the stimulation by isoflurane argued against TASK-1 and the resistance to ruthenium red against TASK-3 homodimers. The pH sensitivity of the native current slightly deviated from pure TASK-1. This pharmacological profile fitted to the characteristics of TASK-1/TASK-3 heterodimers (63), indicating that these channels were responsible for the majority of the background K^+ conductance (21).

The acid-sensitive K^+ current of somatic motoneurons is inhibited by different neurotransmitters (5-hydroxytryptamine, substance P, thyrotropin releasing hormone, and glutamate) via receptors coupled to $G_{q/11}$ proteins (18, 309). In the case of respiratory motoneurons, the transmitters may be released from axons originating in the chemosensory areas, the caudal medullary raphe nuclei, locus coeruleus, and retrotrapezoid nucleus. Thus the inhibition of TASK-1 via G_q-coupled receptors and the resulting depolarization was proposed to regulate the respiratory motor output (18). The same pH-sensitive current of motoneurons was activated by halothane, suggesting that this effect contributed to the anesthetic-induced immobilization (304). This hypothesis was supported by the results that TASK-1 knockout mice needed higher concentrations of the anesthetic to attain immobility than the wild-type animals (203).

7. *Regulation of the action potential firing pattern in cerebellar granule neurons*

Expression of TASK-3 increases as cerebellar granule cells reach their final location and their neuronal connections are formed during the development (187). The depolarizing effect of the gradually intensifying mossy fiber input is considered to induce this augmented expression. Granule cells in culture respond to elevated EC $[K^+]$ with similarly enhanced TASK-3 expression. The upregulation is dependent on the depolarization-induced Ca^{2+} entry and the activation of the calcium/calmodulin-dependent protein phosphatase calcineurin (354). At the end stage of upregulation, TASK-3 becomes the most important K^+ channel subunit determining the background K^+ conductance (mentioned in the literature as standing outward current, IKSO) and the resting membrane potential of mature granule neurons. The expression of TWIK-1 (33), TREK-2c (122), THIK-2 (285), and TASK-1 (33, 234) mRNAs has also been described; however, detailed single-channel analysis indicated the detectable functional expression of only TASK-1 and TASK-3 homodimers, TASK-1/TASK-3 heterodimers, and TREK-2 channels in cerebellar granule cells (126, 148).

The pharmacology and pH sensitivity of the current suggested that TASK-1/TASK-3 heterodimers primarily determined the background K^+ conductance of granule cells in vivo (2), whereas the heterodimers together with TASK-3 homodimers mainly constituted the current in cultured cells (148). Genetic deletion of TASK-1 did not significantly influence the electrophysiological properties of adult granule neurons, but it was demonstrated that TASK-1/TASK-3 heterodimers were functionally substituted by TASK-3 homodimers in TASK-1 knockout animals (2). On the other hand, in TASK-3 knockout mice, the granule neurons were depolarized and their action potential generation was also substantially disfigured. Action potentials were evoked by smaller depolarizing current injections, and the sustained repetitive firing to suprathreshold depolarization was also impaired (32). Substitution of the TASK-like channels during patch-clamp experiments by introducing a nonlinear leak conductance restored the normal tonic action potential generation in the granule neurons of TASK-3 knockout mice. Thus the function of TASK-3 was not restricted to the adjustment of the resting membrane potential and excitability. It also had an important role in the repolarization, as in its absence the depolarization-activated conductances could not completely recover from inactivation, interfering with sustained repetitive firing (32).

In light of the substantial electrophysiological disturbances of granule neuron function in the absence of TASK-3 subunit, it is surprising that the motor coordination and balance performance of TASK-3 knockout animals did not fall significantly behind the wild-type littermates. Their performance was not impaired in most test situations except for having more difficulties in balancing on a thin rotating rod (204).

8. *Glucose-activated K^+ currents of orexin neurons: TASK or not TASK?*

Orexin (hypocretin) neurons of the lateral hypothalamus have complex homeostatic function; they are involved in the coordination of energy homeostasis, arousal, emotion, and reward system and also modulate respiration. They receive multiple regulatory inputs, including the local glucose concentration, pH, P_{CO_2}, dopamine, and also the hormones ghrelin and leptin. Orexin neurons exhibited spontaneous electrical activity in tissue slices. The spontaneous firing was completely inhibited by the activation of a potassium current, when the extracellular glucose concentration was elevated from 0.2 to 4.5 mM. On the basis of immunohistochemical detection of channel proteins, and properties of the current (acid sensitivity, single-channel conductance, activation by halothane, and insensitivity to ruthenium red), TASK-1/TASK-3 heteromer has been proposed to be the glucose-activated K^+ channel. Low subphysiological concentration of glucose (0.2 mM) almost completely suppressed the acid-sensitive K^+ conductance, indicating the dra-

matic glucose dependence of the background K^+ current of orexin neurons (40).

Subsequent experiments confirmed that TASK channels contribute to the background K^+ conductance of orexin neurons; these cells from TASK1$^{-/-}$/TASK-3$^{-/-}$ knock out mice showed reduced background K^+ conductance and impaired high-frequency firing (119). However, glucose hyperpolarized and inhibited spontaneous action potential generation of orexin neurons in the knockout mice as efficiently as in the wild-type animals, and the acid sensitivity of the background K^+ current was also maintained (119, 124). As the glucose-activated proton-sensitive leak K^+ current was also inhibited by low concentrations of Ba^{2+} (which does not inhibit TASK channels), unidentified (41) or weakly inwardly rectifying K_{ir} channels (124) were suggested to be responsible for sensing glucose concentration.

9. *Auditory expression without documented functional significance*

Moderate levels of TASK-1 and TASK-3 mRNAs were detected, and the nonfunctional TASK-5 showed high and selective expression along the central auditory pathway (153). In the bushy cells of the cochlear nucleus, strong immunoreactivity of TASK-1 together with several other K^+ channel subunits was also reported (264), but the hearing of TASK-1$^{-/-}$ mice was not impaired (203). The expression level of all three TASK channels was found to be activity dependent. After cochlear ablation, the expression of TASK channels, especially that of TASK-1 and TASK-5, diminished in the auditory brain stem neurons (138) and in the inferior colliculus (61). Decreased expression of TASK-1 and TASK-3 channels may result in depolarized membrane potential, increased input resistance, and reduced threshold of action potential generation. Further studies are required to understand the significance of the diminished expression of TASK-5, because the function of this K_{2P} subunit is yet unknown.

10. *Changes in the higher neural functions of TASK knockout mice*

The widespread expression of TASK-1 and TASK-3 in the CNS as well as the lack of specific inhibitors make it extremely difficult to evaluate the contribution of these channels to complex neural functions. Knockout experiments may provide some clues; however, permanent absence of the channel(s) may induce compensatory expression of other genes replacing the experimentally eliminated functions. Conditional knockout animals might be required to correct this flaw in the future.

The mammalian startle response has a relatively short and well-described pathway. The sensory information is integrated in the giant pontine neurons, which project directly to motoneurons of the spinal cord. In situ hybridization showed that TASK-3 was abundantly expressed in the giant neurons (332). In accordance with the functional significance of TASK-3 in these cells, a ruthenium red- and acid-sensitive conductance was found to stabilize their resting membrane potential, reduce their excitability, and shorten the repolarizing phase of their action potential (332). Serotonergic fibers from raphe nuclei innervate the giant neurons. The activation of 5-hydroxytryptamine (5-HT_2) receptors depolarized giant neurons by the inhibition of their background K^+ conductance (332). In addition to the experiments indicating the major role of TASK-3, the possible contribution of TASK-1 to the startle response has also been reported; the acoustic startle response was enhanced in the male (but not in the female) TASK-1 knockout mice (203). It is interesting to note that in the same TASK-1 knockout strain (2), the impairment of adrenocortical function was also gender specific; it did not develop in adult males (130). Since the auditory function of the knockout animal was not affected (203), TASK-1 was suggested to influence the central signal processing or the efferent pathway of the startle response.

TASK-1 and TASK-3 are functionally expressed in the thalamocortical relay neurons of the visual pathway in the dorsal lateral geniculate nucleus (dLGN). Neurotransmitters of the ascending activating system, acetylcholine, norepinephrine, and serotonin, inhibited the acid-sensitive background K^+ conductance of these neurons (230). The induced depolarizing shift of the membrane potential altered the firing pattern of the relay neurons in the direction characteristic for wakefulness (from burst to tonic single-spike firing). Halothane hyperpolarized thalamocortical neurons by activating the TASK-like K^+ current and inhibiting hyperpolarization-activated cyclic nucleotide-gated (HCN) nonspecific cation channels (39, 230, 232). In TASK-1 knockout mice, the background K^+ current was reduced and the dLGN neurons were slightly depolarized. These slight electrophysiological changes did not disrupt the cholinergic switch between burst and tonic firing, and accordingly, no impairment in the function of the thalamocortical system was detected. However, TASK-3 substituted TASK-1 in the thalamocortical neurons of knockout mice and became the dominant factor of the background K^+ conductance (228).

TASK-1 knockout influenced higher neural functions marginally. No detectable difference was found in electroencephalogram, sleep/wake cycle, stress-induced hyperthermia, as well as anxiety-related and several other forms of behavior (203, 228). The deficiency of TASK-1 increased the sensitivity to thermal nociceptive stimuli (203). Halothane- and isoflurane-induced analgesia and immobilization were reduced in TASK-1$^{-/-}$ (203) and also in TASK-3$^{-/-}$ (204) mice (similarly to TREK-1 knockout animals), indicating that the activation of multiple K_{2P}

channel types contributed to the in vivo action of these volatile anesthetics.

TASK-3 knockout resulted in somewhat more pronounced behavioral changes than the absence of TASK-1, in accordance with the broader expression pattern of the channel in the CNS. TASK-3 deficiency slightly impaired working memory (in T-maze spontaneous alternation test) and learning (in Morris Water Maze) and also increased the nocturnal activity compared with the wild-type littermates (204).

Although knockout experiments are valuable tools to evaluate the physiological function(s) of the eliminated proteins, unexpected compensatory mechanisms may mask the consequences of the lost function. Upregulation of $GABA_A$ receptor activity functionally substituted for the K^+ channel in TASK-$1^{-/-}$ animals (202). Reciprocal compensation was observed in $GABA_A$ receptor-deficient mice by TASK-1 (33) and TASK-3 (3) overexpression. This example also implies that adaptive regulation of different channels, even with different charge carriers, can protect from the most serious consequences of inactivating mutations.

11. Putative role in epilepsy

TASK-3 (KCNK9) gene is located on chromosome 8 in a locus, which shows positive genetic linkage to human absence epilepsy. In a rat strain with genetic absence epilepsy (GAERS), an insertion mutation of TASK-3 was detected, raising the question whether these genetic variations might be causally related to the disease. However, the expressed current of the mutant channel was indistinguishable from the wild type, and the native background K^+ current in different brain tissue slices of GAERS and nonepileptic control rats was apparently identical (139). In a human genetic study, 63 cases of absence epilepsy were screened for mutations in TASK-3 gene, and only 1 silent polymorphism was found in the coding region of the channel (145). Thus the present data argue against any causal relationship between TASK-3 and the absence epilepsy.

12. Moderate expression and uncertain function in the heart

The expression of TASK-1 in the heart was described in the different publications as moderate (84) or abundant (169, 188, 281). TASK-3 expression was negligible (170, 281), while the silent TASK-5 subunit expression was intermediate (7). TASK-1 mRNA level showed age-related variations with lower amounts detected in the embryonic rat heart than in the adult (209). TASK-1 immunoreactivity was detected by Western blot both in rat atrial and ventricular tissue. TASK-1 immunoflorescence was localized to intercalated disks and t tubule network in ventricular cardiomyocytes (144, 340). In an experiment performed with another anti-TASK-1 antibody, the immunoreactivity of the channel was present throughout the myocardium during the early development, but the expression was found to be restricted to the electrical conduction system of the ventricles in adult mice and chicken (120). The expression of TASK-1 in the heart is highly probable on the basis of the above studies, as it is verified by different experimental approaches. However, the conflicting results of immunolocalization should be considered carefully, as reliable immunodetection of the sparse native channels is usually more difficult than that of the more abundant cytoplasmic proteins.

In the first report, proposing functional significance of TASK-1 in the heart, depolarization of murine ventricular myocytes was induced by platelet activating factor (PAF). PAF inhibited a background K^+ current with pharmacological properties of TASK-1, induced spontaneous activity in otherwise quiescent myocytes, and provoked abnormal automaticity in paced cells (12). TASK-1 current was identified also in rat ventricular cardiomyocytes using A293, an allegedly specific TASK-1 (and TASK-3) inhibitor (281) (A293, however, has been used exclusively in this study as it is commercially unavailable). Although the A293-sensitive current was small, it was detectable in the depolarized range, and its inhibition increased the action potential duration by 10–30%. Thus TASK-1 was suggested to participate in the repolarization of these cells (281). Furthermore, the current attributed to TASK-1 was blocked by stimulation of α_1-adrenergic receptors, suggesting that inhibition of TASK-1 may contribute to the changes of action potential duration in acidosis and/or during sympathetic activation (281). However, these conclusions are at variance with earlier observations which suggested that the voltage-gated, Na^+-activated K^+ channel Slick (Slo2.1) is the target of the α_1-adrenergic receptor (55).

13. Aldosterone production in rodents and primary hyperaldosteronism

Unlike in the bovine gland, in rat adrenal glomerulosa cells, the K^+ channel, responsible for the high resting conductance, was identified as TASK (68). Discovery and pharmacological characterization of TASK-3 allowed differentiation between the two TASK channels, and it was established that ruthenium red-sensitive TASK-3 homodimers dominated the current (64, 214). The functional data were in accordance with the quantitative PCR results, which revealed that TASK-3 mRNA is expressed at the highest abundance among the tested K_{2P} channels (64). In situ hybridization and immunohistochemistry with TASK-3-specific probe or antibody also demonstrated substantial labeling of the glomerulosa layer, while TASK-1 was evenly distributed in the whole

adrenal cortex (17, 74, 276). The background K^+ conductance of rat adrenal glomerulosa cells was inhibited by the stimulation of G_q-coupled AT_1 angiotensin receptor. As depolarization and the concomitant calcium influx via voltage-gated channels is an important mechanism of angiotensin II action, TASK inhibition plays a pivotal role in the regulation of aldosterone secretion (68).

Phenotype of TASK-deficient mice was examined in two independent knockout models. Both subunits (TASK-1 and TASK-3) were knocked out in one of the studies, whereas only TASK-1 was functionally eliminated in the other. In TASK-$1^{-/-}$/TASK-$3^{-/-}$ double-knockout mice, zonation of the adrenal cortex was preserved (74), and the expression of the zone-specific steroidogenic enzyme CYP11β2 (aldosterone synthase) was unaltered. However, the absence of TASK subunits resulted in a marked (~20 mV) depolarization and complete elimination of the halothane-activated, acid-sensitive background K^+ current. TASK-$1^{-/-}$/TASK-$3^{-/-}$ double-knockout mice exhibited the hallmarks of primary hyperaldosteronism in vivo. They developed hypertension, salt retention, and moderate hypokalemia. Their aldosterone production was robustly activated, and the hyperaldosteronism was not suppressed by dietary sodium loading. The increased aldosterone production was maintained despite the low concentrations of plasma renin and was not influenced by the angiotensin receptor antagonist candesartan (74). The other knockout model, where only TASK-1 had been eliminated, also showed disturbance of the mineralocorticoid production, but the picture was a lot more complex (130). Only immature mice and adult females were affected. While the characteristic hyperaldosteronism, salt retention, hypokalemia, and hypertension were present, the defect was the consequence of inappropriate zonation of the adrenal gland. The glomerulosa cell-specific steroidogenic enzyme CYP11B2 was missing in the glomerulosa layer, but its ectopic expression was detected in the deeper zones. This resulted in an inappropriate overproduction of aldosterone under the decisive control of ACTH. Electrophysiological parameters of TASK-$1^{-/-}$ adrenocortical cells deviated slightly from the normal values; mainly TASK-3 provided the outward K^+ current (130).

In spite of the fundamental differences, both reports agreed that primary hyperaldosteronism developed in TASK-deficient mice, indicating the significance of these channels in the regulation of aldosterone production. As similarly convincing data demonstrate the importance of another K_{2P} channel, TREK-1, in the bovine adrenal (see sect. III*C8*), it will be of particular interest to see whether mutations or polymorphisms of TREK or TASK channel genes may be related to human primary hyperaldosteronism.

14. T-lymphocyte function in health and disease

During T-cell activation, a prolonged Ca^{2+} influx and sustained elevation of the cytoplasmic [Ca^{2+}] are necessary for the induction of proliferation and for the production of inflammatory cytokines. Potassium channels of the lymphocytes play a pivotal role in the response; they stabilize negative membrane potential during T-cell activation and augment the driving force for Ca^{2+} influx. Voltage-dependent $K_V1.3$ and Ca^{2+}-activated $K_{Ca}3.1$ channels dominate the potassium conductance in the activated effector T lymphocytes and have been considered as molecular targets during excessive T-cell activation in allergic and autoimmune diseases. Recent reports suggest that in addition to these K^+ channels, TASK-1 and TASK-3 may also contribute to the tuning of immunoreaction and may be pharmacologically targeted for immunomodulation. TASK-1 and TASK-3 immunoreactivity have been detected in $CD3^+$ T lymphocytes, and proliferation and interferon-γ production of these T cells were significantly reduced by the drugs, which are known to inhibit TASK (229). While the detection of the channel proteins was somewhat ambiguous, and the used blockers were considered as "semi-selective" even by the authors, subsequent results in TASK-$1^{-/-}$ animals supported that TASK-1 represented a third functionally important K^+ channel type in T lymphocytes. Experimentally induced autoimmune encephalomyelitis (both the clinical score and the neurodegeneration) was much less severe in TASK-$1^{-/-}$ animals and a similar protection was attained by the administration of the TASK channel inhibitor anandamide to wild-type animals. In TASK-1 knockout mice, however, anandamide lost its beneficial effect on the course of the disease, simultaneously with the lack of effect on T-cell activation and K^+ current (24). It should be recalled, however, that the reduced vulnerability of neurons to the inflammatory injury in the absence of TASK might be the consequence of multiple mechanisms.

Significant sequence homology was identified between the 80 NH_2-terminal amino acids of TASK-1 and Vpu, an accessory transmembrane protein of human immunodeficiency virus (HIV-1), which is known to promote viral release from infected cells (142). The high similarity suggests that the virus acquired the partial sequence of the channel by molecular piracy. When coexpressed, TASK-1 and Vpu showed subcellular colocalization, and they were coimmunoprecipitated from peripheral leukocytes of an AIDS patient. In coexpression experiments, Vpu suppressed TASK current and accelerated the degradation of the channel protein, suggesting that the presence of Vpu prevented normal assembly of TASK-1 subunits to form functional dimers. In turn, TASK-1 reduced the release of HIV-1 particles, interfering functionally with Vpu. Low level of TASK-1 in lymphocytes was suggested to be insufficient to interfere with the viral release,

whereas the high expression of TASK-1 in neurons may prevent spreading but convert these cells to virus reservoirs (142).

15. Apoptosis and oncogenesis

It has been revealed that the expression of TASK-3 may significantly influence cell viability in either direction. Depending on the cell type and also on actual conditions of the particular tissue, TASK-3 may induce apoptosis, but under other circumstances it can help cell survival or promote proliferation.

During the early development of the cerebellum, a significant fraction of granule cells deteriorate, and this is necessary for shaping the appropriate cerebellar structure. The apoptosis coincides with the appearance of TASK-3 channels. Mature granule neurons, which express TASK-3, also die by apoptosis in vitro in physiological K^+ concentration (187), probably reflecting the depletion of intracellular potassium, which is an apoptotic signal in certain cell types, especially in neurons (352). Elevation of the extracellular $[K^+]$ protected the granule neurons from apoptosis, and the same effect was attained by pharmacological inhibition of TASK-3 or expression of a dominant negative TASK-3 mutant. Transfection of cultured hippocampal neurons with TASK-3 in vitro also had a similar apoptotic effect (187).

On the other hand, viral overexpression of TASK-3 in tissue slices from different hippocampal regions increased cell survival during cellular stress conditions, like hypoxia and/or glucose deprivation. The protection was strongly potentiated by activating TASK-3 with isoflurane, which was, however, ineffective on nontransfected cells (206). These results suggested that under certain cellular stress conditions the presence and/or activation of TASK-3 can also be protective in neuronal tissues, in a similar way as observed in the case of TREK channels.

It is generally accepted that potassium channels may influence cell proliferation (306). Overexpression of different potassium channels has been found in different malignant cells, and their activity has been related to tumor progression (6, 79, 105, 262, 353). Ether-á-go-go potassium channel was even considered as a highly significant tumor marker with diagnostic and possibly also with therapeutic relevance (307).

Among the K_{2P} channels, TASK-3 has attracted considerable attention as a channel potentially involved in carcinogenesis and tumor progression. The first data were obtained from a representation difference analysis, which revealed a highly significant (5- to 100-fold) overexpression of TASK-3 gene in 44% of breast and 35% of lung cancer cases (243). In the same study, TASK-3 was verified as an effective oncogene; its overexpression accelerated tumor formation from implanted oncogenically transformed (C8) fibroblasts. Furthermore, under hypoxic conditions, TASK-3 increased the viability of C8 cancer cells in vitro and prevented their apoptosis also during moderate serum deprivation (206, 243). The intact K^+ channel function of TASK-3 was indispensable for tumor promotion. A dominant negative, G95E pore-domain mutant TASK-3 did not influence the evoked apoptosis of C8 cells in vitro and failed to accelerate tumor development in nude mice. Coexpression of TASK-3 G95E with the wild-type channel neutralized the tumor-promoting effect of the latter and also reduced the proliferation rate of *Ben* human lung carcinoma cell line, which overexpresses TASK-3 endogenously (273). Constitutive TASK-3 expression was also found in different cell lines derived from glioblastoma, the most common aggressive primary tumor of the human brain. However, in contrast to other malignomas, activation of TASK-3 in these cells induced apoptosis (231) (similarly to cerebellar granule cells, cultured under identical conditions).

Increased TASK-3 expression, analyzed by immunohistochemistry, was also reported in several other malignant tumors. These reports, however, raise serious doubts and questions, because of the inherently problematic nature of the immunodetection of native channel proteins. Up to 50% of the colorectal cancer cases displayed moderate or high immunoreactivity, but TASK-3 expression did not correlate with the stage of the disease and the protein localized mainly to the cytoplasm (160). Similarly, TASK-3 immunoreactivity was diffusely distributed in the cytoplasm with some perinuclear condensation in gastric carcinoma cells, and the level of expression did not differ significantly from the normal gastric mucosa (177). TASK-3 was also detected predominantly in the perinuclear region of malignant melanoma cells and normal melanocytes (276). Interestingly, in the control experiment, TASK-3 immunolabeling showed clear plasma membrane localization in adrenal glomerulosa cells (276). Closer analysis localized TASK-3 immunopositivity to the mitochondria both in malignantly transformed (melanoma) cells and normal keratinocytes (293). Assuming that the reported immunolabelings are specific for TASK-3, we should conclude that non-plasma membrane localization is preferential in malignancies. However, this far-reaching conclusion would require substantial validation by additional methods.

V. TALK (TWIK-RELATED ALKALINE pH-ACTIVATED K^+ CHANNEL)

A. Expression Patterns, Electrophysiology, and Regulation by Alkaline pH

The first member of the TALK subfamily, TASK-2 (KCNK5), was cloned from human kidney (289). Because of its sensitivity to the extracellular pH, this channel was

originally named as TASK-2. Later, however, it was reassigned to the emerging TALK subfamily based on sequence similarity and according to the alkaline range of its pH sensitivity. TASK-2 mRNA expression was detected in the kidney, pancreas, and liver, while the expression was low in the nervous system (77, 149, 310). Although TASK-2-like immunoreactivity was also reported in selected brain regions (109) and in neural elements of the carotid body (347), the specificity of the used antibodies was not reassuringly verified in these studies.

The TALK subfamily also includes TALK-1 (KCNK16) and TALK-2 (KCNK17) (77, 112). [TALK-2 was named as TASK-4 in one of the initial studies (77).] Interestingly, members of this subfamily form a gene cluster on human chromosome 6 within a 150-kb region. The highest levels of TALK-1 and TALK-2 mRNA were detected in the pancreas (112). Whereas TASK-2 mRNA was also present in the endocrine islets, TALK-1 and TALK-2 channels were restricted to the exocrine cells (83). The strong expression of the alkaline-activated K_{2P} channels in an organ, which produces especially alkaline secretion, suggested their contribution to the exocrine secretory mechanism. The liver, lung, and heart were also abundant sources of TALK-2 mRNA, and this channel was also detected in the brain (77, 112, 149).

TASK-2, TALK-1, and TALK-2 clearly constitute a distinct subfamily of K_{2P} channels phylogenetically and also according to functional properties. All of them can be expressed functionally, and they are activated by EC alkalinization in the pH 7.5–10 range. In symmetrical K^+ solution, TASK-2 single-channel current has nearly linear (289), or according to another report, weakly inwardly rectifying (149) *I-V* relationship. The single-channel conductance of TASK-2, when measured between −60 and +20 mV in 5 mM EC K^+, was 14.5 pS, while the conductance increased to 60–70 pS in symmetrical 155 mM [K^+] (149, 289). At +60 mV, in high [K^+], the conductance was smaller (34 pS) in accordance with the slight inward rectification (149). A unique feature of TASK-2 is that its inward rectification depends on the presence of intracellular Na^+ (whereas intracellular Mg^{2+} and spermine, cations being responsible for the rectification of K_{IR}, inward rectifier K^+ channels, do not affect TASK-2 current). The rectification of TASK-2 (in the presence of intracellular Na^+) was not influenced by mutations of the negatively charged residues of the second transmembrane segment, which form the inner vestibule and to which Mg^{2+} and spermine bind in K_{IR} channels. In contrast, G102A/G207A double mutation in the pore domains of TASK-2, which rendered TASK-2 a nonselective cation channel, also eliminated the Na^+-dependent rectification. This suggests that in the wild-type channel Na^+ binds to and blocks the permeation at the selectivity filter (240).

TALK-1 and TALK-2 are more closely related to each other than to TASK-2. The amino acid sequences of TALK-1 and TALK-2 deviate from TASK-2 even in the region of transmembrane segments. Four splice variants of TALK-1 have been identified, but only two of them were functional. The two functional splice variants differ in their COOH-terminal tail region, but their electrophysiological characteristics seem to be indistinguishable. In the other two splice variants, the fourth transmembrane segment is missing. Not surprisingly, they do not induce current, and in coexpression experiments they did not influence the current of the functional variants (125). The noninactivating macroscopic currents of TALK-1 and TALK-2 show an almost instantaneous activation kinetics (<10 ms). The *I-V* relationship of the macroscopic current is linear in symmetrical K^+ (112), while a slight inward rectification of TALK-1 single-channel current was reported (125). Single-channel openings of TALK-1 are brief (<0.2 ms), showing ~20 and 10 pS conductance at −60 and +60 mV, respectively, in symmetrical 150 mM [K^+] (125). TALK-2 showed a similar inward rectification at the single-channel level: 33 pS conductance at −60 mV and 15 pS at +60 mV (149).

TASK-2 is highly sensitive to pH changes in the alkaline range; 50% activity is attained at pH 8.6 or 7.8, if the current is measured at −50 or +50 mV, respectively. Thus the inhibitory effect of protons is voltage dependent; it is stronger at negative membrane potential values. Acidification reduces the P_o, while the single-channel current amplitude does not change in a wide range of pH (149, 289). The pH sensitivity of TALK-1 and TALK-2 is shifted to the alkaline direction compared with TASK-1, TASK-3, and also TASK-2. Their current is largely (TALK-1) or almost completely (TALK-2) inhibited at the physiological pH 7.4, and maximal activation is attained above pH 10 (77, 112). In contrast to TASK-2, the effect of pH was found to be independent of the membrane potential (112).

The pH sensor of TASK-2 was originally related to multiple titratable residues of the M1-P1 loop (239). As these residues are not conserved in the TALK-1 and TALK-2 channels, the structural basis of their pH sensitivity was considered to be different. However, according to more recent site-directed mutagenesis studies, the pH sensitivity depends on a single amino acid, R224. This residue is located in the vicinity of the second pore domain, allowing an electrostatic effect on the channel pore, and modifying its P_o (252, 253). Basic amino acids are present in the corresponding position of TALK-1 (R242) and TALK-2 (K242). The substitution of these residues by neutral amino acids renders both TALK channels similarly pH insensitive (253). Thus the gating of all members of the TALK subfamily appears to be similarly regulated by alkaline pH at the molecular level.

B. Alkaline pH-Related Functions of TALK Channels

1. Bicarbonate reabsorption in the kidney

The expression of TASK-2 in the kidney is confined to the proximal tubule cells and to the papillary collecting ducts (330). Functional experiments clearly demonstrated that TASK-2 was indirectly engaged in the bicarbonate reabsorption and the accompanying Na^+ and water movements. Increased bicarbonate transport from the proximal tubule cells activated a potassium conductance, as a consequence of alkalinization of the basolateral compartment. The significance of this adaptive regulation in the course of bicarbonate transport is explained in a well-established model (Fig. 8). The effect was lost in TASK-2$^{-/-}$ mice, which had impaired bicarbonate reabsorption capacity, metabolic acidosis, pronounced loss of Na^+ and water, and reduced blood pressure. The condition of these animals resembled the clinical manifestation of proximal renal acidosis syndrome (330). Activation of TASK-2 by alkalinization of the extracellular space during a hypotonic challenge also contributes to the counterregulatory volume decrease of proximal tubular cells (183). Activation of TASK-2 is secondary to the swelling-activated Cl^- efflux, which accelerates Cl^-/HCO_3^- exchange and thereby alkalinizes the basolateral side of the proximal tubular cells.

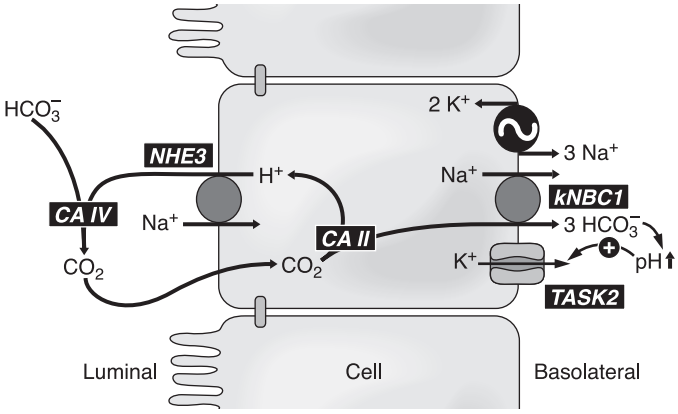

FIG. 8. Contribution of TASK-2 to the bicarbonate reabsorbtion in the proximal tubule of the nephron. TASK-2 in the basolateral membrane of proximal tubule cells is regulated by pH alterations in the extracellular space. During bicarbonate reabsorbtion, this compartment alkalinizes, leading to TASK-2 activation. The increased K^+ conductance allows efficient recycling of the K^+ which had entered the cell via the Na^+-K^+ pump. The K^+ efflux and the resulting hyperpolarization augment the electrical driving force for the electrogenic transport through the basolateral Na^+-$3HCO_3^-$ cotransporter (kNBC1). Intracellular and luminal carboanhydrases, CA II and CA IV, respectively, and the Na^+/H^+ exchanger (NHE3) in the luminal membrane are also involved in the vectorial transport of sodium and bicarbonate ions. [Adapted from Warth et al. (330).]

2. Resting membrane potential of rat pulmonary artery smooth muscle cells

A depolarizing shift of the resting membrane potential of rat pulmonary artery smooth muscle cells was induced by silencing TASK-2 with siRNA. Acidification-induced current changes were reduced in the cells treated with siRNA, suggesting that the closure of this channel contributed to the depolarization and the consequent vasoconstriction in response to acidification, an essential response for appropriate adjustment of the ventilation-to-perfusion ratio (118). Thus, in addition to voltage-gated, ATP-dependent, and TASK-1 potassium channels, TASK-2 also appears to be a significant component of the pH-regulated K^+ conductance of rat pulmonary arterial smooth muscle cells. However, the contribution of TASK-2 may be species dependent, since TASK-2 mRNA was not detected in human pulmonary arterial myocytes, and the pH sensitivity of the human background K^+ current corresponded well to that of TASK-1 (259) (see sect. IV*C4*).

3. Potential role of alkaline-activated channels in the exocrine pancreas

The epithelial cells of the exocrine pancreas produce the most alkaline fluid of the body, with $[HCO_3^-]$ of ~140 mM. Bicarbonate may enter the cell through the basolateral membrane or may be produced from CO_2 by carbonic anhydrase, which operates in concert with the basolateral Na^+/H^+ exchanger. The secretion is regulated primarily by secretin and cholecystokinin via cAMP and the Ca^{2+} signal, activating cystic fibrosis transmembrane conductance regulator (CFTR) and calcium-activated chloride channels (CaCC), respectively. The anion efflux is electrogenic, resulting in a lumen-negative potential. The apical potassium conductance allows potassium entry into the tubular lumen, providing charge compensation for the anion transport, thus interfering with the generation of a rate-limiting lumen-negative tubular potential and facilitating the bicarbonate secretion. The quantitative reflection of the apical efflux is the significantly higher $[K^+]$ in the tubular fluid than in the plasma. Calcium-activated K^+ channels contribute to, but are only responsible for, a fraction of this apical transport. In a malignant pancreatic duct cell line (HPAF), the expression of TASK-2 was verified by RT-PCR (101). An alkaline-activated K^+ conductance with pharmacological properties of TASK-2 was also demonstrated in the apical membrane of HPAF cells (101). Accordingly, it has been suggested that alkaline-activated K_{2P} channels, TASK-2, TALK-1, and TALK-2, which are expressed abundantly in the pancreas, may have a special importance in the apical compensatory K^+ current in the pancreatic duct cells too.

TALK-1 and TALK-2 channels are strongly (2- to 8-fold) activated by NO and reactive oxygen species: su-

peroxide or singlet oxygen (83). Since a NO-ergic component has been demonstrated to contribute to the neural control of the pancreas secretion (337), TALK channels were proposed as auxiliary targets during physiological vagal stimulation. Under pathological conditions, when generation of reactive nitrogen species may become excessive in the pancreas, activation of TALK currents may influence the events, leading to cellular damage and pancreatitis (56).

VI. THIK (TANDEM PORE DOMAIN HALOTHANE-INHIBITED K^+ CHANNEL)

THIK channels, THIK-1 (KCNK13) and THIK-2 (KCNK12), were cloned from rat and human brain (112, 285). Rat THIK-1 was reported to be expressed ubiquitously, while THIK-2 expression was found in the lung, spleen, and different regions of the brain (RT-PCR) (285). Human THIK-2 mRNA was most abundant in the heart, skeletal muscle, and pancreas as determined by Northern blot (112). Recently, both THIK-1 and THIK-2 were detected in the kidney, in the same structures where ROMK ($K_{IR}1.1$) inwardly rectifying K^+ channel is also expressed (315).

Heterologous expression of rat THIK-1 in *Xenopus* oocytes produced leak potassium current, which activated instantaneously and did not inactivate. In symmetrical [K^+] solutions, the current was slightly inwardly rectifying (285). THIK-1 was not influenced by moderate EC or IC acidification, and only moderately responded to temperature changes (it was not temperature sensitive). Its current was not influenced by lysophospholipids; however, it was activated by arachidonic acid (EC_{50} ~1 μM), similarly to the members of the TREK/TRAAK subfamily (285). In contrast to several other K_{2P} channels, THIK-1 is inhibited by halothane with a K_d of 2.83 mM (285). Heterologously expressed THIK-1 channels are weakly inhibited by hypoxia (~10% inhibition by 20 mmHg Po_2). The mechanism of inhibition appeared to be independent of mitochondrial respiration or NADPH oxidases, being in this regard different from other O_2-sensitive K_{2P} channels (45).

A physiological role of THIK-1 has been suggested in cerebellar Purkinje cells, since a fraction of the TEA-resistant background K^+ current exhibited pharmacological properties similar to THIK-1 (stimulation with arachidonic acid, inhibition with halothane, and resistance to moderate acidification to pH 6.9) (42). Activation of the G_i-coupled $GABA_B$ or opioid receptors stimulated, while activation of the group I metabotropic glutamate or muscarinic receptors inhibited the current, attributed to THIK-1 or related channels (42). However, the receptor-mediated effects were not tested on heterologously expressed THIK-1 channels, and thus the significance of THIK-1 in Purkinje cells requires confirmation.

The carotid bodies are innervated by NO synthase-positive glossopharyngeal neurons (GPN). In isolated NOS-immunoreactive GPN, the outward K^+ current was slightly inhibited by hypoxia. The hypoxia-sensitive K^+ current shared pharmacological properties with THIK-1. The physiological significance of this regulation, however, remains enigmatic, as hypoxic activation of NO-ergic GPN neurons exerts efferent inhibition on the chemoreceptor cells. Accordingly, this mechanism would negatively modify the response of the carotid body to a hypoxic challenge (46).

Neither rat (285) nor human (112) THIK-2 could be expressed functionally, although the expressed rat channel was targeted properly to the plasma membrane. Chimera channels of different compositions, constructed from THIK-2 and THIK-1, were also nonfunctional. In coexpression experiments, THIK-2 did not influence THIK-1 current, suggesting that the two channels do not form heterodimers (285). Altered level of expression of THIK-2 was observed under various conditions. Its expression in the brain was turned on only after birth, primarily in thalamic nuclei and in cerebellar granule cells post migration (3). Reduced expression was detected by quantitative RT-PCR in the rat cochlear nucleus (138) and colliculus inferior (61) following deafness. A proteomic analysis revealed a reduction of THIK-2 level in the striatum during nicotine addiction (350). However, in the absence of any known function of THIK-2, the significance of these observations remains to be established.

VII. TRESK (TWIK-RELATED SPINAL CORD K^+ CHANNEL)

A. Unique Single-Channel Behavior

The TRESK subfamily consists of only one channel. TRESK (KCNK18, $K_{2P}18.1$) cDNA has been cloned from human spinal cord (299), mouse cerebellum (70), and testis (152). Human and mouse TRESK channels show unexpectedly low (65%) amino acid sequence identity (152). This could be the reason why mouse TRESK was originally named as TRESK-2 (152). As neither the human nor the mouse genome possesses more than one TRESK gene, it has been accepted that human and mouse TRESK channels are genuine orthologs (67, 70, 150, 158).

TRESK single-channel activity was first characterized in *Xenopus* oocyte inside-out membrane patches (70). The conductance of mouse TRESK was 13 pS in symmetrical 140 mM [K^+] at +90 mV. The channel exhibited a peculiar asymmetrical gating behavior; it produced square wavelike openings at depolarized but bursts of very short (<1–2 ms) openings at hyperpolarized membrane potentials (70). High-resolution analysis revealed that the single-channel conductance and mean open time of these

very short openings were 16 pS and 0.4 ms, respectively (at −60 mV) (150, 152). Demonstration of these unique single-channel properties is currently the most reliable way to distinguish TRESK from other K_{2P} channels (150).

B. Regulation by Ca^{2+} and Protein Interactions

The regulation of TRESK by G_q-coupled receptor activation is qualitatively different from that of any other mammalian K_{2P} channel. While the other channels are not affected or inhibited by calcium-mobilizing agonists (14, 68, 309), TRESK, expressed heterologously in *Xenopus* oocytes, is activated 5- to 15-fold by the stimulation of M_1 muscarinic or AT_{1a} angiotensin II receptors (70). The calcium signal was found to be indispensable for TRESK regulation, and experimental elevation of cytoplasmic calcium concentration was sufficient to activate the current (70). This suggests that irrespectively of the source (Ca^{2+} release or influx), the ion exerts its stimulatory effect.

TRESK was activated by 40–80% via coexpressed M_3 muscarinic receptors in COS-7 cells (150, 151). Similar activation was evoked by acetylcholine, glutamate, or histamine, when the regulation of native TRESK current was studied in isolated DRG neurons in cell-attached configuration (151). Although the mechanism of activation has not been examined in COS-7 and DRG cells, this latter experiment also indicated that the effect was not membrane delimited. The reason for the quantitative difference (the modest stimulation of TRESK in these mammalian cells in contrast to the robust activation in *Xenopus* oocytes) remains to be established.

Regulation of TRESK by calcium fundamentally differs from that of the classic calcium-activated channels, BK and SK, which are directly activated by the ion (225, 295). TRESK single-channel activity in excised patches was not influenced by the elevation of [Ca^{2+}] on the intracellular side (70). However, in *Xenopus* oocytes, cyclosporin A and FK506, the inhibitors of the calcium/calmodulin-dependent protein phosphatase calcineurin, abolished the calcium-dependent TRESK activation. In addition, coexpression of a constitutively active form of the phosphatase permanently activated the channel in the absence of cytoplasmic [Ca^{2+}] elevation. With the assumption that the activation reflected the dephosphorylation of TRESK protein, alanine-scanning mutagenesis was performed. The S276A mutant mouse TRESK, mimicking the dephosphorylated state of the channel, proved to be constitutively active, irrespectively of the calcium signal. Accordingly, serine-276 has been proposed as the likely target of calcineurin (70).

In addition to its enzymatic action, calcineurin interacts directly with TRESK via an NFAT-like (nuclear factor of activated T cells) docking site (66). The PQIVID motif in the intracellular loop of mouse TRESK (conserved as PQIIIS in the human ortholog) resembles the PXIXIT calcineurin-binding consensus sequence of NFAT proteins. The surface of calcineurin, which interacts with this NFAT-like docking motif, is clearly different from the enzymatically active site of the phosphatase (197). The binding of calcineurin is highly facilitated by calcium/calmodulin, indicating that the activated form of the phosphatase more avidly associates to the channel than the resting enzyme (66). This kind of protein-protein interaction of TRESK with calcineurin is exceptional among the ion channels. Moreover, the NFAT-like binding motif of TRESK has the highest affinity (K_d ~5–10 μM) for calcineurin among all the proteins examined so far (198).

A mode I binding motif for the ubiquitous 14-3-3 adaptor protein has been recognized in the intracellular loop of TRESK in silico. This RSNSCP motif is located between the calcineurin-binding PQIVID sequence and the putative calcineurin target site, serine-276 (Fig. 9). Conditional interaction of the two proteins was verified in vitro; phosphorylation of serine-264 in mouse TRESK (the second serine in RSNSCP) by protein kinase A was necessary for the docking of 14-3-3. Coexpression of 14-3-3γ or -η decelerated the return of TRESK current to the

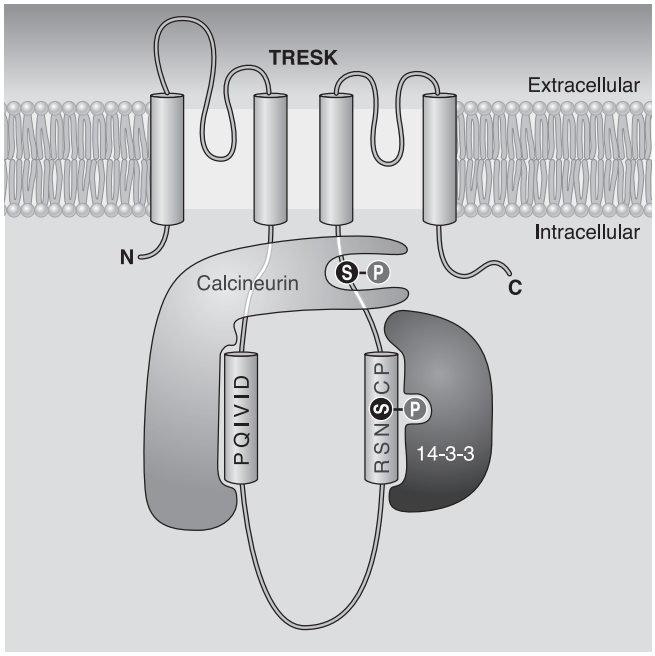

FIG. 9. Schematic representation of the regulatory protein partners directly interacting with TRESK. The calcium/calmodulin-dependent protein phosphatase calcineurin directly and calcium-dependently binds to the nuclear factor of activated T cells (NFAT)-like PQIVID motif of mouse TRESK. Dephosphorylation of phosphoserine-276 in the channel is probably the major mechanism of activation. The ubiquitous adaptor protein, 14-3-3, phosphorylation-dependently associates with the RSNSCP mode I motif of TRESK. Coexpression of 14-3-3 with TRESK decelerates the return of the K^+ current to the resting state after the calcineurin-mediated activation. A possible mechanism of this functional effect may be that 14-3-3 obstructs the inhibitory phosphorylation of the channel.

resting state after calcineurin-dependent activation. It has been speculated that the binding of 14-3-3 to TRESK interferes with the rephosphorylation of serine-276 following the calcineurin-mediated activation, and thus the return of the channel to the resting state is impeded (71). In contrast to TASK channels, 14-3-3 did not change the surface expression of TRESK in *Xenopus* oocytes.

Unlike the mammalian TRESK orthologs, zebrafish (*Danio rerio*) TRESK (GeneBank accession number: GQ304739) does not contain the NFAT-like calcineurin-binding site, and accordingly, it is not regulated by calcium, when expressed in *Xenopus* oocytes (Czirják and Enyedi, unpublished results). However, the 14-3-3 binding motif is also present in the zebrafish TRESK as the KSCSCP sequence. If this motif binds 14-3-3 similarly to the mammalian orthologs, then its ancient function has to be different from the modulation of calcium-dependent regulation in the fish.

C. Physiological Significance of TRESK

TRESK mRNA is expressed at low levels (compared with TASK or TREK channels) and only in few tissues. Originally, human TRESK was found exclusively in the spinal cord (299). Later TRESK mRNA was suggested to be more abundant in the human brain (205). Mouse TRESK was shown to be expressed in the cerebrum, cerebellum, brain stem, spinal cord, and testis (70). TRESK mRNA was detected in the thymus and spleen of both mouse and rat (152) and in mouse DRG (81, 150, 158).

Functional expression of TRESK was demonstrated in cultured neonatal rat DRG neurons (150). TRESK proved to be an abundant background K^+ channel in these cells. It has been detected in 40% of the examined membrane patches (150). Although the single-channel approach does not allow the direct measurement of the contribution of TRESK to the ensemble background K^+ current, it has been estimated that TRESK and TREK-2 together may provide >80% of the background K^+ conductance (150). The relative contribution of these two channels was temperature dependent. TRESK dominated the background K^+ current at room temperature, while TREK-2, activating robustly with an increase of the temperature, prevailed at 37°C. If TREK-2 (and TREK-1) are assumed to be involved in temperature detection in the peripheral subcutaneous endings of DRG neurons (in addition to TRP channels), then TRESK can be envisioned as the temperature-independent (in this respect static) component of the background K^+ current (150).

The significance of TRESK in trigeminal sensory neurons received support from pharmacological data obtained with hydroxy-α-sanshool, the ingredient of Szechuan pepper, which is known to cause tingling oral sensation. The drug which was shown to affect only three members of the K_{2P} channel family (TASK-1, TASK-3, and TRESK) efficiently inhibited the background K^+ current of both large and small neurons (16). On the basis of the mRNA expression levels and additional pharmacological properties (ruthenium red insensitivity and moderate pH sensitivity) of their composite background K^+ current, TRESK was proposed to be an important target of hydroxy-α-sanshool in trigeminal low-threshold mechanoreceptors as well as high-threshold nociceptors (23). The effect of sanshool appeared to be remarkably specific when tested on several other potential target ion channels expressed in *Xenopus* oocytes including different P2X receptors, ASIC, voltage-sensitive K^+ channels, TRPV1, TRPA1, etc. (16). While the efficiency of hydroxy-α-sanshool on TRPV1 and TRPA1 channels is still controversial (176, 291), it has been clearly shown that the calcium signal evoked by sanshool in the sensory neurons, similarly to its behavioral effects, are not dependent on the functional presence of these activating channels (16). It will be interesting to see how the effects of sanshool will be affected in TRESK-deficient animals.

The role of TRESK in DRG neurons has also been examined in functional knockout mice (81). The elimination of TRESK did not induce an apparent phenotype and, interestingly, only marginally affected the electrophysiological parameters of DRG neurons. The amplitude of outward K^+ current (elicited by voltage steps from −70 to −25 mV) was reduced by 27%. Unexpectedly, however, the value of the resting membrane potential has not been changed in the absence of functional TRESK channels. In addition, also in contrast to expectations, the duration of the action potential was reduced and the afterhyperpolarization became more pronounced in the knockout mice. As this second group of data cannot be explained by the simple elimination of a background K^+ current, it has been speculated that the lack of TRESK was compensated for by changes in other ionic currents (81).

In two recent reports, an instantaneous, noninactivating outward K^+ current of human leukemic (Jurkat) T cells was attributed to TRESK (278, 322). The pharmacological properties of this current were comparable to those of TRESK, and the single-channel conductance was also in the appropriate range. However, the characteristic asymmetrical gating behavior of TRESK has not been demonstrated in Jurkat cells. Although the channel protein was also claimed to be present, based on Western blot experiments (278), the specificity of the used antiserum was not clearly verified, and the level of expression was not addressed with the more reliable PCR approach.

While much remains to be learned about the physiological function of TRESK, it is likely that the channel is also regulated by calcineurin in vivo, at least in some locations. Whatever the final impact of the calcineurin-dependent regulation of human TRESK may be, it is

blocked by calcineurin inhibitors. Since these drugs (e.g., cyclosporin A and FK506) are the cornerstones of immunosuppressive therapy (administered, for example, in autoimmune diseases or after organ transplantation), many patients rely on them. These patients suffer from several adverse effects of the medication, some of which may be related to the inhibition of TRESK regulation. The identification of these interactions may aid the alleviation of the adverse effects. Recently, a patent (WO/2008/058399) became accessible, claiming that TRESK is highly expressed in the trigeminal ganglion and also that inactivating mutations of its gene are linked to migraine disease. Migraine headaches are also adverse effects of calcineurin inhibitors (97); thus it is plausible that impaired calcineurin-dependent regulation of TRESK is a pathogenetic mechanism in some cases of this frequent neurological syndrome.

VIII. CONCLUSIONS

K_{2P} potassium channels turned out to be the long searched for molecular entities responsible for the background or leak potassium conductance. Studies in heterologous expression systems revealed their biophysical characteristics and structure-function relationships and also highlighted various mechanisms through which these channels are regulated. The tissue distribution of the individual channels was also characterized, and K_{2P} background currents were identified in many excitable and nonexcitable tissues. The functional significance of the endogenously expressed channels was verified under physiological and also pathophysiological conditions. K_{2P} channels were found to mediate the effect of some drugs, such as volatile anesthetics or therapeutically administered polyunsaturated fatty acids, and they have been considered as promising targets in various diseases.

It should be realized, however, that there are certain ambiguities and pitfalls which impede the understanding of their role and hinder their therapeutic targeting. A major difficulty is the lack of selective pharmacology. Although each channel has a characteristic pharmacological profile that is perfectly suitable to identify the particular current in an expression system, the inhibitors and modifying agents often fall short when the aim is to determine the molecular substrate of a leak conductance in a native tissue. Another restraint is the lack of high-affinity antibodies that could reliably detect the characteristically low level of channel protein expression. Knockout approaches are valuable tools to clarify the functional significance of K_{2P} channels. However, it was demonstrated that persistent lack of the eliminated background K^+ conductance often induces compensatory replacement of the channel by a closely related member of the K_{2P} family. There was also evidence that other types of channels could functionally substitute for the lost activity stabilizing the resting membrane potential. These are the most likely reasons why the knockout of certain K_{2P} genes (e.g., TRAAK, TASK, and TRESK channels) had unexpectedly moderate phenotypic consequences.

With the development of new pharmacological tools, the generation of more specific reagents for immunodetection, and more extensive application of combined or conditional knockout organisms, future studies will be able to provide even more revealing insights into the physiological functions, the pathophysiological mechanisms, and also into the pharmacological potential of this K^+ channel family.

ACKNOWLEDGMENTS

Address for reprint requests and other correspondence: P. Enyedi, Dept. of Physiology, Semmelweis University of Medicine, PO Box 259, Budapest, Hungary H-1444 (e-mail: peter.enyedi@eok.sote.hu).

GRANTS

This work was supported by Hungarian National Research Funds OTKA K75239 (to P. Enyedi) and OTKA F-67743 (to G. Czirják). G. Czirják was supported by the János Bolyai Fellowship of the Hungarian Academy of Sciences.

REFERENCES

1. **Aimond F, Rauzier JM, Bony C, Vassort G.** Simultaneous activation of p38 MAPK and p42/44 MAPK by ATP stimulates the K^+ current I_{TREK} in cardiomyocytes. *J Biol Chem* 275: 39110–39116, 2000.
2. **Aller MI, Veale EL, Linden AM, Sandu C, Schwaninger M, Evans LJ, Korpi ER, Mathie A, Wisden W, Brickley SG.** Modifying the subunit composition of TASK channels alters the modulation of a leak conductance in cerebellar granule neurons. *J Neurosci* 25: 11455–11467, 2005.
3. **Aller MI, Wisden W.** Changes in expression of some two-pore domain potassium channel genes (KCNK) in selected brain regions of developing mice. *Neuroscience* 151: 1154–1172, 2008.
4. **Alloui A, Zimmermann K, Mamet J, Duprat F, Noel J, Chemin J, Guy N, Blondeau N, Voilley N, Rubat-Coudert C, Borsotto M, Romey G, Heurteaux C, Reeh P, Eschalier A, Lazdunski M.** TREK-1, a K^+ channel involved in polymodal pain perception. *EMBO J* 25: 2368–2376, 2006.
5. **Arrighi I, Lesage F, Scimeca JC, Carle GF, Barhanin J.** Structure, chromosome localization, and tissue distribution of the mouse twik K^+ channel gene. *FEBS Lett* 425: 310–316, 1998.
6. **Artym VV, Petty HR.** Molecular proximity of Kv1.3 voltage-gated potassium channels and β_1-integrins on the plasma membrane of melanoma cells: effects of cell adherence and channel blockers. *J Gen Physiol* 120: 29–37, 2002.
7. **Ashmole I, Goodwin PA, Stanfield PR.** TASK-5, a novel member of the tandem pore K^+ channel family. *Pflügers Arch* 442: 828–833, 2001.
8. **Atkinson NS, Robertson GA, Ganetzky B.** A component of calcium-activated potassium channels encoded by the *Drosophila slo* locus. *Science* 253: 551–555, 1991.
9. **Azzalin A, Ferrara V, Arias A, Cerri S, Avella D, Pisu MB, Nano R, Bernocchi G, Ferretti L, Comincini S.** Interaction between the cellular prion (PrPC) and the 2P domain K^+ channel TREK-1 protein. *Biochem Biophys Res Commun* 346: 108–115, 2006.
10. **Baker SA, Hennig GW, Han J, Britton FC, Smith TK, Koh SD.** Methionine and its derivatives increase bladder excitability by

inhibiting stretch-dependent K^+ channels. *Br J Pharmacol* 153: 1259–1271, 2008.
11. **Bang H, Kim Y, Kim D.** TREK-2, a new member of the mechanosensitive tandem-pore K^+ channel family. *J Biol Chem* 275: 17412–17419, 2000.
12. **Barbuti A, Ishii S, Shimizu T, Robinson RB, Feinmark SJ.** Block of the background K^+ channel TASK-1 contributes to arrhythmogenic effects of platelet-activating factor. *Am J Physiol Heart Circ Physiol* 282: H2024–H2030, 2002.
13. **Barel O, Shalev SA, Ofir R, Cohen A, Zlotogora J, Shorer Z, Mazor G, Finer G, Khateeb S, Zilberberg N, Birk OS.** Maternally inherited Birk Barel mental retardation dysmorphism syndrome caused by a mutation in the genomically imprinted potassium channel KCNK9. *Am J Hum Genet* 83: 193–199, 2008.
14. **Barratt L, Fyffe REW, Millar JA, Robertson B, Mathie A.** The two-pore domain potassium channel, TASK-1, is inhibited by activation of muscarinic acetylcholine receptors and is expressed in rat cerebellar granule neurons. *J Physiol Lond* 525: 71P–72P, 2000.
15. **Basbaum AI, Bautista DM, Scherrer G, Julius D.** Cellular and molecular mechanisms of pain. *Cell* 139: 267–284, 2009.
16. **Bautista DM, Sigal YM, Milstein AD, Garrison JL, Zorn JA, Tsuruda PR, Nicoll RA, Julius D.** Pungent agents from Szechuan peppers excite sensory neurons by inhibiting two-pore potassium channels. *Nat Neurosci* 11: 772–779, 2008.
17. **Bayliss DA, Sirois JE, Talley EM.** The TASK family: two-pore domain background K^+ channels. *Mol Interv* 3: 205–219, 2003.
18. **Bayliss DA, Talley EM, Sirois JE, Lei Q.** TASK-1 is a highly modulated pH-sensitive "leak" K^+ channel expressed in brainstem respiratory neurons. *Respir Physiol* 129: 159–174, 2001.
19. **Bearzatto B, Lesage F, Reyes R, Lazdunski M, Laduron PM.** Axonal transport of TREK and TRAAK potassium channels in rat sciatic nerves. *Neuroreport* 11: 927–930, 2000.
20. **Beitzinger M, Hofmann L, Oswald C, Beinoraviciute-Kellner R, Sauer M, Griesmann H, Bretz AC, Burek C, Rosenwald A, Stiewe T.** p73 poses a barrier to malignant transformation by limiting anchorage-independent growth. *EMBO J* 27: 792–803, 2008.
21. **Berg AP, Talley EM, Manger JP, Bayliss DA.** Motoneurons express heteromeric TWIK-related acid-sensitive K^+ (TASK) channels containing TASK-1 (KCNK3) and TASK-3 (KCNK9) subunits. *J Neurosci* 24: 6693–6702, 2004.
22. **Besana A, Barbuti A, Tateyama MA, Symes AJ, Robinson RB, Feinmark SJ.** Activation of protein kinase C epsilon inhibits the two-pore domain K^+ channel, TASK-1, inducing repolarization abnormalities in cardiac ventricular myocytes. *J Biol Chem* 279: 33154–33160, 2004.
23. **Bhattacharya MR, Bautista DM, Wu K, Haeberle H, Lumpkin EA, Julius D.** Radial stretch reveals distinct populations of mechanosensitive mammalian somatosensory neurons. *Proc Natl Acad Sci USA* 105: 20015–20020, 2008.
24. **Bittner S, Meuth SG, Gobel K, Melzer N, Herrmann AM, Simon OJ, Weishaupt A, Budde T, Bayliss DA, Bendszus M, Wiendl H.** TASK1 modulates inflammation and neurodegeneration in autoimmune inflammation of the central nervous system. *Brain* 132: 2501–2516, 2009.
25. **Blondeau N, Petrault O, Manta S, Giordanengo V, Gounon P, Bordet R, Lazdunski M, Heurteaux C.** Polyunsaturated fatty acids are cerebral vasodilators via the TREK-1 potassium channel. *Circ Res* 101: 176–184, 2007.
26. **Blondeau N, Widmann C, Lazdunski M, Heurteaux C.** Polyunsaturated fatty acids induce ischemic and epileptic tolerance. *Neuroscience* 109: 231–241, 2002.
27. **Bockenhauer D, Nimmakayalu MA, Ward DC, Goldstein SA, Gallagher PG.** Genomic organization and chromosomal localization of the murine 2 P domain potassium channel gene Kcnk8: conservation of gene structure in 2 P domain potassium channels. *Gene* 261: 365–372, 2000.
28. **Bockenhauer D, Zilberberg N, Goldstein SA.** KCNK2: reversible conversion of a hippocampal potassium leak into a voltage-dependent channel. *Nat Neurosci* 4: 486–491, 2001.
29. **Bowers BJ, Radcliffe RA, Smith AM, Miyamoto-Ditmon J, Wehner JM.** Microarray analysis identifies cerebellar genes sensitive to chronic ethanol treatment in PKCgamma mice. *Alcohol* 40: 19–33, 2006.
30. **Boyd DF, Millar JA, Watkins CS, Mathie A.** The role of Ca^{2+} stores in the muscarinic inhibition of the K^+ current IK(SO) in neonatal rat cerebellar granule cells. *J Physiol* 529: 321–331, 2000.
31. **Brenner T, O'Shaughnessy KM.** Both TASK-3 and TREK-1 two-pore loop K channels are expressed in H295R cells and modulate their membrane potential and aldosterone secretion. *Am J Physiol Endocrinol Metab* 295: E1480–E1486, 2008.
32. **Brickley SG, Aller MI, Sandu C, Veale EL, Alder FG, Sambi H, Mathie A, Wisden W.** TASK-3 two-pore domain potassium channels enable sustained high-frequency firing in cerebellar granule neurons. *J Neurosci* 27: 9329–9340, 2007.
33. **Brickley SG, Revilla V, Cull-Candy SG, Wisden W, Farrant M.** Adaptive regulation of neuronal excitability by a voltage-independent potassium conductance. *Nature* 409: 88–92, 2001.
34. **Bryan RM Jr, You J, Phillips SC, Andresen JJ, Lloyd EE, Rogers PA, Dryer SE, Marrelli SP.** Evidence for two-pore domain potassium channels in rat cerebral arteries. *Am J Physiol Heart Circ Physiol* 291: H770–H780, 2006.
35. **Buckler KJ, Honore E.** The lipid-activated two-pore domain K^+ channel TREK-1 is resistant to hypoxia: implication for ischaemic neuroprotection. *J Physiol* 562: 213–222, 2005.
36. **Buckler KJ, Vaughan-Jones RD.** Effects of hypercapnia on membrane potential and intracellular calcium in rat carotid body type I cells. *J Physiol* 478: 157–171, 1994.
37. **Buckler KJ, Vaughan-Jones RD.** Effects of hypoxia on membrane potential and intracellular calcium in rat neonatal carotid body type I cells. *J Physiol* 476: 423–428, 1994.
38. **Buckler KJ, Williams BA, Honore E.** An oxygen-, acid- and anaesthetic-sensitive TASK-like background potassium channel in rat arterial chemoreceptor cells. *J Physiol* 525: 135–142, 2000.
39. **Budde T, Coulon P, Pawlowski M, Meuth P, Kanyshkova T, Japes A, Meuth SG, Pape HC.** Reciprocal modulation of I_h and I_{TASK} in thalamocortical relay neurons by halothane. *Pflügers Arch* 456: 1061–1073, 2008.
40. **Burdakov D, Jensen LT, Alexopoulos H, Williams RH, Fearon IM, O'Kelly I, Gerasimenko O, Fugger L, Verkhratsky A.** Tandem-pore K^+ channels mediate inhibition of orexin neurons by glucose. *Neuron* 50: 711–722, 2006.
41. **Burdakov D, Lesage F.** Glucose-induced inhibition: how many ionic mechanisms? *Acta Physiol*. In press.
42. **Bushell T, Clarke C, Mathie A, Robertson B.** Pharmacological characterization of a non-inactivating outward current observed in mouse cerebellar Purkinje neurones. *Br J Pharmacol* 135: 705–712, 2002.
43. **Cain SM, Meadows HJ, Dunlop J, Bushell TJ.** mGlu4 potentiation of K(2P)2.1 is dependant on C-terminal dephosphorylation. *Mol Cell Neurosci* 37: 32–39, 2008.
44. **Caley AJ, Gruss M, Franks NP.** The effects of hypoxia on the modulation of human TREK-1 potassium channels. *J Physiol* 562: 205–212, 2005.
45. **Campanucci VA, Brown ST, Hudasek K, O'Kelly IM, Nurse CA, Fearon IM.** O_2 sensing by recombinant TWIK-related halothane-inhibitable K^+ channel-1 background K^+ channels heterologously expressed in human embryonic kidney cells. *Neuroscience* 135: 1087–1094, 2005.
46. **Campanucci VA, Fearon IM, Nurse CA.** A novel O_2-sensing mechanism in rat glossopharyngeal neurones mediated by a halothane-inhibitable background K^+ conductance. *J Physiol* 548: 731–743, 2003.
47. **Chavez RA, Gray AT, Zhao BB, Kindler CH, Mazurek MJ, Mehta Y, Forsayeth JR, Yost CS.** TWIK-2, a new weak inward rectifying member of the tandem pore domain potassium channel family. *J Biol Chem* 274: 7887–7892, 1999.
48. **Chemin J, Girard C, Duprat F, Lesage F, Romey G, Lazdunski M.** Mechanisms underlying excitatory effects of group I metabotropic glutamate receptors via inhibition of 2P domain K^+ channels. *EMBO J* 22: 5403–5411, 2003.
49. **Chemin J, Monteil A, Perez-Reyes E, Nargeot J, Lory P.** Direct inhibition of T-type calcium channels by the endogenous cannabinoid anandamide. *EMBO J* 20: 7033–7040, 2001.

50. **Chemin J, Patel A, Duprat F, Zanzouri M, Lazdunski M, Honore E.** Lysophosphatidic acid-operated K^+ channels. *J Biol Chem* 280: 4415–4421, 2005.
51. **Chemin J, Patel AJ, Duprat F, Lauritzen I, Lazdunski M, Honore E.** A phospholipid sensor controls mechanogating of the K^+ channel TREK-1. *EMBO J* 24: 44–53, 2005.
52. **Chemin J, Patel AJ, Duprat F, Sachs F, Lazdunski M, Honore E.** Up- and down-regulation of the mechano-gated K(2P) channel TREK-1 by PIP_2 and other membrane phospholipids. *Pflügers Arch* 455: 97–103, 2007.
53. **Chen WC, Davis RL.** Voltage-gated and two-pore-domain potassium channels in murine spiral ganglion neurons. *Hear Res* 222: 89–99, 2006.
54. **Chen X, Talley EM, Patel N, Gomis A, McIntire WE, Dong B, Viana F, Garrison JC, Bayliss DA.** Inhibition of a background potassium channel by Gq protein alpha-subunits. *Proc Natl Acad Sci USA* 103: 3422–3427, 2006.
55. **Choisy SC, Hancox JC, Arberry LA, Reynolds AM, Shattock MJ, James AF.** Evidence for a novel K^+ channel modulated by α_{1A}-adrenoceptors in cardiac myocytes. *Mol Pharmacol* 66: 735–748, 2004.
56. **Chvanov M, Petersen OH, Tepikin A.** Free radicals and the pancreatic acinar cells: role in physiology and pathology. *Philos Trans R Soc Lond B Biol Sci* 360: 2273–2284, 2005.
57. **Clarke CE, Veale EL, Green PJ, Meadows HJ, Mathie A.** Selective block of the human 2-P domain potassium channel, TASK-3, the native leak potassium current, I_{KSO}, by zinc. *J Physiol* 560: 51–62, 2004.
58. **Clarke CE, Veale EL, Wyse K, Vandenberg JI, Mathie A.** The M1P1 loop of TASK3 K2P channels apposes the selectivity filter and influences channel function. *J Biol Chem* 283: 16985–16992, 2008.
59. **Cluzeaud F, Reyes R, Escoubet B, Fay M, Lazdunski M, Bonvalet JP, Lesage F, Farman N.** Expression of TWIK-1, a novel weakly inward rectifying potassium channel in rat kidney. *Am J Physiol Cell Physiol* 275: C1602–C1609, 1998.
60. **Cohen A, Ben Abu Y, Hen S, Zilberberg N.** A novel mechanism for human K2P2.1 channel gating. Facilitation of C-type gating by protonation of extracellular histidine residues. *J Biol Chem* 283: 19448–19455, 2008.
61. **Cui YL, Holt AG, Lomax CA, Altschuler RA.** Deafness associated changes in two-pore domain potassium channels in the rat inferior colliculus. *Neuroscience* 149: 421–433, 2007.
62. **Czempinski K, Zimmermann S, Ehrhardt T, Muller-Rober B.** New structure and function in plant K^+ channels: KCO1, an outward rectifier with a steep Ca^{2+} dependency. *EMBO J* 16: 2565–2575, 1997.
63. **Czirják G, Enyedi P.** Formation of functional heterodimers between the TASK-1 and TASK-3 two-pore domain potassium channel subunits. *J Biol Chem* 277: 5426–5432, 2002.
64. **Czirják G, Enyedi P.** TASK-3 dominates the background potassium conductance in rat adrenal glomerulosa cells. *Mol Endocrinol* 16: 621–629, 2002.
65. **Czirják G, Enyedi P.** Ruthenium red inhibits TASK-3 potassium channel by interconnecting glutamate 70 of the two subunits. *Mol Pharmacol* 63: 646–652, 2003.
66. **Czirják G, Enyedi P.** Targeting of calcineurin to an NFAT-like docking site is required for the calcium-dependent activation of the background K^+ channel, TRESK. *J Biol Chem* 281: 14677–14682, 2006.
67. **Czirják G, Enyedi P.** Zinc and mercuric ions distinguish TRESK from the other two-pore-domain K^+ channels. *Mol Pharmacol* 69: 1024–1032, 2006.
68. **Czirják G, Fischer T, Spät A, Lesage F, Enyedi P.** TASK (TWIK-related acid-sensitive K^+ channel) is expressed in glomerulosa cells of rat adrenal cortex and inhibited by angiotensin II. *Mol Endocrinol* 14: 863–874, 2000.
69. **Czirják G, Pethető GL, Spät A, Enyedi P.** Inhibition of TASK-1 potassium channel by phospholipase C. *Am J Physiol Cell Physiol* 281: C700–C708, 2001.
70. **Czirják G, Tóth ZE, Enyedi P.** The two-pore domain K^+ channel, TRESK, is activated by the cytoplasmic calcium signal through calcineurin. *J Biol Chem* 279: 18550–18558, 2004.
71. **Czirják G, Vuity D, Enyedi P.** Phosphorylation-dependent binding of 14-3-3 proteins controls TRESK regulation. *J Biol Chem* 283: 15672–15680, 2008.
72. **Dallas ML, Scragg JL, Peers C.** Modulation of hTREK-1 by carbon monoxide. *Neuroreport* 19: 345–348, 2008.
73. **Danthi S, Enyeart JA, Enyeart JJ.** Modulation of native TREK-1 and Kv1.4 K^+ channels by polyunsaturated fatty acids and lysophospholipids. *J Membr Biol* 195: 147–164, 2003.
74. **Davies LA, Hu C, Guagliardo NA, Sen N, Chen X, Talley EM, Carey RM, Bayliss DA, Barrett PQ.** TASK channel deletion in mice causes primary hyperaldosteronism. *Proc Natl Acad Sci USA* 105: 2203–2208, 2008.
75. **Davis KA, Cowley EA.** Two-pore-domain potassium channels support anion secretion from human airway Calu-3 epithelial cells. *Pflügers Arch* 451: 631–641, 2006.
76. **De la Cruz IP, Levin JZ, Cummins C, Anderson P, Horvitz HR.** Sup-9, sup-10, and unc-93 may encode components of a two-pore K^+ channel that coordinates muscle contraction in *Caenorhabditis elegans*. *J Neurosci* 23: 9133–9145, 2003.
77. **Decher N, Maier M, Dittrich W, Gassenhuber J, Bruggemann A, Busch AE, Steinmeyer K.** Characterization of TASK-4, a novel member of the pH-sensitive, two-pore domain potassium channel family. *FEBS Lett* 492: 84–89, 2001.
78. **Decressac S, Franco M, Bendahhou S, Warth R, Knauer S, Barhanin J, Lazdunski M, Lesage F.** ARF6-dependent interaction of the TWIK1 K^+ channel with EFA6, a GDP/GTP exchange factor for ARF6. *EMBO Rep* 5: 1171–1175, 2004.
79. **Desai R, Peretz A, Idelson H, Lazarovici P, Attali B.** Ca^{2+}-activated K^+ channels in human leukemic Jurkat T cells. Molecular cloning, biochemical and functional characterization. *J Biol Chem* 275: 39954–39963, 2000.
80. **Dhaka A, Murray AN, Mathur J, Earley TJ, Petrus MJ, Patapoutian A.** TRPM8 is required for cold sensation in mice. *Neuron* 54: 371–378, 2007.
81. **Dobler T, Springauf A, Tovornik S, Weber M, Schmitt A, Sedlmeier R, Wischmeyer E, Doring F.** TRESK two-pore-domain K^+ channels constitute a significant component of background potassium currents in murine dorsal root ganglion neurones. *J Physiol* 585: 867–879, 2007.
82. **Dorai T, Gehani N, Katz A.** Therapeutic potential of curcumin in human prostate cancer. I. Curcumin induces apoptosis in both androgen-dependent and androgen-independent prostate cancer cells. *Prostate Cancer Prostatic Dis* 3: 84–93, 2000.
83. **Duprat F, Girard C, Jarretou G, Lazdunski M.** Pancreatic two P domain K^+ channels TALK-1 and TALK-2 are activated by nitric oxide and reactive oxygen species. *J Physiol* 562: 235–244, 2005.
84. **Duprat F, Lesage F, Fink M, Reyes R, Heurteaux C, Lazdunski M.** TASK, a human background K^+ channel to sense external pH variations near physiological pH. *EMBO J* 16: 5464–5471, 1997.
85. **Duprat F, Lesage F, Patel AJ, Fink M, Romey G, Lazdunski M.** The neuroprotective agent riluzole activates the two P domain K^+ channels TREK-1 and TRAAK. *Mol Pharmacol* 57: 906–912, 2000.
86. **Ellinghaus P, Scheubel RJ, Dobrev D, Ravens U, Holtz J, Huetter J, Nielsch U, Morawietz H.** Comparing the global mRNA expression profile of human atrial and ventricular myocardium with high-density oligonucleotide arrays. *J Thorac Cardiovasc Surg* 129: 1383–1390, 2005.
87. **Enyeart JA, Danthi S, Enyeart JJ.** Corticotropin induces the expression of TREK-1 mRNA and K^+ current in adrenocortical cells. *Mol Pharmacol* 64: 132–142, 2003.
88. **Enyeart JA, Danthi SJ, Enyeart JJ.** TREK-1 K^+ channels couple angiotensin II receptors to membrane depolarization and aldosterone secretion in bovine adrenal glomerulosa cells. *Am J Physiol Endocrinol Metab* 287: E1154–E1165, 2004.
89. **Enyeart JA, Liu H, Enyeart JJ.** Curcumin inhibits bTREK-1 K^+ channels and stimulates cortisol secretion from adrenocortical cells. *Biochem Biophys Res Commun* 370: 623–628, 2008.
90. **Enyeart JJ, Gomora JC, Xu L, Enyeart JA.** Adenosine triphosphate activates a noninactivating K^+ current in adrenal cortical cells through nonhydrolytic binding. *J Gen Physiol* 110: 679–692, 1997.
91. **Enyeart JJ, Mlinar B, Enyeart JA.** Adrenocorticotropic hormone and cAMP inhibit noninactivating K^+ current in adrenocor-

tical cells by an A-kinase-independent mechanism requiring ATP hydrolysis. *J Gen Physiol* 108: 251–264, 1996.
92. **Enyeart JJ, Xu L, Danthi S, Enyeart JA.** An ACTH- and ATP-regulated background K^+ channel in adrenocortical cells is TREK-1. *J Biol Chem* 277: 49186–49199, 2002.
93. **Enyeart JJ, Xu L, Gomora JC, Enyeart JA.** Reciprocal modulation of voltage-gated and background K^+ channels mediated by nucleotides and corticotropin. *Mol Pharmacol* 60: 114–123, 2001.
94. **Evans AM, Hardie DG, Galione A, Peers C, Kumar P, Wyatt CN.** AMP-activated protein kinase couples mitochondrial inhibition by hypoxia to cell-specific Ca^{2+} signalling mechanisms in oxygen-sensing cells. *Novartis Found Symp* 272: 234–252, 2006.
95. **Fearon IM, Zhang M, Vollmer C, Nurse CA.** GABA mediates autoreceptor feedback inhibition in the rat carotid body via presynaptic $GABA_B$ receptors and TASK-1. *J Physiol* 553: 83–94, 2003.
96. **Feliciangeli S, Bendahhou S, Sandoz G, Gounon P, Reichold M, Warth R, Lazdunski M, Barhanin J, Lesage F.** Does sumoylation control K2P1/TWIK1 background K^+ channels? *Cell* 130: 563–569, 2007.
97. **Ferrari U, Empl M, Kim KS, Sostak P, Forderreuther S, Straube A.** Calcineurin inhibitor-induced headache: clinical characteristics and possible mechanisms. *Headache* 45: 211–214, 2005.
98. **Filosa JA, Putnam RW.** Multiple targets of chemosensitive signaling in locus coeruleus neurons: role of K^+ and Ca^{2+} channels. *Am J Physiol Cell Physiol* 284: C145–C155, 2003.
99. **Fink M, Duprat F, Lesage F, Reyes R, Romey G, Heurteaux C, Lazdunski M.** Cloning, functional expression and brain localization of a novel unconventional outward rectifier K^+ channel. *EMBO J* 15: 6854–6862, 1996.
100. **Fink M, Lesage F, Duprat F, Heurteaux C, Reyes R, Fosset M, Lazdunski M.** A neuronal two P domain K^+ channel stimulated by arachidonic acid and polyunsaturated fatty acids. *EMBO J* 17: 3297–3308, 1998.
101. **Fong P, Argent BE, Guggino WB, Gray MA.** Characterization of vectorial chloride transport pathways in the human pancreatic duct adenocarcinoma cell line HPAF. *Am J Physiol Cell Physiol* 285: C433–C445, 2003.
102. **Franco M, Peters PJ, Boretto J, van Donselaar E, Neri A, D'Souza-Schorey C, Chavrier P.** EFA6, a sec7 domain-containing exchange factor for ARF6, coordinates membrane recycling and actin cytoskeleton organization. *EMBO J* 18: 1480–1491, 1999.
103. **Franks NP, Lieb WR.** Molecular and cellular mechanisms of general anaesthesia. *Nature* 367: 607–614, 1994.
104. **Fraser DD, Hoehn K, Weiss S, MacVicar BA.** Arachidonic acid inhibits sodium currents and synaptic transmission in cultured striatal neurons. *Neuron* 11: 633–644, 1993.
105. **Fraser SP, Grimes JA, Diss JK, Stewart D, Dolly JO, Djamgoz MB.** Predominant expression of Kv1.3 voltage-gated K^+ channel subunit in rat prostate cancer cell lines: electrophysiological, pharmacological and molecular characterisation. *Pflügers Arch* 446: 559–571, 2003.
106. **Frech GC, VanDongen AM, Schuster G, Brown AM, Joho RH.** A novel potassium channel with delayed rectifier properties isolated from rat brain by expression cloning. *Nature* 340: 642–645, 1989.
107. **Frizzo ME, Dall'Onder LP, Dalcin KB, Souza DO.** Riluzole enhances glutamate uptake in rat astrocyte cultures. *Cell Mol Neurobiol* 24: 123–128, 2004.
108. **Gaborit N, Steenman M, Lamirault G, Le Meur N, Le Bouter S, Lande G, Leger J, Charpentier F, Christ T, Dobrev D, Escande D, Nattel S, Demolombe S.** Human atrial ion channel and transporter subunit gene-expression remodeling associated with valvular heart disease and atrial fibrillation. *Circulation* 112: 471–481, 2005.
109. **Gabriel A, Abdallah M, Yost CS, Winegar BD, Kindler CH.** Localization of the tandem pore domain K^+ channel KCNK5 (TASK-2) in the rat central nervous system. *Brain Res* 98: 153–163, 2002.
110. **Gardener MJ, Johnson IT, Burnham MP, Edwards G, Heagerty AM, Weston AH.** Functional evidence of a role for two-pore domain potassium channels in rat mesenteric and pulmonary arteries. *Br J Pharmacol* 142: 192–202, 2004.
111. **Garry A, Fromy B, Blondeau N, Henrion D, Brau F, Gounon P, Guy N, Heurteaux C, Lazdunski M, Saumet JL.** Altered acetylcholine, bradykinin and cutaneous pressure-induced vasodilation in mice lacking the TREK1 potassium channel: the endothelial link. *EMBO Rep* 8: 354–359, 2007.
112. **Girard C, Duprat F, Terrenoire C, Tinel N, Fosset M, Romey G, Lazdunski M, Lesage F.** Genomic and functional characteristics of novel human pancreatic 2P domain K^+ channels. *Biochem Biophys Res Commun* 282: 249–256, 2001.
113. **Girard C, Tinel N, Terrenoire C, Romey G, Lazdunski M, Borsotto M.** p11, an annexin II subunit, an auxiliary protein associated with the background K^+ channel, TASK-1. *EMBO J* 21: 4439–4448, 2002.
114. **Goldman DE.** Potential, impedance and rectification in membranes. *J Gen Physiol* 27: 37–60, 1943.
115. **Goldstein SA, Bayliss DA, Kim D, Lesage F, Plant LD, Rajan S.** International Union of Pharmacology. LV. Nomenclature and molecular relationships of two-P potassium channels. *Pharmacol Rev* 57: 527–540, 2005.
116. **Goldstein SA, Price LA, Rosenthal DN, Pausch MH.** ORK1, a potassium-selective leak channel with two pore domains cloned from *Drosophila melanogaster* by expression in *Saccharomyces cerevisiae*. *Proc Natl Acad Sci USA* 93: 13256–13261, 1996.
117. **Goldstein SA, Wang KW, Ilan N, Pausch MH.** Sequence and function of the two P domain potassium channels: implications of an emerging superfamily. *J Mol Med* 76: 13–20, 1998.
118. **Gönczi M, Szentandrássy N, Johnson IT, Heagerty AM, Weston AH.** Investigation of the role of TASK-2 channels in rat pulmonary arteries: pharmacological and functional studies following RNA interference procedures. *Br J Pharmacol* 147: 496–505, 2006.
119. **Gonzalez JA, Jensen LT, Doyle SE, Miranda-Anaya M, Menaker M, Fugger L, Bayliss DA, Burdakov D.** Deletion of TASK1 and TASK3 channels disrupts intrinsic excitability but does not abolish glucose or pH responses of orexin/hypocretin neurons. *Eur J Neurosci* 30: 57–64, 2009.
120. **Graham V, Zhang H, Willis S, Creazzo TL.** Expression of a two-pore domain K^+ channel (TASK-1) in developing avian and mouse ventricular conduction systems. *Dev Dyn* 235: 143–151, 2006.
121. **Gruss M, Bushell TJ, Bright DP, Lieb WR, Mathie A, Franks NP.** Two-pore-domain K^+ channels are a novel target for the anesthetic gases xenon, nitrous oxide, and cyclopropane. *Mol Pharmacol* 65: 443–452, 2004.
122. **Gu W, Schlichthorl G, Hirsch JR, Engels H, Karschin C, Karschin A, Derst C, Steinlein OK, Daut J.** Expression pattern and functional characteristics of two novel splice variants of the two-pore-domain potassium channel TREK-2. *J Physiol* 539: 657–668, 2002.
123. **Gurney AM, Osipenko ON, MacMillan D, McFarlane KM, Tate RJ, Kempsill FE.** Two-pore domain K channel, TASK-1, in pulmonary artery smooth muscle cells. *Circ Res* 93: 957–964, 2003.
124. **Guyon A, Tardy MP, Rovere C, Nahon JL, Barhanin J, Lesage F.** Glucose inhibition persists in hypothalamic neurons lacking tandem-pore K^+ channels. *J Neurosci* 29: 2528–2533, 2009.
125. **Han J, Kang D, Kim D.** Functional properties of four splice variants of a human pancreatic tandem-pore K^+ channel, TALK-1. *Am J Physiol Cell Physiol* 285: C529–C538, 2003.
126. **Han J, Truell J, Gnatenco C, Kim D.** Characterization of four types of background potassium channels in rat cerebellar granule neurons. *J Physiol* 542: 431–444, 2002.
127. **Harinath S, Sikdar SK.** Trichloroethanol enhances the activity of recombinant human TREK-1 and TRAAK channels. *Neuropharmacology* 46: 750–760, 2004.
128. **Hartness ME, Lewis A, Searle GJ, O'Kelly I, Peers C, Kemp PJ.** Combined antisense and pharmacological approaches implicate hTASK as an airway O_2 sensing K^+ channel. *J Biol Chem* 276: 26499–26508, 2001.
129. **Hebert T, Drapeau P, Pradier L, Dunn RJ.** Block of the rat brain IIA sodium channel alpha subunit by the neuroprotective drug riluzole. *Mol Pharmacol* 45: 1055–1060, 1994.
130. **Heitzmann D, Derand R, Jungbauer S, Bandulik S, Sterner C, Schweda F, El Wakil A, Lalli E, Guy N, Mengual R, Reichold**

M, Tegtmeier I, Bendahhou S, Gomez-Sanchez CE, Aller MI, Wisden W, Weber A, Lesage F, Warth R, Barhanin J. Invalidation of TASK1 potassium channels disrupts adrenal gland zonation and mineralocorticoid homeostasis. *EMBO J* 27: 179–187, 2008.

131. **Heurteaux C, Guy N, Laigle C, Blondeau N, Duprat F, Mazzuca M, Lang-Lazdunski L, Widmann C, Zanzouri M, Romey G, Lazdunski M.** TREK-1, a K^+ channel involved in neuroprotection and general anesthesia. *EMBO J* 23: 2684–2695, 2004.
132. **Heurteaux C, Laigle C, Blondeau N, Jarretou G, Lazdunski M.** Alpha-linolenic acid and riluzole treatment confer cerebral protection and improve survival after focal brain ischemia. *Neuroscience* 137: 241–251, 2006.
133. **Heurteaux C, Lucas G, Guy N, El Yacoubi M, Thummler S, Peng XD, Noble F, Blondeau N, Widmann C, Borsotto M, Gobbi G, Vaugeois JM, Debonnel G, Lazdunski M.** Deletion of the background potassium channel TREK-1 results in a depression-resistant phenotype. *Nat Neurosci* 9: 1134–1141, 2006.
134. **Hiraoka M, Kawano S, Hirano Y, Furukawa T.** Role of cardiac chloride currents in changes in action potential characteristics and arrhythmias. *Cardiovasc Res* 40: 23–33, 1998.
135. **Hodgkin AL, Huxley AF.** Potassium leakage from an active nerve fibre. *J Physiol* 106: 341–367, 1947.
136. **Hodgkin AL, Huxley AF.** A quantitative description of membrane current and its application to conduction and excitation in nerve. *J Physiol* 117: 500–544, 1952.
137. **Hodgkin AL, Katz B.** The effect of sodium ions on the electrical activity of the giant axon of the squid. *J Physiol* 108: 37–77, 1949.
138. **Holt AG, Asako M, Duncan RK, Lomax CA, Juiz JM, Altschuler RA.** Deafness associated changes in expression of two-pore domain potassium channels in the rat cochlear nucleus. *Hear Res* 216–217: 146–153, 2006.
139. **Holter J, Carter D, Leresche N, Crunelli V, Vincent P.** A TASK3 channel (KCNK9) mutation in a genetic model of absence epilepsy. *J Mol Neurosci* 25: 37–51, 2005.
140. **Honore E, Maingret F, Lazdunski M, Patel AJ.** An intracellular proton sensor commands lipid- and mechano-gating of the K^+ channel TREK-1. *EMBO J* 21: 2968–2976, 2002.
141. **Hopwood SE, Trapp S.** TASK-like K^+ channels mediate effects of 5-HT and extracellular pH in rat dorsal vagal neurones in vitro. *J Physiol* 568: 145–154, 2005.
142. **Hsu K, Seharaseyon J, Dong P, Bour S, Marban E.** Mutual functional destruction of HIV-1 Vpu and host TASK-1 channel. *Mol Cell* 14: 259–267, 2004.
143. **Inglis SK, Brown SG, Constable MJ, McTavish N, Olver RE, Wilson SM.** A Ba^{2+}-resistant, acid-sensitive K^+ conductance in Na^+-absorbing H441 human airway epithelial cells. *Am J Physiol Lung Cell Mol Physiol* 292: L1304–L1312, 2007.
144. **Jones SA, Morton MJ, Hunter M, Boyett MR.** Expression of TASK-1, a pH-sensitive twin-pore domain K^+ channel, in rat myocytes. *Am J Physiol Heart Circ Physiol* 283: H181–H185, 2002.
145. **Kananura C, Sander T, Rajan S, Preisig-Muller R, Grzeschik KH, Daut J, Derst C, Steinlein OK.** Tandem pore domain K^+-channel TASK-3 (KCNK9) and idiopathic absence epilepsies. *Am J Med Genet* 114: 227–229, 2002.
146. **Kang D, Choe C, Kim D.** Thermosensitivity of the two-pore domain K^+ channels TREK-2 and TRAAK. *J Physiol* 564: 103–116, 2005.
147. **Kang D, Han J, Kim D.** Mechanism of inhibition of TREK-2 (K2P10.1) by the Gq-coupled M3 muscarinic receptor. *Am J Physiol Cell Physiol* 291: C649–C656, 2006.
148. **Kang D, Han J, Talley EM, Bayliss DA, Kim D.** Functional expression of TASK-1/TASK-3 heteromers in cerebellar granule cells. *J Physiol* 554: 64–77, 2004.
149. **Kang D, Kim D.** Single-channel properties and pH sensitivity of two-pore domain K^+ channels of the TALK family. *Biochem Biophys Res Commun* 315: 836–844, 2004.
150. **Kang D, Kim D.** TREK2 (K2P10.1) and TRESK (K2P18.1) are major background K^+ channels in dorsal root ganglion neurons. *Am J Physiol Cell Physiol* 291: C138–C146, 2006.
151. **Kang D, Kim GT, Kim EJ, La JH, Lee JS, Lee ES, Park JY, Hong SG, Han J.** Lamotrigine inhibits TRESK regulated by G-protein coupled receptor agonists. *Biochem Biophys Res Commun* 367: 609–615, 2008.
152. **Kang D, Mariash E, Kim D.** Functional expression of TRESK-2, a new member of the tandem-pore K^+ channel family. *J Biol Chem* 279: 28063–28070, 2004.
153. **Karschin C, Wischmeyer E, Preisig-Muller R, Rajan S, Derst C, Grzeschik KH, Daut J, Karschin A.** Expression pattern in brain of TASK-1, TASK-3, a tandem pore domain K^+ channel subunit, and TASK-5, associated with the central auditory nervous system. *Mol Cell Neurosci* 18: 632–648, 2001.
154. **Kelly D, Mackenzie L, Hunter P, Smaill B, Saint DA.** Gene expression of stretch-activated channels and mechanoelectric feedback in the heart. *Clin Exp Pharmacol Physiol* 33: 642–648, 2006.
155. **Kemp PJ, Lewis A, Hartness ME, Searle GJ, Miller P, O'Kelly I, Peers C.** Airway chemotransduction: from oxygen sensor to cellular effector. *Am J Respir Crit Care Med* 166: S17–S24, 2002.
156. **Kemp PJ, Searle GJ, Hartness ME, Lewis A, Miller P, Williams S, Wootton P, Adriaensen D, Peers C.** Acute oxygen sensing in cellular models: relevance to the physiology of pulmonary neuroepithelial and carotid bodies. *Anat Rec A Discov Mol Cell Evol Biol* 270: 41–50, 2003.
157. **Kennard LE, Chumbley JR, Ranatunga KM, Armstrong SJ, Veale EL, Mathie A.** Inhibition of the human two-pore domain potassium channel, TREK-1, by fluoxetine and its metabolite norfluoxetine. *Br J Pharmacol* 144: 821–829, 2005.
158. **Keshavaprasad B, Liu C, Au JD, Kindler CH, Cotten JF, Yost CS.** Species-specific differences in response to anesthetics and other modulators by the K2P channel TRESK. *Anesth Analg* 101: 1042–1049, 2005.
159. **Ketchum KA, Joiner WJ, Sellers AJ, Kaczmarek LK, Goldstein SA.** A new family of outwardly rectifying potassium channel proteins with two pore domains in tandem. *Nature* 376: 690–695, 1995.
160. **Kim CJ, Cho YG, Jeong SW, Kim YS, Kim SY, Nam SW, Lee SH, Yoo NJ, Lee JY, Park WS.** Altered expression of KCNK9 in colorectal cancers. *APMIS* 112: 588–594, 2004.
161. **Kim D.** A mechanosensitive K^+ channel in heart cells. Activation by arachidonic acid. *J Gen Physiol* 100: 1021–1040, 1992.
162. **Kim D, Cavanaugh EJ, Kim I, Carroll J.** Heteromeric TASK-1/TASK-3 is the major oxygen-sensitive background K^+ channel in rat carotid body glomus cells. *J Physiol* 2009.
163. **Kim D, Clapham DE.** Potassium channels in cardiac cells activated by arachidonic acid and phospholipids. *Science* 244: 1174–1176, 1989.
164. **Kim D, Fujita A, Horio Y, Kurachi Y.** Cloning and functional expression of a novel cardiac two-pore background K^+ channel (cTBAK-1). *Circ Res* 82: 513–518, 1998.
165. **Kim D, Gnatenco C.** TASK-5, a new member of the tandem-pore K^+ channel family. *Biochem Biophys Res Commun* 284: 923–930, 2001.
166. **Kim D, Sladek CD, Aguado-Velasco C, Mathiasen JR.** Arachidonic acid activation of a new family of K^+ channels in cultured rat neuronal cells. *J Physiol* 484: 643–660, 1995.
167. **Kim HI, Kim TH, Shin YK, Lee CS, Park M, Song JH.** Anandamide suppression of Na^+ currents in rat dorsal root ganglion neurons. *Brain Res* 1062: 39–47, 2005.
168. **Kim Y, Bang H, Gnatenco C, Kim D.** Synergistic interaction and the role of C-terminus in the activation of TRAAK K^+ channels by pressure, free fatty acids and alkali. *Pflügers Arch* 442: 64–72, 2001.
169. **Kim Y, Bang H, Kim D.** TBAK-1 and TASK-1, two-pore K^+ channel subunits: kinetic properties and expression in rat heart. *Am J Physiol Heart Circ Physiol* 277: H1669–H1678, 1999.
170. **Kim Y, Bang H, Kim D.** TASK-3, a new member of the tandem pore K^+ channel family. *J Biol Chem* 275: 9340–9347, 2000.
171. **Kim Y, Gnatenco C, Bang H, Kim D.** Localization of TREK-2 K^+ channel domains that regulate channel kinetics and sensitivity to pressure, fatty acids and pH_i. *Pflügers Arch* 442: 952–960, 2001.
172. **Kindler CH, Yost CS, Gray AT.** Local anesthetic inhibition of baseline potassium channels with two pore domains in tandem. *Anesthesiology* 90: 1092–1102, 1999.
173. **Koh SD, Monaghan K, Sergeant GP, Ro S, Walker RL, Sanders KM, Horowitz B.** TREK-1 regulation by nitric oxide and cGMP-dependent protein kinase. An essential role in smooth muscle inhibitory neurotransmission. *J Biol Chem* 276: 44338–44346, 2001.

174. **Koh SD, Sanders KM.** Stretch-dependent potassium channels in murine colonic smooth muscle cells. *J Physiol* 533: 155–163, 2001.
175. **Konu O, Kane JK, Barrett T, Vawter MP, Chang R, Ma JZ, Donovan DM, Sharp B, Becker KG, Li MD.** Region-specific transcriptional response to chronic nicotine in rat brain. *Brain Res* 909: 194–203, 2001.
176. **Koo JY, Jang Y, Cho H, Lee CH, Jang KH, Chang YH, Shin J, Oh U.** Hydroxy-alpha-sanshool activates TRPV1 and TRPA1 in sensory neurons. *Eur J Neurosci* 26: 1139–1147, 2007.
177. **Kovács I, Pocsai K, Czifra G, Sarkadi L, Szűcs G, Nemes Z, Rusznák Z.** TASK-3 immunoreactivity shows differential distribution in the human gastrointestinal tract. *Virchows Arch* 446: 402–410, 2005.
178. **Kreneisz O, Benoit JP, Bayliss DA, Mulkey DK.** AMP-activated protein kinase inhibits TREK channels. *J Physiol* 587: 5819–5830, 2009.
179. **Kubo Y, Baldwin TJ, Jan YN, Jan LY.** Primary structure and functional expression of a mouse inward rectifier potassium channel. *Nature* 362: 127–133, 1993.
180. **Kumar P.** Sensing hypoxia in the carotid body: from stimulus to response. *Essays Biochem* 43: 43–60, 2007.
181. **Kummer W, Yamamoto Y.** Cellular distribution of oxygen sensor candidates-oxidases, cytochromes, and K^+-channels–in the carotid body. *Microsc Res Tech* 59: 234–242, 2002.
182. **Kunkel MT, Johnstone DB, Thomas JH, Salkoff L.** Mutants of a temperature-sensitive two-P domain potassium channel. *J Neurosci* 20: 7517–7524, 2000.
183. **L'Hoste S, Poet M, Duranton C, Belfodil R, Barriere H, Rubera I, Tauc M, Poujeol C, Barhanin J, Poujeol P.** Role of TASK2 in the control of apoptotic volume decrease in proximal kidney cells. *J Biol Chem* 282: 36692–36703, 2007.
184. **Larkman PM, Perkins EM.** A TASK-like pH- and amine-sensitive "leak" K^+ conductance regulates neonatal rat facial motoneuron excitability in vitro. *Eur J Neurosci* 21: 679–691, 2005.
185. **Lauritzen I, Blondeau N, Heurteaux C, Widmann C, Romey G, Lazdunski M.** Polyunsaturated fatty acids are potent neuroprotectors. *EMBO J* 19: 1784–1793, 2000.
186. **Lauritzen I, Chemin J, Honore E, Jodar M, Guy N, Lazdunski M, Jane PA.** Cross-talk between the mechano-gated K2P channel TREK-1 and the actin cytoskeleton. *EMBO Rep* 6: 642–648, 2005.
187. **Lauritzen I, Zanzouri M, Honore E, Duprat F, Ehrengruber MU, Lazdunski M, Patel AJ.** K^+-dependent cerebellar granule neuron apoptosis. Role of task leak K^+ channels. *J Biol Chem* 278: 32068–32076, 2003.
188. **Leonoudakis D, Gray AT, Winegar BD, Kindler CH, Harada M, Taylor DM, Chavez RA, Forsayeth JR, Yost CS.** An open rectifier potassium channel with two pore domains in tandem cloned from rat cerebellum. *J Neurosci* 18: 868–877, 1998.
189. **Lesage F, Guillemare E, Fink M, Duprat F, Lazdunski M, Romey G, Barhanin J.** A pH-sensitive yeast outward rectifier K^+ channel with two pore domains and novel gating properties. *J Biol Chem* 271: 4183–4187, 1996.
190. **Lesage F, Guillemare E, Fink M, Duprat F, Lazdunski M, Romey G, Barhanin J.** TWIK-1, a ubiquitous human weakly inward rectifying K^+ channel with a novel structure. *EMBO J* 15: 1004–1011, 1996.
191. **Lesage F, Lauritzen I, Duprat F, Reyes R, Fink M, Heurteaux C, Lazdunski M.** The structure, function and distribution of the mouse TWIK-1 K^+ channel. *FEBS Lett* 402: 28–32, 1997.
192. **Lesage F, Maingret F, Lazdunski M.** Cloning and expression of human TRAAK, a polyunsaturated fatty acids-activated and mechano-sensitive K^+ channel. *FEBS Lett* 471: 137–140, 2000.
193. **Lesage F, Reyes R, Fink M, Duprat F, Guillemare E, Lazdunski M.** Dimerization of TWIK-1 K^+ channel subunits via a disulfide bridge. *EMBO J* 15: 6400–6407, 1996.
194. **Lesage F, Terrenoire C, Romey G, Lazdunski M.** Human TREK2, a 2P domain mechano-sensitive K^+ channel with multiple regulations by polyunsaturated fatty acids, lysophospholipids, G_s, G_i, and G_q protein-coupled receptors. *J Biol Chem* 275: 28398–28405, 2000.
195. **Levy DI, Velazquez H, Goldstein SA, Bockenhauer D.** Segment-specific expression of 2P domain potassium channel genes in human nephron. *Kidney Int* 65: 918–926, 2004.
196. **Lewis A, Hartness ME, Chapman CG, Fearon IM, Meadows HJ, Peers C, Kemp PJ.** Recombinant hTASK1 is an O_2-sensitive K^+ channel. *Biochem Biophys Res Commun* 285: 1290–1294, 2001.
197. **Li H, Rao A, Hogan PG.** Structural delineation of the calcineurin-NFAT interaction and its parallels to PP1 targeting interactions. *J Mol Biol* 342: 1659–1674, 2004.
198. **Li H, Zhang L, Rao A, Harrison SC, Hogan PG.** Structure of calcineurin in complex with PVIVIT peptide: portrait of a low-affinity signalling interaction. *J Mol Biol* 369: 1296–1306, 2007.
199. **Liedtke W.** Transient receptor potential vanilloid channels functioning in transduction of osmotic stimuli. *J Endocrinol* 191: 515–523, 2006.
200. **Lin W, Burks CA, Hansen DR, Kinnamon SC, Gilbertson TA.** Taste receptor cells express pH-sensitive leak K^+ channels. *J Neurophysiol* 92: 2909–2919, 2004.
201. **Lin W, Ogura T, Kinnamon SC.** Acid-activated cation currents in rat vallate taste receptor cells. *J Neurophysiol* 88: 133–141, 2002.
202. **Linden AM, Aller MI, Leppa E, Rosenberg PH, Wisden W, Korpi ER.** K^+ channel TASK-1 knockout mice show enhanced sensitivities to ataxic and hypnotic effects of $GABA_A$ receptor ligands. *J Pharmacol Exp Ther* 327: 277–286, 2008.
203. **Linden AM, Aller MI, Leppa E, Vekovischeva O, Aitta-Aho T, Veale EL, Mathie A, Rosenberg P, Wisden W, Korpi ER.** The in vivo contributions of TASK-1-containing channels to the actions of inhalation anesthetics, the α_2 adrenergic sedative dexmedetomidine, and cannabinoid agonists. *J Pharmacol Exp Ther* 317: 615–626, 2006.
204. **Linden AM, Sandu C, Aller MI, Vekovischeva OY, Rosenberg PH, Wisden W, Korpi ER.** TASK-3 knockout mice exhibit exaggerated nocturnal activity, impairments in cognitive functions, and reduced sensitivity to inhalation anesthetics. *J Pharmacol Exp Ther* 323: 924–934, 2007.
205. **Liu C, Au JD, Zou HL, Cotten JF, Yost CS.** Potent activation of the human tandem pore domain K channel TRESK with clinical concentrations of volatile anesthetics. *Anesth Analg* 99: 1715–1722, 2004.
206. **Liu C, Cotten JF, Schuyler JA, Fahlman CS, Au JD, Bickler PE, Yost CS.** Protective effects of TASK-3 (KCNK9) and related 2P K channels during cellular stress. *Brain Res* 1031: 164–173, 2005.
207. **Liu H, Enyeart JA, Enyeart JJ.** Angiotensin II inhibits native bTREK-1 K^+ channels through a PLC-, kinase C-, and PIP_2-independent pathway requiring ATP hydrolysis. *Am J Physiol Cell Physiol* 293: C682–C695, 2007.
208. **Liu H, Enyeart JA, Enyeart JJ.** ACTH inhibits bTREK-1 K^+ channels through multiple cAMP-dependent signaling pathways. *J Gen Physiol* 132: 279–294, 2008.
209. **Liu W, Saint DA.** Heterogeneous expression of tandem-pore K^+ channel genes in adult and embryonic rat heart quantified by real-time polymerase chain reaction. *Clin Exp Pharmacol Physiol* 31: 174–178, 2004.
210. **Lopes CM, Gallagher PG, Buck ME, Butler MH, Goldstein SA.** Proton block and voltage gating are potassium-dependent in the cardiac leak channel Kcnk3. *J Biol Chem* 275: 16969–16978, 2000.
211. **Lopes CM, Remon JI, Matavel A, Sui JL, Keselman I, Medei E, Shen Y, Rosenhouse-Dantsker A, Rohács T, Logothetis DE.** Protein kinase A modulates PLC-dependent regulation and PIP_2-sensitivity of K^+ channels. *Channels* 1: 124–134, 2007.
212. **Lopes CM, Rohács T, Czirják G, Balla T, Enyedi P, Logothetis DE.** PIP_2 hydrolysis underlies agonist-induced inhibition and regulates voltage gating of two-pore domain K^+ channels. *J Physiol* 564: 117–129, 2005.
213. **Lopes CM, Zilberberg N, Goldstein SA.** Block of Kcnk3 by protons. Evidence that 2-P-domain potassium channel subunits function as homodimers. *J Biol Chem* 276: 24449–24452, 2001.
214. **Lotshaw DP.** Biophysical and pharmacological characteristics of native two-pore domain TASK channels in rat adrenal glomerulosa cells. *J Membr Biol* 210: 51–70, 2006.
215. **Luedi PP, Dietrich FS, Weidman JR, Bosko JM, Jirtle RL, Hartemink AJ.** Computational and experimental identification of novel human imprinted genes. *Genome Res* 17: 1723–1730, 2007.
216. **Magloire H, Lesage F, Couble ML, Lazdunski M, Bleicher F.** Expression and localization of TREK-1 K^+ channels in human odontoblasts. *J Dent Res* 82: 542–545, 2003.

217. **Maingret F, Fosset M, Lesage F, Lazdunski M, Honore E.** TRAAK is a mammalian neuronal mechano-gated K^+ channel. *J Biol Chem* 274: 1381–1387, 1999.
218. **Maingret F, Honore E, Lazdunski M, Patel AJ.** Molecular basis of the voltage-dependent gating of TREK-1, a mechano-sensitive K^+ channel. *Biochem Biophys Res Commun* 292: 339–346, 2002.
219. **Maingret F, Lauritzen I, Patel AJ, Heurteaux C, Reyes R, Lesage F, Lazdunski M, Honore E.** TREK-1 is a heat-activated background K^+ channel. *EMBO J* 19: 2483–2491, 2000.
220. **Maingret F, Patel AJ, Lazdunski M, Honore E.** The endocannabinoid anandamide is a direct and selective blocker of the background K^+ channel TASK-1. *EMBO J* 20: 47–54, 2001.
221. **Maingret F, Patel AJ, Lesage F, Lazdunski M, Honore E.** Mechano- or acid stimulation, two interactive modes of activation of the TREK-1 potassium channel. *J Biol Chem* 274: 26691–26696, 1999.
222. **Maingret F, Patel AJ, Lesage F, Lazdunski M, Honore E.** Lysophospholipids open the two-pore domain mechano-gated K^+ channels TREK-1 and TRAAK. *J Biol Chem* 275: 10128–10133, 2000.
223. **Maruyama Y, Yamada M.** TREK-1: a potential target for novel antidepressants. *Nihon Shinkei Seishin Yakurigaku Zasshi* 27: 147–151, 2007.
224. **Mathie A, Veale EL.** Therapeutic potential of neuronal two-pore domain potassium-channel modulators. *Curr Opin Invest Drugs* 8: 555–562, 2007.
225. **Maylie J, Bond CT, Herson PS, Lee WS, Adelman JP.** Small conductance Ca^{2+}-activated K^+ channels and calmodulin. *J Physiol* 554: 255–261, 2004.
226. **Meadows HJ, Randall AD.** Functional characterisation of human TASK-3, an acid-sensitive two-pore domain potassium channel. *Neuropharmacology* 40: 551–559, 2001.
227. **Medhurst AD, Rennie G, Chapman CG, Meadows H, Duckworth MD, Kelsell RE, Gloger II, Pangalos MN.** Distribution analysis of human two pore domain potassium channels in tissues of the central nervous system and periphery. *Brain Res* 86: 101–114, 2001.
228. **Meuth SG, Aller MI, Munsch T, Schuhmacher T, Seidenbecher T, Meuth P, Kleinschnitz C, Pape HC, Wiendl H, Wisden W, Budde T.** The contribution of TWIK-related acid-sensitive K^+-containing channels to the function of dorsal lateral geniculate thalamocortical relay neurons. *Mol Pharmacol* 69: 1468–1476, 2006.
229. **Meuth SG, Bittner S, Meuth P, Simon OJ, Budde T, Wiendl H.** TWIK-related acid-sensitive K^+ channel 1 (TASK1) and TASK3 critically influence T lymphocyte effector functions. *J Biol Chem* 283: 14559–14570, 2008.
230. **Meuth SG, Budde T, Kanyshkova T, Broicher T, Munsch T, Pape HC.** Contribution of TWIK-related acid-sensitive K^+ channel 1 (TASK1) and TASK3 channels to the control of activity modes in thalamocortical neurons. *J Neurosci* 23: 6460–6469, 2003.
231. **Meuth SG, Herrmann AM, Ip CW, Kanyshkova T, Bittner S, Weishaupt A, Budde T, Wiendl H.** The two-pore domain potassium channel TASK3 functionally impacts glioma cell death. *J Neurooncol* 87: 263–270, 2008.
232. **Meuth SG, Kanyshkova T, Meuth P, Landgraf P, Munsch T, Ludwig A, Hofmann F, Pape HC, Budde T.** Membrane resting potential of thalamocortical relay neurons is shaped by the interaction among TASK3 and HCN2 channels. *J Neurophysiol* 96: 1517–1529, 2006.
233. **Millar ID, Taylor HC, Cooper GJ, Kibble JD, Barhanin J, Robson L.** Adaptive downregulation of a quinidine-sensitive cation conductance in renal principal cells of TWIK-1 knockout mice. *Pflügers Arch* 453: 107–116, 2006.
234. **Millar JA, Barratt L, Southan AP, Page KM, Fyffe REW, Robertson B, Mathie A.** A functional role for the two-pore domain potassium channel TASK-1 in cerebellar granule neurons. *Proc Natl Acad Sci USA* 97: 3614–3618, 2000.
235. **Miller P, Kemp PJ, Lewis A, Chapman CG, Meadows HJ, Peers C.** Acute hypoxia occludes hTREK-1 modulation: re-evaluation of the potential role of tandem P domain K^+ channels in central neuroprotection. *J Physiol* 548: 31–37, 2003.
236. **Miller P, Peers C, Kemp PJ.** Polymodal regulation of hTREK1 by pH, arachidonic acid, and hypoxia: physiological impact in acidosis and alkalosis. *Am J Physiol Cell Physiol* 286: C272–C282, 2004.
237. **Mlinar B, Biagi BA, Enyeart JJ.** A novel K^+ current inhibited by adrenocorticotropic hormone and angiotensin II in adrenal cortical cells. *J Biol Chem* 268: 8640–8644, 1993.
238. **Morais-Cabral JH, Zhou Y, MacKinnon R.** Energetic optimization of ion conduction rate by the K^+ selectivity filter. *Nature* 414: 37–42, 2001.
239. **Morton MJ, Abohamed A, Sivaprasadarao A, Hunter M.** pH sensing in the two-pore domain K^+ channel, TASK2. *Proc Natl Acad Sci USA* 102: 16102–16106, 2005.
240. **Morton MJ, Chipperfield S, Abohamed A, Sivaprasadarao A, Hunter M.** Na^+-induced inward rectification in the two-pore domain K^+ channel, TASK-2. *Am J Physiol Renal Physiol* 288: F162–F169, 2005.
241. **Morton MJ, O'Connell AD, Sivaprasadarao A, Hunter M.** Determinants of pH sensing in the two-pore domain K^+ channels TASK-1 and -2. *Pflügers Arch* 445: 577–583, 2003.
242. **Moshelion M, Becker D, Czempinski K, Mueller-Roeber B, Attali B, Hedrich R, Moran N.** Diurnal and circadian regulation of putative potassium channels in a leaf moving organ. *Plant Physiol* 128: 634–642, 2002.
243. **Mu D, Chen L, Zhang X, See LH, Koch CM, Yen C, Tong JJ, Spiegel L, Nguyen KC, Servoss A, Peng Y, Pei L, Marks JR, Lowe S, Hoey T, Jan LY, McCombie WR, Wigler MH, Powers S.** Genomic amplification and oncogenic properties of the KCNK9 potassium channel gene. *Cancer Cell* 3: 297–302, 2003.
244. **Mulkey DK, Stornetta RL, Weston MC, Simmons JR, Parker A, Bayliss DA, Guyenet PG.** Respiratory control by ventral surface chemoreceptor neurons in rats. *Nat Neurosci* 7: 1360–1369, 2004.
245. **Mulkey DK, Talley EM, Stornetta RL, Siegel AR, West GH, Chen X, Sen N, Mistry AM, Guyenet PG, Bayliss DA.** TASK channels determine pH sensitivity in select respiratory neurons but do not contribute to central respiratory chemosensitivity. *J Neurosci* 27: 14049–14058, 2007.
246. **Muller S, Hoege C, Pyrowolakis G, Jentsch S.** SUMO, ubiquitin's mysterious cousin. *Nat Rev Mol Cell Biol* 2: 202–210, 2001.
247. **Murbartian J, Lei Q, Sando JJ, Bayliss DA.** Sequential phosphorylation mediates receptor- and kinase-induced inhibition of TREK-1 background potassium channels. *J Biol Chem* 280: 30175–30184, 2005.
248. **Musset B, Meuth SG, Liu GX, Derst C, Wegner S, Pape HC, Budde T, Preisig-Muller R, Daut J.** Effects of divalent cations and spermine on the K^+ channel TASK-3 and on the outward current in thalamic neurons. *J Physiol* 572: 639–657, 2006.
249. **Nattel S.** New ideas about atrial fibrillation 50 years on. *Nature* 415: 219–226, 2002.
250. **Nicolas MT, Barhanin J, Reyes R, Dememes D.** Cellular localization of TWIK-1, a two-pore-domain potassium channel in the rodent inner ear. *Hear Res* 181: 20–26, 2003.
251. **Nie X, Arrighi I, Kaissling B, Pfaff I, Mann J, Barhanin J, Vallon V.** Expression and insights on function of potassium channel TWIK-1 in mouse kidney. *Pflügers Arch* 451: 479–488, 2005.
252. **Niemeyer MI, Gonzalez-Nilo FD, Zuniga L, Gonzalez W, Cid LP, Sepulveda FV.** Gating of two-pore domain K^+ channels by extracellular pH. *Biochem Soc Trans* 34: 899–902, 2006.
253. **Niemeyer MI, Gonzalez-Nilo FD, Zuniga L, Gonzalez W, Cid LP, Sepulveda FV.** Neutralization of a single arginine residue gates open a two-pore domain, alkali-activated K^+ channel. *Proc Natl Acad Sci USA* 104: 666–671, 2007.
254. **Noel J, Zimmermann K, Busserolles J, Deval E, Alloui A, Diochot S, Guy N, Borsotto M, Reeh P, Eschalier A, Lazdunski M.** The mechano-activated K^+ channels TRAAK and TREK-1 control both warm and cold perception. *EMBO J* 28: 1308–1318, 2009.
255. **O'Kelly I, Butler MH, Zilberberg N, Goldstein Forward transport SA.** 14-3-3 binding overcomes retention in endoplasmic reticulum by dibasic signals. *Cell* 111: 577–588, 2002.
256. **O'Kelly I, Goldstein SA.** Forward transport of K2p3.1: mediation by 14-3-3 and COPI, modulation by p11. *Traffic* 9: 72–78, 2008.
257. **O'Kelly I, Lewis A, Peers C, Kemp PJ.** O_2 sensing by airway chemoreceptor-derived cells. Protein kinase c activation reveals functional evidence for involvement of NADPH oxidase. *J Biol Chem* 275: 7684–7692, 2000.

258. **O'Kelly I, Stephens RH, Peers C, Kemp PJ.** Potential identification of the O_2-sensitive K^+ current in a human neuroepithelial body-derived cell line. *Am J Physiol Lung Cell Mol Physiol* 276: L96–L104, 1999.
259. **Olschewski A, Li Y, Tang B, Hanze J, Eul B, Bohle RM, Wilhelm J, Morty RE, Brau ME, Weir EK, Kwapiszewska G, Klepetko W, Seeger W, Olschewski H.** Impact of TASK-1 in human pulmonary artery smooth muscle cells. *Circ Res* 98: 1072–1080, 2006.
260. **Ordway RW, Walsh JV Jr, Singer JJ.** Arachidonic acid and other fatty acids directly activate potassium channels in smooth muscle cells. *Science* 244: 1176–1179, 1989.
261. **Orias M, Velazquez H, Tung F, Lee G, Desir GV.** Cloning and localization of a double-pore K channel, KCNK1: exclusive expression in distal nephron segments. *Am J Physiol Renal Physiol* 273: F663–F666, 1997.
262. **Ouadid-Ahidouch H, Ahidouch A.** K^+ channel expression in human breast cancer cells: involvement in cell cycle regulation and carcinogenesis. *J Membr Biol* 221: 1–6, 2008.
263. **Ozaita A, Vega-Saenz DM.** Cloning of two transcripts, HKT41a and HKT41b, from the human two-pore K^+ channel gene KCNK4 Chromosomal localization, tissue distribution and functional expression. *Brain Res* 102: 18–27, 2002.
264. **Pál B, Por A, Pocsai K, Szűcs G, Rusznák Z.** Voltage-gated and background K^+ channel subunits expressed by the bushy cells of the rat cochlear nucleus. *Hearing Res* 199: 57–70, 2005.
265. **Park KJ, Baker SA, Cho SY, Sanders KM, Koh SD.** Sulfur-containing amino acids block stretch-dependent K^+ channels and nitrergic responses in the murine colon. *Br J Pharmacol* 144: 1126–1137, 2005.
266. **Park KS, Jung KH, Kim SH, Kim KS, Choi MR, Kim Y, Chai YG.** Functional expression of ion channels in mesenchymal stem cells derived from umbilical cord vein. *Stem Cells* 25: 2044–2052, 2007.
267. **Patel AJ, Honore E.** Molecular physiology of oxygen-sensitive potassium channels. *Eur Respir J* 18: 221–227, 2001.
268. **Patel AJ, Honore E, Lesage F, Fink M, Romey G, Lazdunski M.** Inhalational anesthetics activate two-pore-domain background K^+ channels. *Nat Neurosci* 2: 422–426, 1999.
269. **Patel AJ, Honore E, Maingret F, Lesage F, Fink M, Duprat F, Lazdunski M.** A mammalian two pore domain mechano-gated S-like K^+ channel. *EMBO J* 17: 4283–4290, 1998.
270. **Patel AJ, Maingret F, Magnone V, Fosset M, Lazdunski M, Honore E.** TWIK2, an inactivating domain K^+ channel. *J Biol Chem* 275: 28722–28730, 2000.
271. **Peers C.** Effect of lowered extracellular pH on Ca^{2+}-dependent K^+ currents in type I cells from the neonatal rat carotid body. *J Physiol* 422: 381–395, 1990.
272. **Peers C.** Hypoxic suppression of K^+ currents in type I carotid body cells: selective effect on the Ca^{2+}-activated K^+ current. *Neurosci Lett* 119: 253–256, 1990.
273. **Pei L, Wiser O, Slavin A, Mu D, Powers S, Jan LY, Hoey T.** Oncogenic potential of TASK3 (Kcnk9) depends on K^+ channel function. *Proc Natl Acad Sci USA* 100: 7803–7807, 2003.
274. **Perez-Garcia MT, Colinas O, Miguel-Velado E, Moreno-Dominguez A, Lopez-Lopez JR.** Characterization of the Kv channels of mouse carotid body chemoreceptor cells and their role in oxygen sensing. *J Physiol* 557: 457–471, 2004.
275. **Perez-Garcia MT, Lopez-Lopez JR, Riesco AM, Hoppe UC, Marban E, Gonzalez C, Johns DC.** Viral gene transfer of dominant-negative Kv4 construct suppresses an O_2-sensitive K^+ current in chemoreceptor cells. *J Neurosci* 20: 5689–5695, 2000.
276. **Pocsai K, Kosztka L, Bakondi G, Gönczi M, Fodor J, Dienes B, Szentesi P, Kovács I, Feniger-Barish R, Kopf E, Zharhary D, Szucs G, Csernoch L, Rusznák Z.** Melanoma cells exhibit strong intracellular TASK-3-specific immunopositivity in both tissue sections and cell culture. *Cell Mol Life Sci* 63: 2364–2376, 2006.
277. **Poling JS, Rogawski MA, Salem N Jr, Vicini S.** Anandamide, an endogenous cannabinoid, inhibits Shaker-related voltage-gated K^+ channels. *Neuropharmacology* 35: 983–991, 1996.
278. **Pottosin II, Bonales-Alatorre E, Valencia-Cruz G, Mendoza-Magana ML, Dobrovinskaya OR.** TRESK-like potassium channels in leukemic T cells. *Pflügers Arch* 456: 1037–1048, 2008.
279. **Pountney DJ, Gulkarov I, Vega-Saenz DM, Holmes D, Saganich M, Rudy B, Artman M, Coetzee WA**. Identification and cloning of TWIK-originated similarity sequence (TOSS): a novel human 2-pore K^+ channel principal subunit. *FEBS Lett* 450: 191–196, 1999.
280. **Putzke C, Hanley PJ, Schlichthorl G, Preisig-Muller R, Rinne S, Anetseder M, Eckenhoff R, Berkowitz C, Vassiliou T, Wulf H, Eberhart L.** Differential effects of volatile and intravenous anesthetics on the activity of human TASK-1. *Am J Physiol Cell Physiol* 293: C1319–C1326, 2007.
281. **Putzke C, Wemhoner K, Sachse FB, Rinne S, Schlichthorl G, Li XT, Jae L, Eckhardt I, Wischmeyer E, Wulf H, Preisig-Muller R, Daut J, Decher N.** The acid-sensitive potassium channel TASK-1 in rat cardiac muscle. *Cardiovasc Res* 75: 59–68, 2007.
282. **Raghavendra Rao V, Dhodda VK, Song G, Bowen KK, Dempsey RJ.** Traumatic brain injury-induced acute gene expression changes in rat cerebral cortex identified by GeneChip analysis. *J Neurosci Res* 71: 208–219, 2003.
283. **Rajan S, Plant LD, Rabin ML, Butler MH, Goldstein SA.** Sumoylation silences the plasma membrane leak K^+ channel K2P1. *Cell* 121: 37–47, 2005.
284. **Rajan S, Preisig-Muller R, Wischmeyer E, Nehring R, Hanley PJ, Renigunta V, Musset B, Schlichthorl G, Derst C, Karschin A, Daut J.** Interaction with 14-3-3 proteins promotes functional expression of the potassium channels TASK-1 and TASK-3. *J Physiol* 545: 13–26, 2002.
285. **Rajan S, Wischmeyer E, Karschin C, Preisig-Muller R, Grzeschik KH, Daut J, Karschin A, Derst C.** THIK-1 and THIK-2, a novel subfamily of tandem pore domain K^+ channels. *J Biol Chem* 276: 7302–7311, 2001.
286. **Rajan S, Wischmeyer E, Xin LG, Preisig-Muller R, Daut J, Karschin A, Derst C.** TASK-3, a novel tandem pore domain acid-sensitive K^+ channel. An extracellular histidine as pH sensor. *J Biol Chem* 275: 16650–16657, 2000.
287. **Reid G, Flonta M.** Cold transduction by inhibition of a background potassium conductance in rat primary sensory neurones. *Neurosci Lett* 297: 171–174, 2001.
288. **Renigunta V, Yuan H, Zuzarte M, Rinne S, Koch A, Wischmeyer E, Schlichthorl G, Gao Y, Karschin A, Jacob R, Schwappach B, Daut J, Preisig-Muller R.** The retention factor p11 confers an endoplasmic reticulum-localization signal to the potassium channel TASK-1. *Traffic* 7: 168–181, 2006.
289. **Reyes R, Duprat F, Lesage F, Fink M, Salinas M, Farman N, Lazdunski M.** Cloning and expression of a novel pH-sensitive two pore domain K^+ channel from human kidney. *J Biol Chem* 273: 30863–30869, 1998.
290. **Richter TA, Dvoryanchikov GA, Chaudhari N, Roper SD.** Acid-sensitive two-pore domain potassium (K2P) channels in mouse taste buds. *J Neurophysiol* 92: 1928–1936, 2004.
291. **Riera CE, Menozzi-Smarrito C, Affolter M, Michlig S, Munari C, Robert F, Vogel H, Simon SA, le Coutre J.** Compounds from Sichuan and Melegueta peppers activate, covalently and non-covalently, TRPA1 and TRPV1 channels. *Br J Pharmacol* 157: 1398–1409, 2009.
292. **Rohács T, Chen J, Prestwich GD, Logothetis DE.** Distinct specificities of inwardly rectifying K^+ channels for phosphoinositides. *J Biol Chem* 274: 36065–36072, 1999.
293. **Rusznák Z, Bakondi G, Kosztka L, Pocsai K, Dienes B, Fodor J, Telek A, Gönczi M, Szűcs G, Csernoch L.** Mitochondrial expression of the two-pore domain TASK-3 channels in malignantly transformed and non-malignant human cells. *Virchows Arch* 452: 415–426, 2008.
294. **Salinas M, Reyes R, Lesage F, Fosset M, Heurteaux C, Romey G, Lazdunski M.** Cloning of a new mouse two-P domain channel subunit and a human homologue with a unique pore structure. *J Biol Chem* 274: 11751–11760, 1999.
295. **Salkoff L, Butler A, Ferreira G, Santi C, Wei A.** High-conductance potassium channels of the SLO family. *Nat Rev Neurosci* 7: 921–931, 2006.
296. **Sanders KM, Koh SD.** Two-pore-domain potassium channels in smooth muscles: new components of myogenic regulation. *J Physiol* 570: 37–43, 2006.

297. **Sandoz G, Tardy MP, Thummler S, Feliciangeli S, Lazdunski M, Lesage F.** Mtap2 is a constituent of the protein network that regulates twik-related K^+ channel expression and trafficking. *J Neurosci* 28: 8545–8552, 2008.
298. **Sandoz G, Thummler S, Duprat F, Feliciangeli S, Vinh J, Escoubas P, Guy N, Lazdunski M, Lesage F.** AKAP150, a switch to convert mechano-, pH- and arachidonic acid-sensitive TREK K^+ channels into open leak channels. *EMBO J* 25: 5864–5872, 2006.
299. **Sano Y, Inamura K, Miyake A, Mochizuki S, Kitada C, Yokoi H, Nozawa K, Okada H, Matsushime H, Furuichi K.** A novel two-pore domain K^+ channel, TRESK, is localized in the spinal cord. *J Biol Chem* 278: 27406–27412, 2003.
300. **Searle GJ, Hartness ME, Hoareau R, Peers C, Kemp PJ.** Lack of contribution of mitochondrial electron transport to acute O_2 sensing in model airway chemoreceptors. *Biochem Biophys Res Commun* 291: 332–337, 2002.
301. **Shyng SL, Nichols CG.** Membrane phospholipid control of nucleotide sensitivity of K_{ATP} channels. *Science* 282: 1138–1141, 1998.
302. **Sigurdson WJ, Morris CE.** Stretch-activated ion channels in growth cones of snail neurons. *J Neurosci* 9: 2801–2808, 1989.
303. **Simkin D, Cavanaugh EJ, Kim D.** Control of the single channel conductance of K2P10.1 (TREK-2) by the amino-terminus: role of alternative translation initiation. *J Physiol* 586: 5651–5663, 2008.
304. **Sirois JE, Lei Q, Talley EM, Lynch C, III, Bayliss DA.** The TASK-1 two-pore domain K^+ channel is a molecular substrate for neuronal effects of inhalation anesthetics. *J Neurosci* 20: 6347–6354, 2000.
305. **Spät A, Hunyady L.** Control of aldosterone secretion: a model for convergence in cellular signaling pathways. *Physiol Rev* 84: 489–539, 2004.
306. **Spitzner M, Martins JR, Soria RB, Ousingsawat J, Scheidt K, Schreiber R, Kunzelmann K.** Eag1 and Bestrophin 1 are up-regulated in fast-growing colonic cancer cells. *J Biol Chem* 283: 7421–7428, 2008.
307. **Stuhmer W, Alves F, Hartung F, Zientkowska M, Pardo LA.** Potassium channels as tumour markers. *FEBS Lett* 580: 2850–2852, 2006.
308. **Talley EM, Bayliss DA.** Modulation of TASK-1 (Kcnk3) and TASK-3 (Kcnk9) potassium channels: volatile anesthetics and neurotransmitters share a molecular site of action. *J Biol Chem* 277: 17733–17742, 2002.
309. **Talley EM, Lei Q, Sirois JE, Bayliss DA.** TASK-1, a two-pore domain K^+ channel, is modulated by multiple neurotransmitters in motoneurons. *Neuron* 25: 399–410, 2000.
310. **Talley EM, Solorzano G, Lei Q, Kim D, Bayliss DA.** CNS distribution of members of the two-pore-domain (KCNK) potassium channel family. *J Neurosci* 21: 7491–7505, 2001.
311. **Tan JH, Liu W, Saint DA.** Differential expression of the mechanosensitive potassium channel TREK-1 in epicardial and endocardial myocytes in rat ventricle. *Exp Physiol* 89: 237–242, 2004.
312. **Taylor NC, Li A, Nattie EE.** Medullary serotonergic neurones modulate the ventilatory response to hypercapnia, but not hypoxia in conscious rats. *J Physiol* 566: 543–557, 2005.
313. **Terrenoire C, Lauritzen I, Lesage F, Romey G, Lazdunski M.** A TREK-1-like potassium channel in atrial cells inhibited by beta-adrenergic stimulation and activated by volatile anesthetics. *Circ Res* 89: 336–342, 2001.
314. **Tertyshnikova S, Knox RJ, Plym MJ, Thalody G, Griffin C, Neelands T, Harden DG, Signor L, Weaver D, Myers RA, Lodge NJ.** BL-1249 [(5,6,7,8-tetrahydro-naphthalen-1-yl)-[2-(1H-tetrazol-5-yl)-phenyl]-amine]: a putative potassium channel opener with bladder-relaxant properties. *J Pharmacol Exp Ther* 313: 250–259, 2005.
315. **Theilig F, Goranova I, Hirsch JR, Wieske M, Unsal S, Bachmann S, Veh RW, Derst C.** Cellular localization of THIK-1 (K(2P)13.1) and THIK-2 (K(2P)121) K channels in the mammalian kidney. *Cell Physiol Biochem* 21: 63–74, 2008.
316. **Thomas D, Plant LD, Wilkens CM, McCrossan ZA, Goldstein SA.** Alternative translation initiation in rat brain yields K2P2.1 potassium channels permeable to sodium. *Neuron* 58: 859–870, 2008.
317. **Thummler S, Duprat F, Lazdunski M.** Antipsychotics inhibit TREK but not TRAAK channels. *Biochem Biophys Res Commun* 354: 284–289, 2007.
318. **Thut PD, Wrigley D, Gold MS.** Cold transduction in rat trigeminal ganglia neurons in vitro. *Neuroscience* 119: 1071–1083, 2003.
319. **Torborg CL, Berg AP, Jeffries BW, Bayliss DA, McBain CJ.** TASK-like conductances are present within hippocampal CA1 stratum oriens interneuron subpopulations. *J Neurosci* 26: 7362–7367, 2006.
320. **Trapp S, Aller MI, Wisden W, Gourine AV.** A role for TASK-1 (KCNK3) channels in the chemosensory control of breathing. *J Neurosci* 28: 8844–8850, 2008.
321. **Tsai SJ.** Sipatrigine could have therapeutic potential for major depression and bipolar depression through antagonism of the two-pore-domain K^+ channel TREK-1. *Med Hypotheses* 70: 548–550, 2008.
322. **Valencia-Cruz G, Shabala L, Delgado-Enciso I, Shabala S, Bonales-Alatorre E, Pottosin II, Dobrovinskaya OR.** K(bg) and Kv1.3 channels mediate potassium efflux in the early phase of apoptosis in Jurkat T lymphocytes. *Am J Physiol Cell Physiol* 297: C 1544–C1553, 2009.
323. **Veale EL, Buswell R, Clarke CE, Mathie A.** Identification of a region in the TASK3 two pore domain potassium channel that is critical for its blockade by methanandamide. *Br J Pharmacol* 152: 778–786, 2007.
324. **Veale EL, Kennard LE, Sutton GL, MacKenzie G, Sandu C, Mathie A.** G alpha(q)-mediated regulation of TASK3 two-pore domain potassium channels: the role of protein kinase C. *Mol Pharmacol* 71: 1666–1675, 2007.
325. **Vega-Saenz DM, Lau DH, Zhadina M, Pountney D, Coetzee WA, Rudy B.** KT32 and KT33, two novel human two-pore K^+ channels closely related to TASK-1. *J Neurophysiol* 86: 130–142, 2001.
326. **Voloshyna I, Besana A, Castillo M, Matos T, Weinstein IB, Mansukhani M, Robinson RB, Cordon-Cardo C, Feinmark SJ.** TREK-1 is a novel molecular target in prostate cancer. *Cancer Res* 68: 1197–1203, 2008.
327. **Vreugdenhil M, Bruehl C, Voskuyl RA, Kang JX, Leaf A, Wadman WJ.** Polyunsaturated fatty acids modulate sodium and calcium currents in CA1 neurons. *Proc Natl Acad Sci USA* 93: 12559–12563, 1996.
328. **Wang J, Zhang C, Li N, Su L, Wang G.** Expression of TASK-1 in brainstem and the occurrence of central sleep apnea in rats. *Respir Physiol Neurobiol* 161: 23–28, 2008.
329. **Wang Z, Yue L, White M, Pelletier G, Nattel S.** Differential distribution of inward rectifier potassium channel transcripts in human atrium versus ventricle. *Circulation* 98: 2422–2428, 1998.
330. **Warth R, Barriere H, Meneton P, Bloch M, Thomas J, Tauc M, Heitzmann D, Romeo E, Verrey F, Mengual R, Guy N, Bendahhou S, Lesage F, Poujeol P, Barhanin J.** Proximal renal tubular acidosis in TASK2 K^+ channel-deficient mice reveals a mechanism for stabilizing bicarbonate transport. *Proc Natl Acad Sci USA* 101: 8215–8220, 2004.
331. **Washburn CP, Sirois JE, Talley EM, Guyenet PG, Bayliss DA.** Serotonergic raphe neurons express TASK channel transcripts and a TASK-like pH- and halothane-sensitive K^+ conductance. *J Neurosci* 22: 1256–1265, 2002.
332. **Weber M, Schmitt A, Wischmeyer E, Doring F.** Excitability of pontine startle processing neurones is regulated by the two-pore-domain K^+ channel TASK-3 coupled to 5-HT_{2C} receptors. *Eur J Neurosci* 28: 931–940, 2008.
333. **Westphalen RI, Hemmings HC Jr.** Volatile anesthetic effects on glutamate versus GABA release from isolated rat cortical nerve terminals: basal release. *J Pharmacol Exp Ther* 316: 208–215, 2006.
334. **Westphalen RI, Krivitski M, Amarosa A, Guy N, Hemmings HC Jr.** Reduced inhibition of cortical glutamate and GABA release by halothane in mice lacking the K^+ channel, TREK-1. *Br J Pharmacol* 152: 939–945, 2007.
335. **Wijffels MC, Kirchhof CJ, Dorland R, Allessie MA.** Atrial fibrillation begets atrial fibrillation. A study in awake chronically instrumented goats. *Circulation* 92: 1954–1968, 1995.

336. **Williams RH, Jensen LT, Verkhratsky A, Fugger L, Burdakov D.** Control of hypothalamic orexin neurons by acid and CO_2. *Proc Natl Acad Sci USA* 104: 10685–10690, 2007.
337. **Wrenn RW, Currie MG, Herman LE.** Nitric oxide participates in the regulation of pancreatic acinar cell secretion. *Life Sci* 55: 511–518, 1994.
338. **Wyatt CN, Buckler KJ.** The effect of mitochondrial inhibitors on membrane currents in isolated neonatal rat carotid body type I cells. *J Physiol* 556: 175–191, 2004.
339. **Wyatt CN, Mustard KJ, Pearson SA, Dallas ML, Atkinson L, Kumar P, Peers C, Hardie DG, Evans AM.** AMP-activated protein kinase mediates carotid body excitation by hypoxia. *J Biol Chem* 282: 8092–8098, 2007.
340. **Xian TL, Dyachenko V, Zuzarte M, Putzke C, Preisig-Muller R, Isenberg G, Daut J.** The stretch-activated potassium channel TREK-1 in rat cardiac ventricular muscle. *Cardiovasc Res* 69: 86–97, 2006.
341. **Xiao Y, Li X.** Polyunsaturated fatty acids modify mouse hippocampal neuronal excitability during excitotoxic or convulsant stimulation. *Brain Res* 846: 112–121, 1999.
342. **Xiao YF, Sigg DC, Ujhelyi MR, Wilhelm JJ, Richardson ES, Iaizzo PA.** Pericardial delivery of omega-3 fatty acid: a novel approach to reducing myocardial infarct sizes and arrhythmias. *Am J Physiol Heart Circ Physiol* 294: H2212–H2218, 2008.
343. **Xiao Z, Deng PY, Rojanathammanee L, Yang C, Grisanti L, Permpoonputtana K, Weinshenker D, Doze VA, Porter JE, Lei S.** Noradrenergic depression of neuronal excitability in the entorhinal cortex via activation of TREK-2 K^+ channels. *J Biol Chem* 284: 10980–10991, 2009.
344. **Xu F, Tse FW, Tse A.** Pituitary adenylate cyclase-activating polypeptide (PACAP) stimulates the oxygen sensing type I (glomus) cells of rat carotid bodies via reduction of a background TASK-like K^+ current. *J Neurochem* 101: 1284–1293, 2007.
345. **Xu F, Xu J, Tse FW, Tse A.** Adenosine stimulates depolarization and rise in cytoplasmic $[Ca^{2+}]$ in type I cells of rat carotid bodies. *Am J Physiol Cell Physiol* 290: C1592–C1598, 2006.
346. **Yamamoto S, Kanno T, Yamada K, Yasuda Y, Nishizaki T.** Dual regulation of heat-activated K^+ channel in rat DRG neurons via alpha(1) and beta adrenergic receptors. *Life Sci* 85: 167–171, 2009.
347. **Yamamoto Y, Kummer W, Atoji Y, Suzuki Y.** TASK-1, TASK-2, TASK-3 and TRAAK immunoreactivities in the rat carotid body. *Brain Res* 950: 304–307, 2002.
348. **Yamamoto Y, Taniguchi K.** Expression of tandem P domain K^+ channel, TREK-1, in the rat carotid body. *J Histochem Cytochem* 54: 467–472, 2006.
349. **Yehuda S, Carasso RL, Mostofsky DI.** Essential fatty acid preparation (SR-3) raises the seizure threshold in rats. *Eur J Pharmacol* 254: 193–198, 1994.
350. **Yeom M, Shim I, Lee HJ, Hahm DH.** Proteomic analysis of nicotine-associated protein expression in the striatum of repeated nicotine-treated rats. *Biochem Biophys Res Commun* 326: 321–328, 2005.
351. **Youm JB, Han J, Kim N, Zhang YH, Kim E, Joo H, Hun LC, Joon KS, Cha KA, Earm YE.** Role of stretch-activated channels on the stretch-induced changes of rat atrial myocytes. *Prog Biophys Mol Biol* 90: 186–206, 2006.
352. **Yu SP.** Regulation and critical role of potassium homeostasis in apoptosis. *Prog Neurobiol* 70: 363–386, 2003.
353. **Yu SP, Yeh CH, Sensi SL, Gwag BJ, Canzoniero LM, Farhangrazi ZS, Ying HS, Tian M, Dugan LL, Choi DW.** Mediation of neuronal apoptosis by enhancement of outward potassium current. *Science* 278: 114–117, 1997.
354. **Zanzouri M, Lauritzen I, Lazdunski M, Patel A.** The background K^+ channel TASK-3 is regulated at both the transcriptional and post-transcriptional levels. *Biochem Biophys Res Commun* 348: 1350–1357, 2006.
355. **Zhang H, Craciun LC, Mirshahi T, Rohács T, Lopes CM, Jin T, Logothetis DE.** PIP_2 activates KCNQ channels, its hydrolysis underlies receptor-mediated inhibition of M currents. *Neuron* 37: 963–975, 2003.
356. **Zhang H, Shepherd N, Creazzo TL.** Temperature-sensitive TREK currents contribute to setting the resting membrane potential in embryonic atrial myocytes. *J Physiol* 586: 3645–3656, 2008.
357. **Zygmunt PM, Petersson J, Andersson DA, Chuang H, Sorgard M, Di M, V, Julius D, Hogestatt ED.** Vanilloid receptors on sensory nerves mediate the vasodilator action of anandamide. *Nature* 400: 452–457, 1999.